3D-printed Object Authentication using Micro and Macro Surface Textures and Geometric Features

Ankit Seal, M. Phil

Student ID:16029808

Supervised by: Professor Melvyn Smith, Dr Shwe Soe, Dr Gary Atkinson, and Dr Abdul Farooq

Centre for Machine Vision University of the West of England

School Of Computing And Creative Technologies

Feb 2024

Abstract

As the speed, quality, and affordability of additive manufacturing (AM) processes improve, more organisations and consumers are adopting the technology. Customising products, localising production, and lowering logistics are just a few of the primary advantages of AM. Because of these and other advantages, AM allows for a worldwide distributed manufacturing and supply chain involving several parties. This raises questions regarding the manufactured product's authenticity, and consequently its quality and reliability in use. In this research, we first explore the various hazards that exist in the additive manufacturing cyber-physical environment. The results highlight the security challenges for the AM supply chain. We then evaluate some of the currently implemented security measures to identify drawbacks and vulnerabilities in them. A core aspect of our investigation involves developing an algorithm that leverages extracted features to identify and characterize the unique signatures of glyphs and watermarks on the surface of 3D-printed objects. Based on the findings, the research then proposes three different levels of security that can be implemented and a novel authentication technique that utilises the intrinsic surface texture of the 3D-printed object. The experimental results and analysis demonstrate that the proposed method can successfully authenticate a 3-D printed object with high precision, as well as achieve a high level of security and robustness.

Contents

Table of Tables

Table of Figures

Glossary

Additive Manufacturing: A process of joining materials to make objects from 3D model data, usually layer upon layer, as opposed to subtractive manufacturing methodologies. Also refers to the industrial process starting from the inception of part till manufacturing using 3D printers.

Anomalies: Anomalies are any deviations that occur either on a 3D-printed surface or inside the object that are not part of the design but do not amount to a defect. They do not leave the objects unusable.

Watermark: a pattern of geometrical features embedded during the manufacturing process that is extracted by scanning to authenticate the given 3D-printed part.

Glyph: Macroscopic structures (greater than 1mm) that form a pattern or a 3D QR code on the printed surface, such as a 3D QR code, to provide a basic level of authentication.

Elaborate geometrical features: Specialised and intricate surface textures or patterns are added during the manufacturing process to provide a higher level of security compared to glyphs. Examples include custom surface patterns or micro-features.

Intrinsic geometrical features/texture: The unique, naturally occurring surface characteristics and printing traits of a 3D-printed object, which can be used for authentication without adding any artificial markers or patterns. Examples include layer lines or surface roughness resulting from the printing process.

Fiducial: A fiducial marker or fiducial is an object placed in the field of view of an imaging system which appears in the image produced, for use as a point of reference or a measure.

Fingerprinting: Fingerprinting is the process of examining the unique and distinctive surface features or patterns that naturally occur during additive manufacturing. These intrinsic geometrical features and printing properties serve as a unique signature or "fingerprint" for each product, providing reliable identification, verification, and counterfeiting protection.

G-Code: G-Code is a generic name for a control language understandable by 3D printers that encodes the motion of the toolpath (Printer head) for printing.

ArUco QR code: A type of QR code optimized for fast detection, used for embedding information on 3D-printed objects for authentication.

ArUco markers: Square markers used in vision applications for camera positioning. In 3D printing, they serve as embedded identifiers for quick object authentication.

1. Introduction

The latest industrial revolution, Industry 4.0, envisions the integration of intelligent production systems and advanced information technologies. Additive Layer Manufacturing (ALM) or Additive Manufacturing (AM) is a core component in this vision, enabling both manufacturing automation and the creation of objects with properties that could not be achieved with traditional subtractive manufacturing (Yampolskiy *et al.*, 2018). AM technologies, which are also referred to as additive fabrication, additive processes, additive techniques, additive layer manufacturing, layer manufacturing, three-dimensional (3D) printing, and freeform fabrication, offer unparalleled flexibility in component design and fabrication. This flexibility has fuelled a demand for AM applications in industries such as aerospace and automotive manufacturing. Most objects manufactured through AM technologies have a substantially reduced weight. A study by Airbus Group Innovation (UK) and its partners, showed that up to 75% of raw material usage can be reduced using AM techniques for greater fuel efficiency (Chen *et al.*, 2019; Chen, Mac and Gupta, 2017). In early 2015, the Federal Aviation Administration (FAA) qualified the first 3D-printed commercial jet engine part from General Electric (Belikovetsky *et al.*, 2016; Joshi and Sheikh, 2015). Following this trend, there have been several advancements in 3D printing technologies such as Fused Deposition Modelling (FDM), Stereolithography Apparatus (SLA) and Selective Laser Sintering (SLS) (Vora and Sanyal, 2020). Hewlett-Packard has developed a 3D printer that uses its proprietary Multi Jet Fusion (MJF) 3D printing process to be a pioneer in this $12 trillion manufacturing industry by producing high volume objects at low costs (*HP and Jabil Revolutionize $12 trillion Manufacturing Industry | Jabil.*, 2021).

Unfortunately, this rapid adoption of AM has also motivated a broad array of cyber and cyber-physical attacks (Yampolskiy *et al.*, 2018). The ease with which these 3D-printed products can be counterfeited, and the feasibility of such attacks, have been demonstrated in a study (Belikovetsky *et al.*, 2016). If any unauthorised reproduction of a part is carried out, even a simple sub-millimetre change in scale or a change in orientation, then its performance can be reduced significantly (Zeltmann *et al.*, 2016). Counterfeit objects can therefore be flawed which could result in dire consequences when used in safety-critical industries such as aviation. Such unauthorised objects are very difficult to identify in a supply chain.

Anti-counterfeiting measures such as embedded identification tags or glyphs have been used in the past to tackle this issue, as exemplified by Figure 1 (Pollard *et al.*, 2018). These glyphs are usually in the form of macroscopic

structures (greater than 1mm) that form a pattern or a 3D QR code on the printed surface. They can be easily identified by users before being scanned for verification. Another method is to deliberately introduce patterns scattered inside a 3D-printed object or on the surface as a way to form a *watermark*[1] to distinguish authentic 3D objects from fake ones (Dachowicz *et al.*, 2017) (Figure 2). This watermark is usually extracted and verified using specialist equipment. All these methods draw on the concept of a Physically Unclonable Function (PUF). A PUF is some protocol or algorithm applied to a single or a set of physical features derived from a part that defines a unique fingerprint that is easy to compute but difficult to replicate (Dachowicz *et al.*, 2017). Although the fingerprints are unique, this does not mean that they cannot be cloned easily, due to their small scale. Any macroscopic structure on the surface, by contrast, can be easily identified and replicated. In this research, we exploit the randomness of the 3D-printed surface texture to uniquely fingerprint the object. This randomness occurs due to the traits of the printing process as shown in Figure 3. This will provide the same unique fingerprint as the methods described above but provides the highest level of security due to the difficulty in replicating the fingerprint.

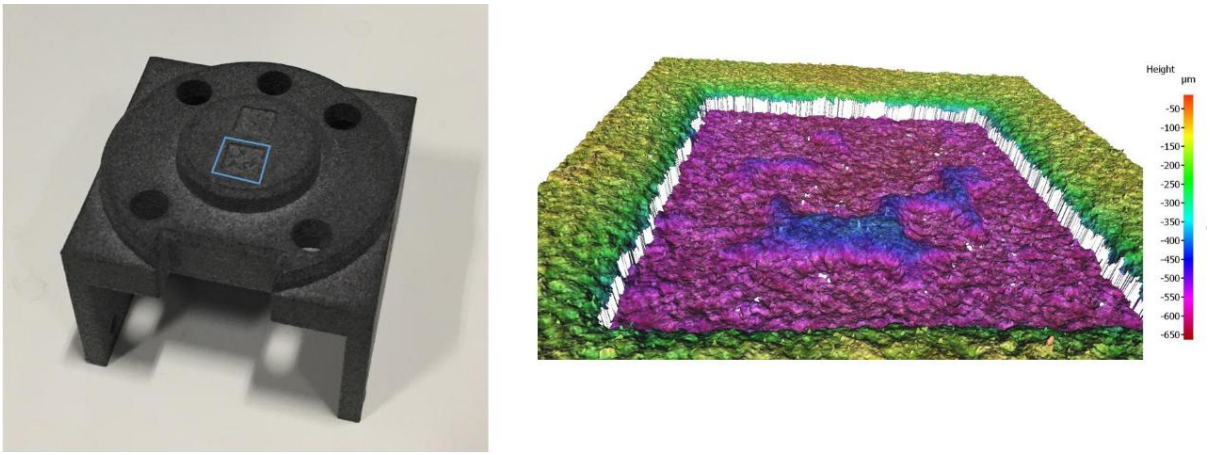

Figure 1: Multi-jet-fusion printed part on the left and a high-resolution scan of the indicated portion of it on the right showing the glyph used for authentication (HP Labs, 2017)

[1] Watermark: a pattern of geometrical features embedded during the manufacturing process that is extracted by scanning.

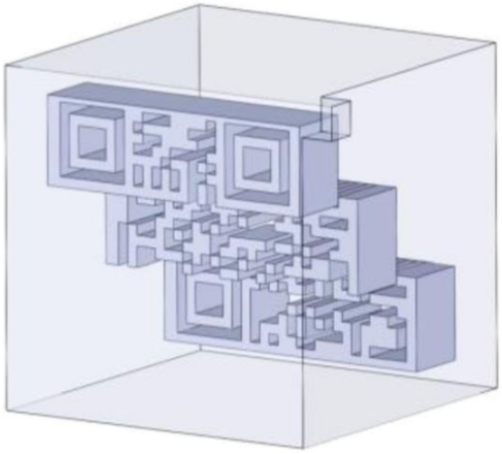

Figure 2: Embedded watermark formed using anomalies (Chen et al.*, 2019)*

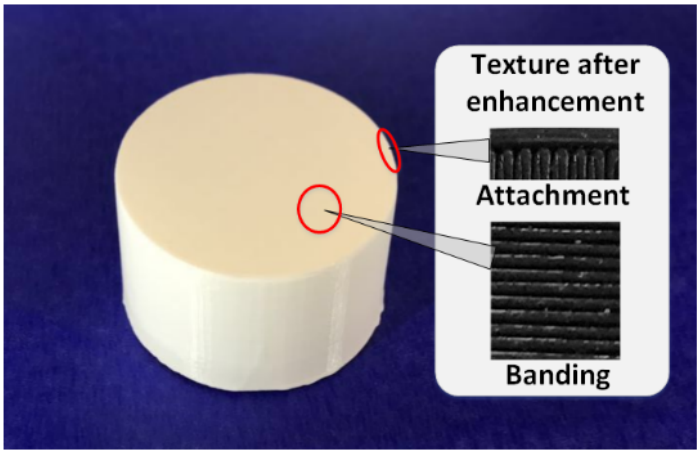

Figure 3: Printing process traits of a fused deposition model showcasing typical textures observed on the surface (Li et al.*, 2018)*

1.1. Problem Statement and Hypothesis

The major drawbacks of the current authentication approaches are that they offer limited authentication features against counterfeiting, making it easy for adversaries to bypass security and counterfeit objects that end up in the supply chain. Table 1 compares the various authentication features currently used in the industry with the proposed features. It draws this comparison based on the level of security provided by each of these methods using various aspects of authentication ranging from the formation of authentication markers to retrieval of these markers for authentication. Each level of security is implemented at a different scale.

Table 1: Taxonomy of printed object security features

Authentication features	Glyph	Elaborate geometrical features	Surface features (Proposed)
Formation of feature	Part of the CAD model is in the form of a randomly generated 3D QR code that is larger by 1mm in size.	Part of the CAD model with Specialised Surface Texture. Size and type depend on the printing technique, but each feature is less than 100 µm.	The intrinsic structure that forms the surface of the printed object.
Part of the design file	Yes	Yes	No
Level of security	Low	Medium	High
Difficulty to Counterfeit	Easy	Moderate	Hard
Scale of capture	Macro (large scale)	Meso (medium scale)	Micro (small scale)
Capture Complexity	Low	Medium	High
Definition of features	High	Medium	Low
Randomness of geometry	Low	Medium	High

Current methods of authentication are implemented by scanning either the glyph added on the surface or the elaborate geometrical features that were added during manufacturing. Glyphs can be in the form of 3D QR codes that are larger than 1mm and provide the lowest level of security due to their lack of complexity. Elaborate geometrical features are specialised surface textures that are carefully positioned, and more intricate than the glyphs. These provide a much greater level of security when compared to Glyphs as their structure definition is much harder to replicate. However, both these methods present surface structures that are highly defined with little

variation (randomness) in between each 3D-printed object when compared to the intrinsic surface of a 3D-printed object. Advanced knowledge of these security measures by an adversary, and access to high-resolution capture methods, means that these objects can be counterfeited with low to moderate difficulty. Having access to the original digital files of these objects will allow the adversary to replicate these security measures. This will make them completely indistinguishable from their original counterpart during verification. Moreover, assigning a unique authentication marker to all printed parts might be a tedious process that requires additional steps, adding complexity to production. Introducing additional geometrical features or glyphs during production may not be feasible or possible at all for some manufacturing requirements. Some manufacturers might desire an unmarked surface for aesthetics. All these drawbacks and limitations presented by the current methods motivate this research into a new authentication. The aim is to be least disruptive to the current manufacturing process and rely on the intrinsic geometrical features and printing traits of a 3D-printed object to provide the highest level of security in the authentication.

The hypothesis that is presented in this research is as follows:

Surface characteristics are unique to each 3D-printed part as each part is printed individually even when manufactured in the same batch from the same device.

None of the current authentication approaches use the intrinsic surface characteristics of 3D-printed objects to identify unique reliable and repeatable surface features that occur naturally during the AM processes. The intrinsic surface features are those characteristics that are inherent to the surface itself, without any external influence or modification. If the research hypothesis is successfully proven, then each manufactured 3D-printed object will present a unique signature on the surface that defines the PUF (Physically Unclonable Function). The highly random microscale features make it extremely difficult to counterfeit these objects, thus providing the highest security.

2. Research Aim

2.1. Research Proposal

The current research will involve implementing novel approaches to detect, capture and characterise the 3D surface texture and surface topography of 3D-printed objects to derive unique signatures that can be used for authentication purposes.

The novelty of the proposed approach lies in achieving a high level of accuracy in authentication by recovering the surface for both, macro (greater than 1mm) and microscale (less than 100 µm) features, and using glyphs and elaborate geometrical features along with intrinsic surface characteristics to derive a unique signature of the surface to identify the PUF. This approach relies on the hypothesis mentioned above as any surface that is highly random is also unique by nature. To achieve this, the current research will investigate surface characteristics derived from 3D object surfaces' topography and surface texture recovered. The capturing resolution limits of these features are based on previously established standards of manufacturability limits of the chosen AM processes of this research.

Investigating surface characteristics involves looking at using localised surface properties (including surface texture and other metrological 3D properties such as surface roughness) at the microscale and combining it with macroscale surface information and geometry to build a more generalised meta-surface structure characterisation that employs localisation and mapping techniques.

2.2. Research Questions

1. Are there any capture systems available that can capture high-resolution surface texture and geometry? Is there a need for a capture system to capture multiscale data for 3D-printed objects? If not, what are the requirements to build such a system?

The research would require the capture of high-resolution 3D surface data. An investigation into industry-leading capture methods is carried out in this research to determine the current standards for capturing 3D surface data. The capture system should be able to recover surface structure at high resolution (less than 25 µm). The capture methods would be **tested for their capture resolution, speed, cost and their ability to span across multiscale**. This would also provide an understanding of whether all surface details can be captured at just one scale or if there is a need to capture at a multiscale.

2. How can we recover reliable surface texture and surface topography information to uniquely characterise surfaces of 3D-printed objects? How can we derive a unique signature using this information?

To answer this question, this study will **investigate current 3D and 2D surface texture analysis approaches** that have been implemented to characterise a surface. This investigation will lead to the development of a novel feature extraction method to **derive a unique signature of the 3D-printed object** by recovering surface data using a combination of 3D (as necessary) and 2D surface information for authentication purposes. The derived unique signature will establish the hypothesis presented in this research. The **features extracted should be reliable and repeatable** to obtain a unique signature. A unique signature obtained from the surface of a 3D-printed object should also be **scale, rotation, and skewness invariant**.

3. How are we able to use a unique signature from a 3D-printed part for robust and accurate authentication? Would the derived signature be enough or is there a need to use additional structural and/or positional information?

As mentioned previously, we hypothesise that the 3D surface characteristics are unique to each printed part, since each part is printed individually even when printed in the same batch. The investigation will first establish if the surface characteristics are the same at each point of a given 3D-printed surface. This will establish the requirement for additional information such as position. The unique signature obtained would be tested to see if it is sufficiently robust for authentication.

Lastly, if additional information is required, we investigate the implementation of additional structures on the 3D-printed surface that form a watermark and use **machine vision techniques** to analyse this watermark for additional markers and propose a comprehensive robust solution that doesn't compromise on the security for authentication with respect to the overall geometry of the object.

2.3. Project Scope

It should be noted that no security and product authentication approach applies to all AM technologies. Thus, here we define the scope of this research.

- The glyphs are larger at 1mm in size whereas the anomalies are less than 100 µm. These anomalies would be deliberately placed around the glyph to form the watermark.
- The objects are not subjected to any post-processing, such as sanding/painted/etc, that will distort or eliminate the glyph.
- The objects are only printed in plastic using 3D printing techniques that are widely adopted in the AM industry.
- The capture system should adhere to industry standards with high-resolution output and high capture speed.

2.4. Objectives

1. Develop comprehensive methods for extracting and analysing localised surface properties at the microscale. This includes creating advanced algorithms and utilising state-of-the-art equipment to capture detailed surface textures and geometric features. The aim is to build a nuanced meta-surface structure characterisation, which is vital for authenticating 3D-printed objects with high precision.
    - **Linked Research Question:** This supports the question about recovering reliable surface texture and topography information (Question 2).
2. Conduct an extensive investigation into the existing and potential technologies for capturing 3D surface textures. This involves not only assessing the capabilities of current systems but also identifying gaps and developing specifications for a new system that can handle both macro and micro-scale data, focusing on high resolution, speed, and cost-effectiveness.
    - **Linked Research Question:** Directly related to exploring available capture systems and the requirements for a multiscale capture system (Question 1).

3. Create innovative feature extraction techniques that can isolate and utilise unique signatures from 3D-printed objects. This requires exploring a combination of 3D and 2D data to formulate reliable, repeatable, and viewpoint invariant features, contributing to a novel approach in object authentication.
    - **Linked Research Question:** Aligns with the question on deriving unique signatures from surface data (Question 2).
4. Design a sophisticated watermarking scheme that seamlessly integrates artificial elements like glyphs and geometric patterns with natural surface textures. This approach aims to increase the security of 3D-printed objects, ensuring the watermarking does not compromise the object's integrity or aesthetic value.
    - **Linked Research Question:** Relates to the exploration of using additional structural and positional information for robust authentication (Question 3).
5. Develop and implement advanced algorithms for object identification using captured surface data. This involves ensuring that the algorithms are robust, accurate, and efficient in authenticating 3D-printed objects, possibly using machine learning techniques to enhance performance.
    - **Linked Research Question:** Ties in with the question of utilising a unique signature for authentication (Question 3).

2.5. Contribution and Impact

1. Publishable work will be undertaken by cataloguing various anomalies that can be deliberately introduced on 3D-printed surfaces.
2. This research will lead to a publishable investigative survey, testing existing methods for their capabilities at multi-scale data capturing.
3. Novel feature extraction techniques to characterise unique signatures based on viewpoint invariant features will be developed for 3D-printed objects.
4. Novel authentication techniques will be designed and developed to address specific needs for 3D-printed objects. This would help to uniquely identify and localise watermarks and glyphs on the 3D-printed surfaces for authentication.

2.6. Potential Commercial Interest in Additive Manufacturing Security and Authentication

As additive manufacturing (AM) becomes increasingly popular across various industries, the need for effective security and authentication measures grows. Several businesses and organizations operating in sectors that depend on the production of high-quality, reliable, and secure components may be interested in this research area. The following is a list of key industries that could potentially benefit from advancements in AM security and authentication.

Aviation and Defence: Aerospace and defence system manufacturers rely on additive manufacturing to create complex, lightweight components. Ensuring the authenticity and integrity of these components is critical, as a single component's failure could have severe consequences. Integrating advanced authentication mechanisms into their AM processes could help these companies maintain strict quality control and prevent counterfeit components from entering their supply chains.

Automotive: Car manufacturers are increasingly using additive manufacturing to produce complex and customised parts for their vehicles. Ensuring the security and authenticity of these components is essential for maintaining safety standards and brand reputation. These manufacturers could utilise advanced AM authentication methods to verify the origin and quality of their 3D-printed items.

Medical Devices and Implants: Medical device and implant manufacturers are increasingly turning to additive manufacturing for patient-specific production. Given the critical nature of these products and the strict regulatory standards they must adhere to, manufacturers need to implement reliable authentication techniques. The development of new AM authentication methods could help these companies ensure the safety and effectiveness of their products while complying with regulatory requirements.

Consumer Electronics: Major consumer device manufacturers could also benefit from advancements in AM security and authentication. As the prevalence of counterfeit products in the electronics market continues to rise, companies need effective methods to protect their intellectual property and ensure the quality of their products. AM authentication methods could provide an additional layer of protection, making it more difficult for counterfeiters to replicate authentic components.

A wide range of industries and businesses stand to gain from advances in AM security and authentication. As 3D printing technology continues to grow and become more widespread across various industries, the demand for secure and reliable authentication solutions will only increase. Enabling researchers and companies working on AM authentication to safeguard the integrity and security of 3D-printed components can offer significant benefits for numerous industries.

3. Literature Review

As outlined in the introduction, a slight deviation in 3D-printed objects can have a significantly negative impact, especially when used within safety-critical environments (Straub, 2018). This established the need for authentication in AM. As this research proposes to prove a hypothesis and develop a novel feature extraction technique, there needs to be a clear understanding of a few aspects of the AM manufacturing and authentication process. Thus, this literature review is divided into 5 major sections:

1. Additive Manufacturing (AM) and Material Science
2. Capture Methods
3. Surface Feature Extraction and Texture analysis
4. Security in AM and Authentication using the 3D-printed surface.
5. Surface Fingerprinting Techniques

The first section provides a clear understanding of the AM process and discusses the material that forms the 3D-printed parts. This will help us understand some of the surface characteristics of these parts. We then identify the 3D printing techniques and printing materials that fit our scope which has been defined in Section 2.3 and understand how they manufacture given objects. Every 3D printing technique, although seem to follow the basic layering model, is slightly different. This can lead to variations in surface finish. It is also known that different 3D printing techniques can result in different types of surface anomalies (Simplify3D, 2018). This information is presented as a taxonomy of the anomalies that can occur naturally or due to error during printing using the most common printing techniques. All these anomalies are part of the surface texture. A better understanding of how they are formed can help understand the limitations of each of these printing techniques. This will help guide the formation of the watermark that can be used for authentication purposes. To detect and identify these watermarks in 3D-printed objects, it is critical to be able to characterise the objects' surfaces and geometries to a high degree of precision. To achieve this, the features used to characterise the surface textures must be obtained from different printing techniques and are distinctively captured at the appropriate resolution. The second section explores the various capture methods that are currently state-of-the-art techniques to capture the surface texture at the appropriate resolution. It also identifies which of these techniques are best suited for our use case. The third section talks about the extraction of the information from the surface a 3D-printed part and presents the expected texture of it. This would lead to an

examination of the current cyber-physical vulnerabilities in AM and the defence techniques against AM sabotage that either implements or can benefit from an authentication system. This is then followed by techniques that can fingerprint the surface for authentication purposes.

3.1. Additive Manufacturing (AM) and Material Science

AM processes take the information from a CAD and create a layer-by-layer 3D object.

The British Standards Institution (BSI) has defined AM as *"the process of joining materials to make parts from 3D model data, usually layer upon layer, as opposed to subtractive manufacturing and formative manufacturing methodologies"* (British Standards Institution, 2015).

Additive Manufacturing (AM) is a complex process that involves both automated and manual workflows. It is integral to understand that 3D printing, a term commonly used by the public, is a crucial component of the broader Additive Manufacturing process. This process can be categorised into three distinct phases as illustrated in Figure 4 (Yampolskiy *et al.*, 2018). At the design phase, a CAD model is created based on the desired dimensions, properties, and functionalities; followed by the optional finite element analysis (FEA) on the optimization model. FEA is typical for safety-critical parts. The manufacturing phase includes the slicing process of the 3D model and the generation of G-Code for 3D printing. G-Code is a generic name for a control language understandable by 3D printers that encodes the motion of the toolpath (Printer head) for printing (Wickramasinghe, Do and Tran, 2020). However, it's important to acknowledge that laser-based AM systems such as SLS (Selective Laser Sintering) and SLA (Stereolithography) typically do not require G-Code programs, which differentiates them from the FDM or Material Extrusion methods. During the testing phase, the printed part is subjected to mechanical and physical testing. It can be destructive or non-destructive testing. It is at this stage that the 3D-printed object is also tested for authenticity.

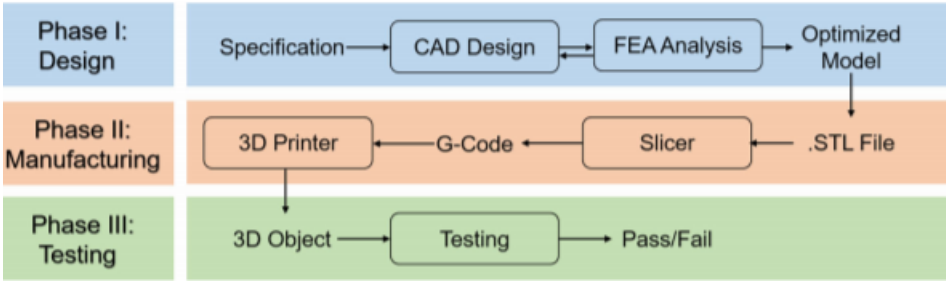

Figure 4: A typical process chain of Additive Manufacturing (Yampolskiy et al.*, 2018)*

Furthermore, 3D printing can be classified into three processes based on the form of material used; Liquid-based, Powder Based and Solid Based (Wong and Hernandez, 2012) as illustrated in Figure 5. Under the scope of this research, we would be concentrating on plastic-based 3D-printed parts due to their prevalent use in the industry and the versatility of plastic materials in a wide range of applications. The printing techniques capable of printing these materials, highlighted in green in Figure 5: , were selected for their industry relevance, compatibility with the desired materials, and accessibility for research and experimental purposes. These dark green techniques are the ones studied in this research. In the following sections, a detailed description of these printing techniques is presented.

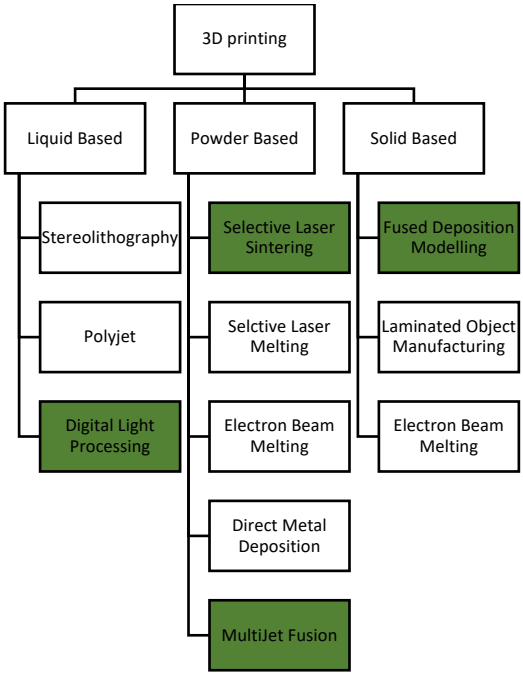

Figure 5: A material-based classification of AM processes and technologies

3.1.1. Fused Deposition Modelling (FDM)

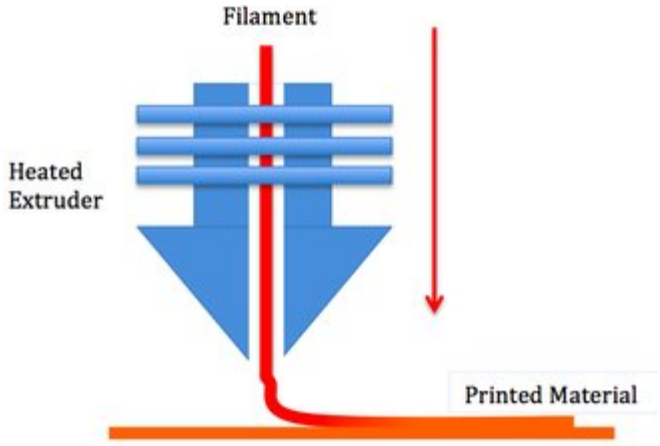

Figure 6: A schematic diagram of the FDM process

In the field of 3D printing, Fused Deposition Modelling (FDM) is a widely adopted technique due to its low cost, high speed, and simplicity (Sharma and Rai, 2022; Vyavahare *et al.*, 2020). According to Sharma and Rai (Sharma & Rai, 2022), FDM comprises the layer-by-layer deposition of thermoplastic polymer filaments extruded through a heated nozzle at high temperatures onto a flatbed (Figure 6). This method allows for the precise and easy development of complicated, bespoke items. The more intricate details of FDM processes have lately been investigated, with subjects including filament processing, materials, and printing parameters covered (Kristiawan *et al.*, 2021; Lalegani Dezaki, Mohd Ariffin and Hatami, 2021)

One of the components of the environmentally friendly FDM process is polylactic acid (PLA), which is produced from renewable biomass sources such as vegetable fats, oils, and maize starch (Sharma & Rai, 2022). Due to its natural degradation, PLA is a desirable material for both domestic and commercial applications, making it perfect for toys and decorative items (Sharma and Rai, 2022). In addition to PLA, several materials have been thoroughly investigated and used in FDM methods, including acrylonitrile butadiene styrene (ABS), polyethene terephthalate glycol (PETG), and thermoplastic polyurethane (TPU) (Kristiawan et al., 2021).

Smart materials that react to external stimuli like heat, magnetic, and electric fields that may modify their physical and chemical characteristics are used in the development of FDM in the field of 4D printing (Sharma & Rai, 2022). This increases the potential uses of FDM-based printing processes by enabling the construction of structures with memory effects and shape-shifting capabilities which can be used for authentication. A deeper comprehension of elements like extrusion temperature, layer height, printing speed, and infill patterns will aid in the creation of more complex and varied applications for FDM technology as researchers continue to refine the process (Lalegani Dezaki et al., 2021).

Surface roughness is mentioned in both Kristiawan et al. (2021) and Lalegani Dezaki et al. (2021) as a crucial element influencing the quality of FDM 3D-printed items. A printed object's surface irregularity, or surface roughness, can have an impact on both its mechanical and aesthetic qualities(Dey and Yodo, 2019). This is discussed further in Section 3.1.7.

3.1.2. Stereolithography (SLA)

Stereolithography (SLA) is a 3D printing technology that uses a liquid photopolymer resin and a UV laser to create solid objects layer by layer.

The SLA printing process, as illustrated in Figure 7, begins by filling a vat with liquid photopolymer resin. A build platform is lowered into the vat, and a UV laser traces a pattern on the surface of the resin, corresponding to the first layer of the 3D model. The laser's energy initiates a chemical reaction that solidifies the resin, forming the first layer of the object. This process was developed in the early 1980s and has been commercialized since 1986, representing one of the first practical applications of additive manufacturing technologies. The build platform then moves up slightly, allowing the fresh resin to flow beneath the solidified layer. The laser traces the next layer, which adheres to the previous one, and the process is repeated until the entire object is formed (Melchels, Feijen and Grijpma, 2010).

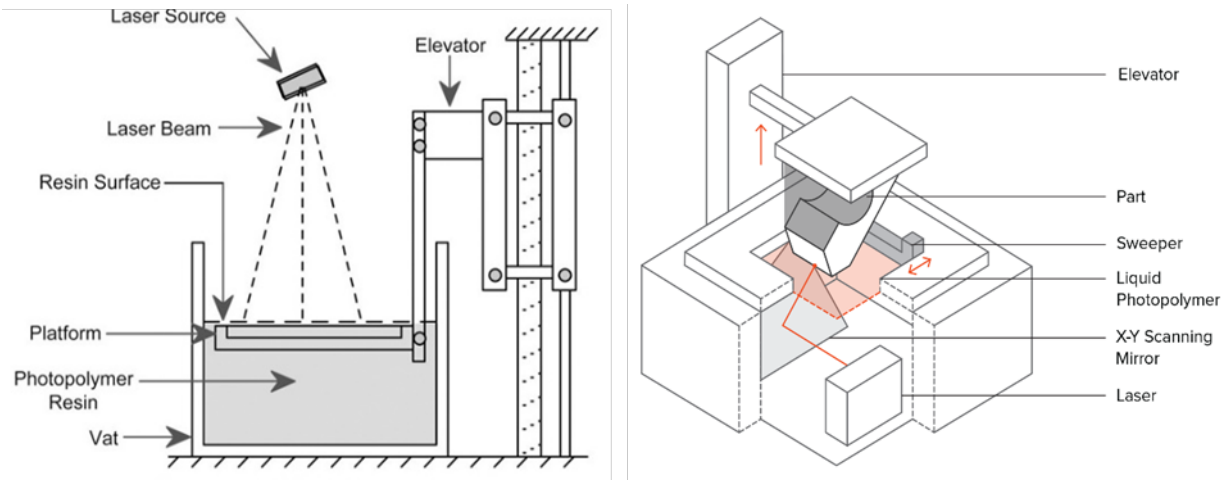

Figure 7: A schematic diagram of the SLA process

SLA has several advantages over other 3D printing technologies, such as high surface quality, fine resolution, and the ability to produce intricate and complex geometries. However, SLA-printed parts are often more brittle than those produced using other methods, and the resin can be expensive and sensitive to UV light, which may cause the objects to degrade over time if exposed to sunlight (Melchels, Feijen and Grijpma, 2010). Despite these challenges, SLA remains a popular choice for applications that require precise detail and a smooth finish.

3.1.3. Polyjet Printing (PP)

Polyjet uses inkjet technologies developed by MIT (Massachusetts Institute of Technology) to produce physical models. The inkjet head moves in the x and y axes depositing a photopolymer which is cured by ultraviolet lamps after each layer is finished (Figure 8). It can achieve very high resolution (up to 5 µm). However, the parts produced by this process are weaker than others like stereolithography and selective laser sintering due to lack of adhesion between the layers. A gel-type polymer is used for supporting the overhang features and after the process is finished this material is water-jetted (Patpatiya *et al.*, 2022; Kechagias and Maropoulos, 2015).

Moreover, Polyjet printing enables the production of delicate features and complicated shapes that would not be achievable with other additive manufacturing processes. This is because it enables the manufacturing of multi-material and multi-coloured parts by allowing printing in many materials and colours inside a single print job. The method is also appropriate for generating small, intricate pieces quickly and for making moulds and patterns for casting operations.

To determine the surface finish of a Polyjet printed object, a test conducted by Cazón et al., (2014) concluded that statistically there are significant differences between the mean roughness in all directions measured(Wei, Zeng and Pei, 2019). This suggests that while preparing the print, care should be given to how the item is oriented throughout the printing process since it may influence the surface quality. Additionally, if necessary, the surface finish of Polyjet printed items can be improved by using post-processing processes like sanding, polishing, or chemical treatments.

Polyjet printing has various limitations despite its benefits. The technology can be more expensive compared to other additive manufacturing techniques due to the high cost of materials and the requirement for specialist equipment, such as UV lights, in addition to the weaker portions. Moreover, UV radiation, moisture, or temperature fluctuations may cause the photopolymers used in Polyjet printing to degrade more quickly over time, which may reduce the printed components' long-term usefulness and durability.

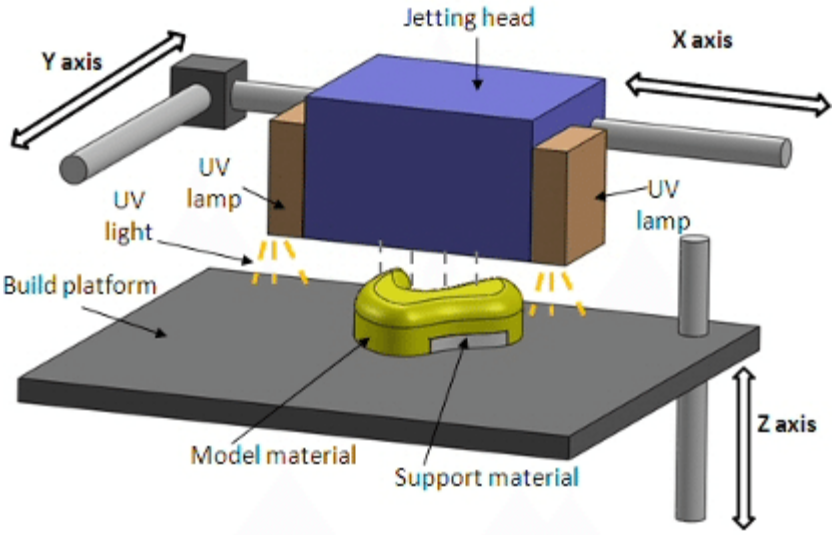

Figure 8: A schematic diagram of the Polyjet Printing process

3.1.4. Digital Light Processing (DLP)

Digital Light Processing (DLP) is an additive manufacturing technique that uses a digital light projector to selectively cure photopolymer resins one layer at a time. A vat of liquid photopolymer resin and a build stage is used in the first step, immediately below the resin's surface (Figure 9). A UV light picture of a single layer is projected onto the resin via a digital light projector, which is typically based on a Digital Micromirror Device (DMD) chip. The liquid resin solidifies after being exposed to UV light, creating the correct layer shape. Up until the entire thing is finished, the build platform is then elevated or lowered, exposing a new layer of resin to the light source(Dilberoglu *et al.*, 2017).

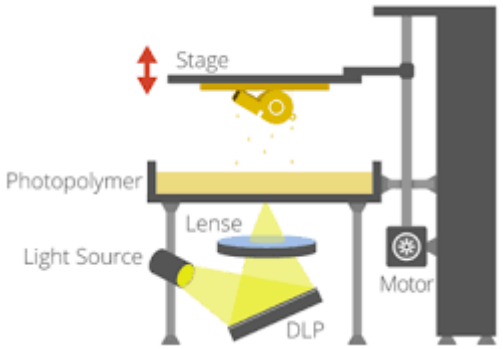

Figure 9: A schematic diagram of the DLP 3D Printing process

DLP technology is known for its capacity to create components with a high degree of resolution and a smooth surface finish, often between 25 and 100 microns. Because of the projection-based process's ability to continuously cure resin layers with less apparent layer lines than conventional layer-by-layer additive manufacturing methods, the smooth surface finish is made possible (Thompson and Mischkot, 2015).

The orientation of the item during printing, the kind and characteristics of the photopolymer resin used, and the methods utilised for post-processing can all have an impact on surface quality. Post-processing techniques like sanding, polishing, or chemical treatments can be used to enhance the surface finish (Chua, Wong and Yeong, 2017; Rebaioli and Fassi, 2017).

3.1.5. Multi Jet Fusion (MJF)

Multijet Jet Fusion (MJF) implement a unique powder-based process developed by HP. The main process in HP's Multi Jet Fusion 3D printing technology is illustrated in Figure 10. First, the build material is recoated on the surface layer as shown in Figure 10 (a). The printing process applies a fusing agent selectively to the places where the 3D object is to be (Figure 10 (b)) and also applies a detailing agent where the fusing action needs to be controlled (Figure 10 (c)). Heat energy using an array of infrared lamps is applied on the entire surface as shown in Figure 10 (d) so that the area for the 3D object is fused (Figure 10 (e)). This process is repeated layer by layer until the full 3D object is printed. The process prints using a plastic-based powder called PA12. A powered material is deposited across the build platform to support the overhangs (Cai *et al.*, 2021).

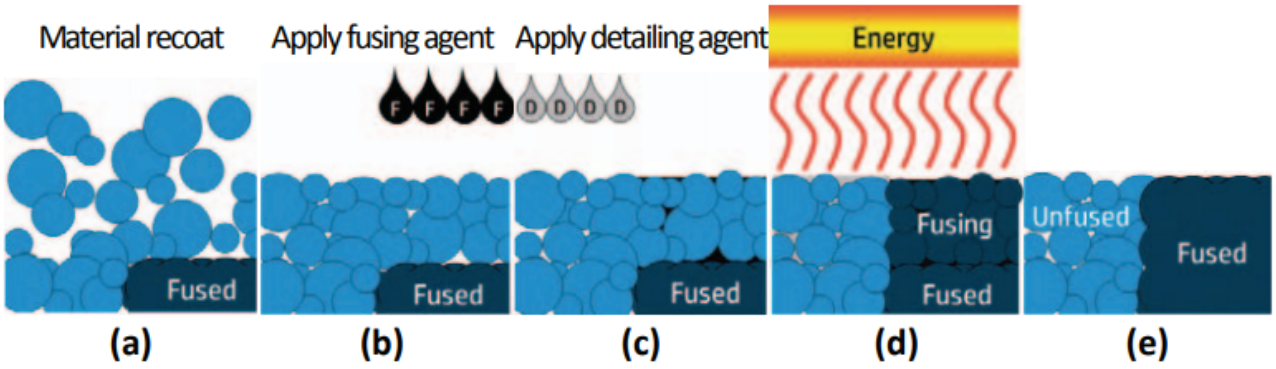

Figure 10: HP's multi-agent printing process of Multi Jet Fusion technology (Cai et al.*, 2021)*

The MJF process generates items with reasonably smooth surfaces due to the fine control given by the fusing and detailing agents. The constant layer bonding and reduced layer visibility are made possible by the regulated application of these agents and the uniform heat distribution provided by the infrared lights. Nonetheless, elements including component orientation, material characteristics, and layer thickness continue to have an impact on the surface finish. Bead blasting or penetration with a sealant are two post-processing methods that can be used to further improve the surface finish and look of MJF-printed objects (Kim, Zhao and Zhao, 2016).

3.1.6. Selective Laser Sintering (SLS)

SLS (Selective Laser Sintering) is commonly deployed in industry. SLS is a powder-based procedure that uses PA12 material, just like MJF. SLS selectively fuses (sinters) the thin layer of deposited plastic-based polymer powder using a laser rather than using an infrared lamp. First, the powder is delivered into the reservoir platform, and then a sledge distributes the powder evenly across the building area to make a uniform coating. The printer must be heated to warm the powder before sintering. The laser's processing temperature needs to be precisely regulated between the melting and crystallisation points of the particular polymer. The "sintering window" of SLS processing for a particular polymer is the name given to this meta-stable thermodynamic area of undercooled polymer melt (Cai *et al.*, 2021). The printing process begins with the activation of the laser (CO2 lasers or fibre lasers), which scans the powder bed along the X and Y axes in accordance with the object's predetermined design. Depending on the amount of transferred energy, powder particles are fused partially or entirely together. Subsequently, the printing bed is lowered, and another layer of powder is deposited on top of the previously sintered layer to enable the Z-axis construction of the item. These stages are repeated until the object is completed. The printed dosage forms are then removed from the construction platform and brushed to eliminate any excess powder (Figure 11) (Gueche *et al.*, 2021).

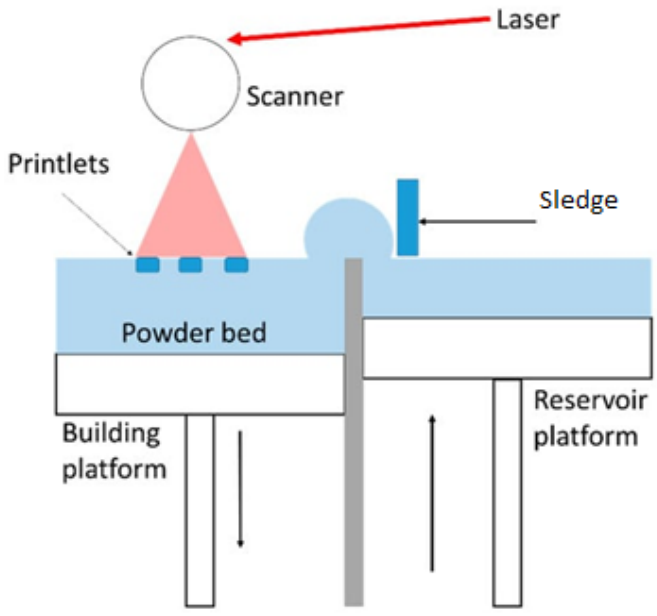

Figure 11: A schematic diagram of the SLS process(Gueche et al.*, 2021)*

Due to the powder-based nature of the process, SLS items often have a little rough texture in terms of surface polish. Particle size, layer thickness, laser power, and scan speed are a few examples of variables that have an impact on

surface roughness. The orientation of the component during the printing process might also have an impact on the roughness (Cai et al., 2021). Sanding, bead blasting, or vibratory finishing are post-processing methods that can be used to enhance the surface finish of SLS-manufactured items (Cai *et al.*, 2021; Tey, Cai and Zhou, 2021).

3.1.7. Surface Characteristics and Anomalies

Different 3D printing technologies produce parts with distinct surface characteristics and potential anomalies. These unique features, influenced by a multitude of printing parameters, can help in determining a surface signature for authentication purposes. In this section, we will discuss the surface finish and anomalies observed in various 3D printing processes.

Various printing parameters affect the surface characteristics of a 3D-printed object, including layer thickness, support angle, extrusion temperature, platform temperature, print speed, extruder flow ratio, nozzle distance, infill type, infill density, surface layers, supports, seam type, and fan speed (Gunaydin, Kadir & S. Türkmen, 2018).

For other AM processes such as Selective Laser Sintering (SLS) and Stereolithography (SLA), additional factors come into play. In SLS, parameters like laser power, scan speed, layer thickness, and powder material properties can significantly impact surface quality and characteristics (Doubrovski, Verlinden and Horvath, 2012). In SLA, factors affecting surface characteristics include laser power, scan speed, layer thickness, resin material properties, and recoating process (Tumbleston *et al.*, 2015).

Each 3D printing technology has a unique visual surface finish, as summarised in Table 2.

Table 2: Overview of surface finish

Printing technology	Surface finish	Surface Roughness (Ra)	XYZ Resolution	Smallest Layer Thickness	Smallest Thin Wall	Image
Fused Deposition Modeling (FDM)	Prominently visible layer lines	Varies with layer height and nozzle size 2-22 µm	0.4 mm (Typical nozzle diameter)	0.1-0.3 mm (Typical)	0.8 mm (Minimum)	
Stereolithography (SLA)	Smooth surface, layer lines may be visible but less prominent	6-12 µm	25-100 µm (Typical)	25-100 µm (Typical)	0.6 mm (Minimum)	
Polyjet/DLP	A smooth surface finish that is either glossy or matt	2-32 µm	16-42 µm (Typical)	16-42 µm (Typical)	0.6 mm (Minimum)	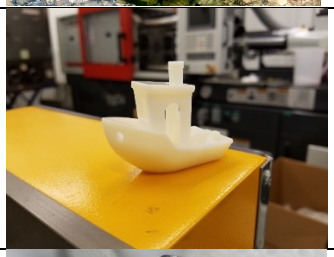
Multi Jet Fusion (MJF)	Grainy texture	10-25 µm	80 µm (Typical)	80 µm (Typical)	0.7 mm (Minimum)	
Selective Laser Sintering (SLS)	Grainy texture. Like MJF but a bit rougher along the layer lines	10-75 µm	100-120 µm (Typical)	100-120 µm (Typical)	0.7 mm (Minimum)	
Laminated Object Manufacturing (LOM)	Rough surface, visible seams between layers	94-101 µm	NA	Layer thickness of used material	Depends on material and layer size	NA

In all Additive Manufacturing (AM) processes, layer thickness, width, and overlap interval between layers affect surface roughness and mechanical properties, resulting in a 'staircase effect' on occasion (Bochmann *et al.*, 2015). This impact and surface roughness can be mitigated by thinning the layer (Sai and Yeole, 2010). Surface roughness measurements (Ra) have been extensively analysed for various 3D printing processes, but no clear trend has been

identified due to location-dependent variability (Reddy, 2018; Cazón *et al.*, 2014; Negi, Dhiman and Sharma, 2014; Ahn *et al.*, 2009). However, Pérez et al. (2018) found that certain printer parameters had a considerable impact on surface properties. A staircase effect can occur due to the sampling of a curved surface in a CAD based on the layer height a 3D printer can print (Figure 12). These effects are visible significantly in Figure 13.

Kazuhisa Miyoshi's work (Miyoshi, 2021) also emphasizes the importance of understanding the physical, mechanical, and chemical changes induced by surface modifications for better surface characterization. This is particularly relevant when considering thin films and coatings, as well as tribological engineering surfaces, which are crucial in 3D printing.

Wall thickness, layer height, temperature, extrusion rate, and printing speed have a substantial impact on the surface properties of FDM-printed objects (Bochmann et al., 2015). Pérez et al. (2018) discovered that increasing layer height and wall thickness diminished surface quality, whereas toolpath, speed, and temperature had no effect. Material storage conditions and the type of material employed can also influence surface quality (Dey and Yodo, 2019; Valerga *et al.*, 2019).

Due to their layer-by-layer procedures and photopolymer resins, SLA, PolyJet and Digital Light Processing (DLP) printers produce smooth surface finishes (Wei, Zeng, and Pei, 2019; Kechagias and Maropoulos, 2015; Cazón et al., 2014). Supporting materials are simply removable, leaving clean surfaces behind. However, the quality of the surface finish may vary based on the printer and materials utilised.

For Multi Jet Fusion (MJF) and Selective Laser Sintering (SLS) procedures, complete polymer particle fusion and adhesion with prior layers are required. Insufficient sintering windows or excessive heat might result in surface finish concerns like lateral development (Cai et al., 2021; Petzold et al., 2019).

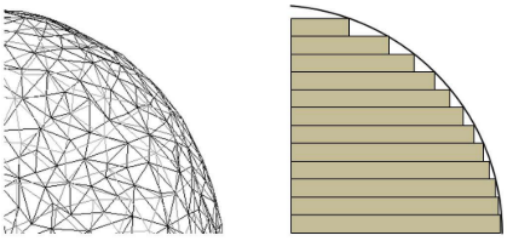

3D mesh model Layered model

Figure 12: CAD model (left), stair stepping effect model (right) (Hou et al.*, 2015)*

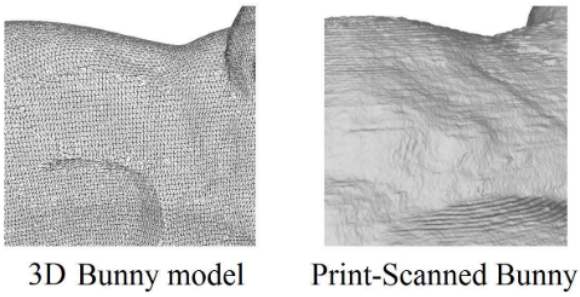

Figure 13: Theoretical stair-stepping effect (left), the real stair-stepping effect of 3D printing content (right) (Hou et al.*, 2015)*

This might be true when the surface was analysed at the macroscale, but another study showed that change in extrusion temperature and rate causes significant porosity on the surface (Gordeev, Galushko and Ananikov, 2018; Valerga *et al.*, 2018). Figure 14 shows a change in extrusion rate that is indistinguishable to human eyes but can alter the strength of the part significantly. The difference is extrusion rate should result in different characteristics for the surface.

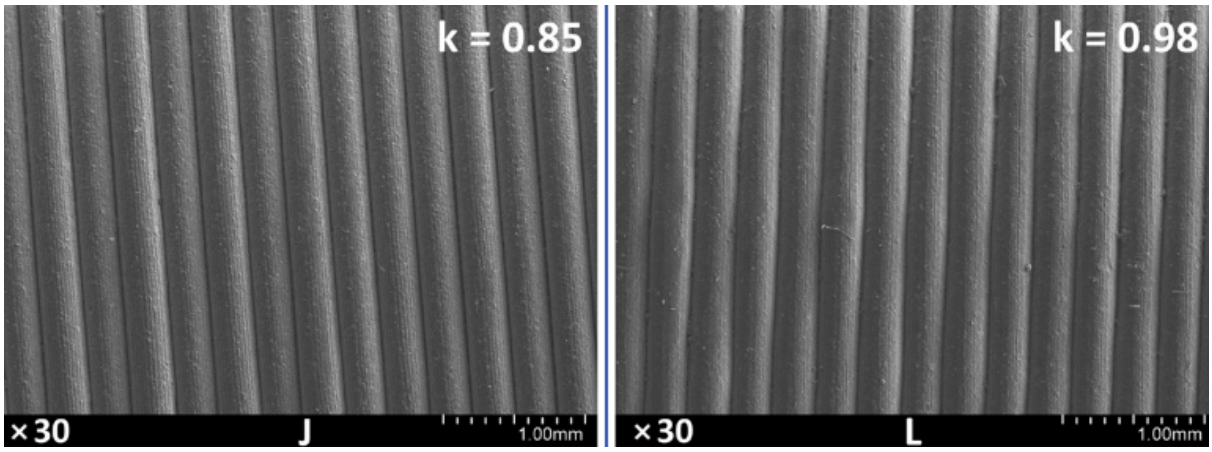

Figure 14: 85% extrusion rate vs 98% extrusion rate on an FDM printer (Gordeev, Galushko and Ananikov, 2018)

Table 3: Influence of storage conditions of the material and operating temperature of the 3D printer on the surface finish (Valerga et al., 2018)

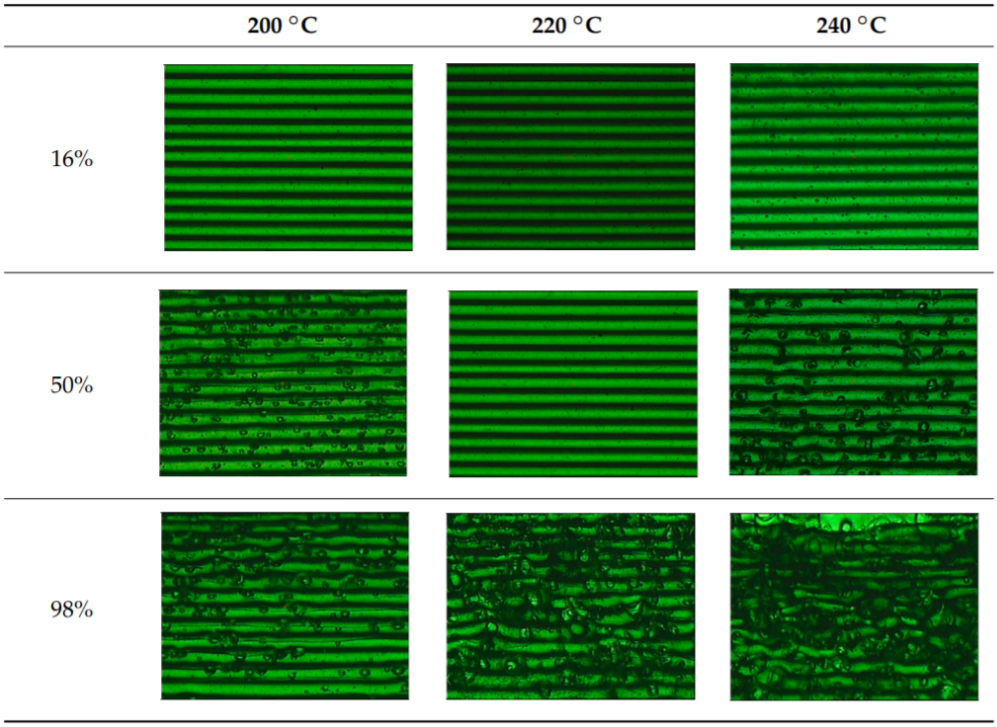

Furthermore, Table 3 reveals that the material's storage circumstances are even more essential than temperature or pigmentation, even though it is rarely studied. This can cause microscopic changes that are not captured by conventional surface testing. Moreover, the surface roughness can present a high variability depending on the measuring location (Pérez *et al.*, 2018).

Materials also influence the print surface quality. For example, PLA (Poly Lactic Acid) polymer, one of the most common materials used in FDM printing, has an uncontrolled and arbitrary appearance due to its low homogeneity (Valerga *et al.*, 2018). Despite replicating the same printing conditions. Similar results were observed with other popular FDM printing materials (Dey and Yodo, 2019; Valerga *et al.*, 2018).

In the case of Polyjet, photopolymers used for printing also present a distinct surface finish. Previous investigations have shown the top surface finish has a uniform pattern for roughness parameters, indicating higher reliability on the measurements taken, while the side surface clearly shows the discrete deposited built layers, indicating the parts have uniform-built structure (Wei, Zeng and Pei, 2019; Kechagias and Maropoulos, 2015; Cazón *et al.*, 2014). However, the surface roughness values calculated were unique for each part measured. Figure 15 shows a microscopic image of the two types of surfaces that a Polyjet printer can achieve. The glossy finish has smooth surfaces, but the matte finish contains repeated lines with peaks and valleys.

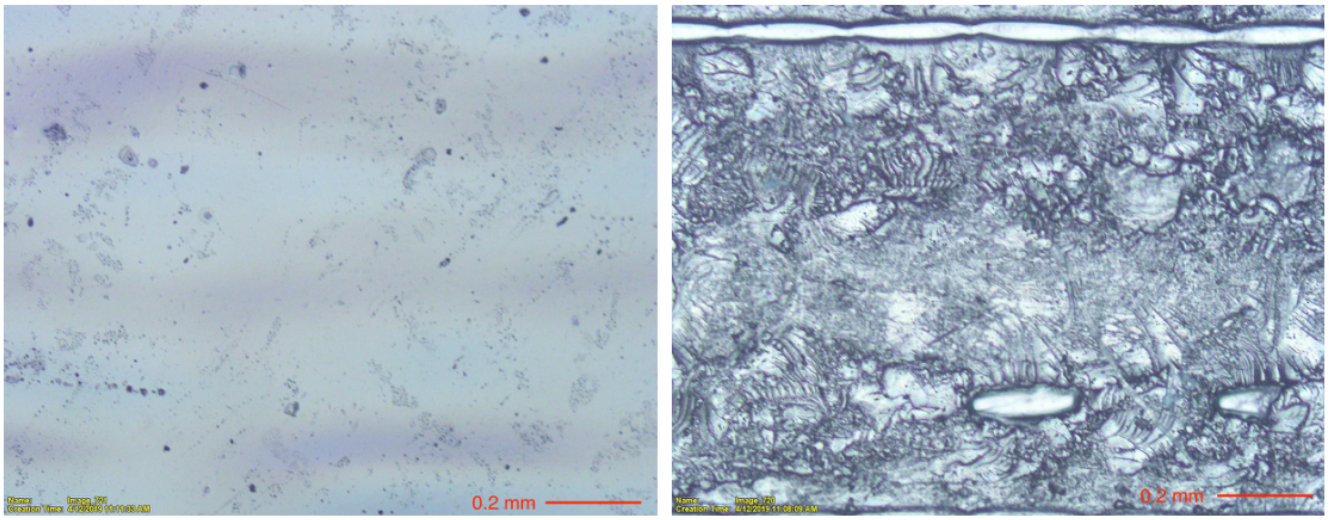

Figure 15: Microscope images of surfaces of Polyjet prints with black material using (a) glossy and (b) matte finish (Wei et. al. , 2019)

As other techniques like MJF and SLS, as they share their traits in printing, they also share some of their flaws. Full fusion of polymer particles in the top powder layer is necessary as well as adhesion with previous sintered layers. Figure 16 shows what can happen if the sintering window is too small for it to happen. It also shows the effects of too much heat that can cause the surrounding polymer powder of the heat focus to reheat to a molten state preventing a high-resolution output. This is called lateral growth. Also, specific to MJF, as the materials fuse to form the object, there is some compression within the powdered layers that cause a 'dip' on the top surface.

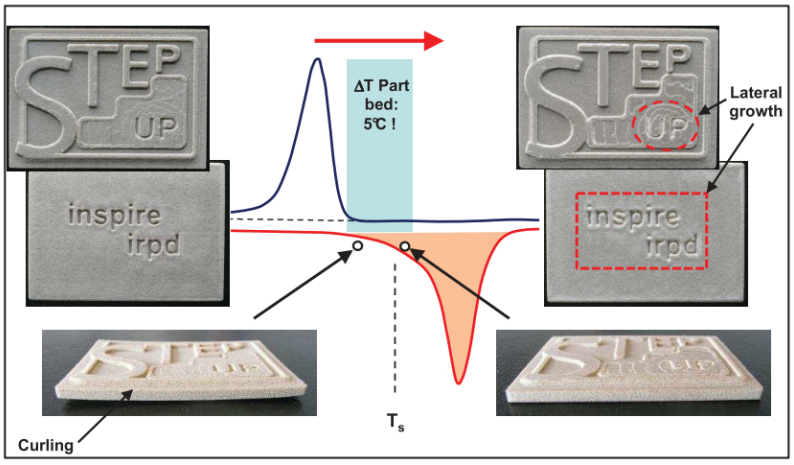

Figure 16: SLS anomaly due to small 'sintering window': curling or lateral growth

Moreover, different print orientations produce different surface textures. Figure 17 depicts the surface roughness values and surface profiles for the top, front, and side surfaces of the PA11 and TPU specimens. The PA11 specimen's

front and side surfaces were noticeably rougher than the top surface. The rougher front and side surfaces are the result of surrounding powder adhering to the specimen. The surface roughness of the PA11 specimens was lower on all surfaces than that of the MJF-printed PA12 specimens(Cai *et al.*, 2021; Petzold *et al.*, 2019).

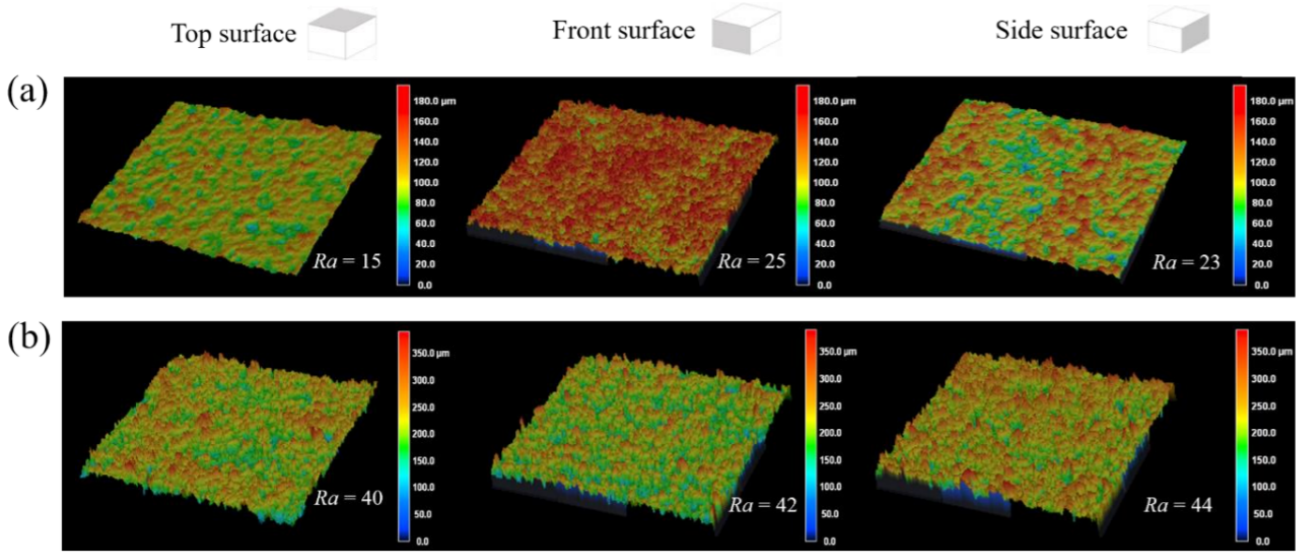

Figure 17:Surface roughness profiles of specimens: (a) PA11 and (b) TPU (Tey et. al. , 2021)

These processes discussed above can also introduce various anomalies to the printed objects due to several factors (external and internal). External factors such as running out of printing material, machine failure or extruder jam can cause print failures. Whereas internal factors are those that can influence surface roughness and introduce anomalies to the print. These internal factors or parameters can be manipulated to deliberately introduce anomalies to the print. The source of these anomalies can be divided into 3 categories (Pérez *et al.*, 2018):

- Material: temperature, viscosity, density, type of material, and mechanical properties.
- Platform: temperature, pressure, vibrations, the position of the platform, position of the extruder, system coordinates, and heat evacuation.
- Printer head: speed, angle of inclination, diameter of extrusion, vibration, and acceleration.

Some of these anomalies can even lead to defects as they render the objects completely unusable, which is undesirable. In FDM printing, sudden oscillating movement of the printer head may result in visible vibrational anomalies (Figure 18). These anomalies can still be acceptable, depending on the use case. But some anomalies as shown in Figure 19, more commonly lead to defective objects. Overheating the filament changes its viscosity and reducing the flow rate of the filament leads to poor adhesion of the layers.

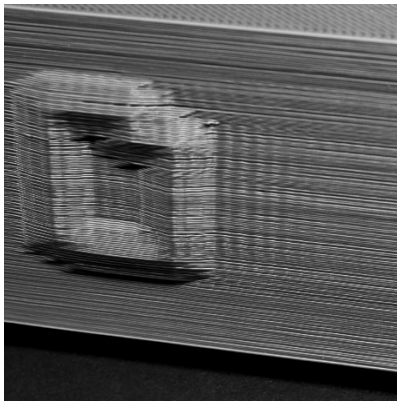

Figure 18: Anomalies due to Vibrations

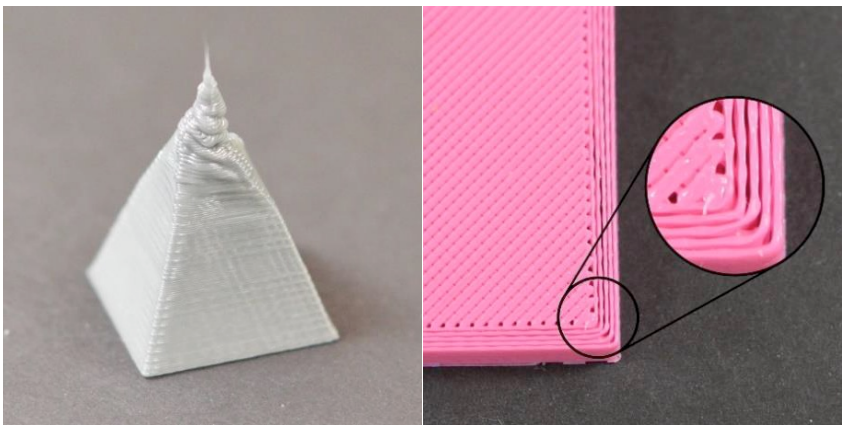

Figure 19: Defect due to over-heating and under extrusion respectively

All of these anomalies described were due to internal factors. Internal factors that can be set or modified by the user can cause certain desired effects on the parts. (Simplify3D, 2018) has identified 41 such anomalies and their sources; out of which only 18 are caused due to external factors. Table 15, in APPENIDX, shows all the types of anomalies that can occur in the identified printing processes due to internal factors and their sources.

Summary

Objects from different printing technologies can be usually easily identified by observing the part but certain printer parameters influence the surface finish slightly which can't be observed by the naked eye. Even subtle changes, such as changing the object orientation during print can alter the roughness of the surface (Myshkin *et al.*, 2003). For example, by manipulating the extrusion rate on a FDM printer, we can create micro pores between the layer lines that are only visible under a microscope (Gordeev, Galushko and Ananikov, 2018). Also, notice that some of the anomalies are unique to a particular printing technique. Along with certain intrinsic properties of the surface, these anomalies can also help us understand the limitation of our deliberately introduced patterns and determine a unique signature for the printing technology.

These unique surface features introduced on the surface, along with widely varying printing parameters, can help determine a unique surface signature that can be used for authentication of the object, not just the printing technology. This requires a capture method that can meet our requirements of being able to capture their intricate surface features.

3.2. Capture Methods

To authenticate 3D-printed objects accurately, it's essential to capture their surface data precisely. This section reviews commercial state-of-the-art techniques for capturing 3D surfaces at both macro and micro scales. The resolution of capture is determined by the print resolution of 3D-printed objects, and the analysis spans the range as per the research scope mentioned in Section 2.3, with systems evaluated based on their output resolution and capture speed.

3D sensing methodologies vary depending on the desired level of detail and field of view. While the market offers a variety of systems with improved accuracy, validated independent studies corroborating these claims, particularly under conditions similar to those specified in this study, are limited. This review seeks to close that gap by providing an in-depth examination of available technologies and their applicability in the precise authentication of 3D-printed artefacts.

3.2.1. Non-Contact Methods

Micro-scale

Multi-focus 3D Microscopy: This technique combines multiple images taken at different focus depths to create a detailed 3D model of the surface. With z-accuracy as high as 2 µm and an x-field of view up to 1 mm, Multi-focus 3D Microscopy is ideal for examining microscale features on surfaces, offering unparalleled detail for research and quality control in materials science and microfabrication(Zamofing and Hugli, 2004).

White Light Interferometry: White Light Interferometry utilizes the interference pattern of light to measure surface topography. It offers a z-accuracy range from 0.01 to 10 µm and a narrow x-field of view (0.2 to 2 µm), suitable for capturing high-precision surface measurements. This method is widely used in semiconductor inspection, micro-electromechanical systems (MEMS), and other applications requiring nanometric precision.

Confocal Microscopy: Confocal Microscopy provides high-resolution images by using a pinhole to eliminate out-of-focus light in specimens that are thicker than the focal plane. It achieves a z-accuracy of 0.05 to 1 µm across an x-field of view ranging from 0.2 to 40 µm. Confocal microscopy is essential for detailed analysis of live cells, microstructures in materials science, and complex surface geometries(Krzewina, 2006).

Micro-scale non-contact capture techniques, as summarized in **Error! Reference source not found.**, offer the precision and resolution essential for analysing the intricate details of microstructures. Each method serves different but complementary roles in micro-scale analysis, from providing a broad overview with Multi-focus 3D Microscopy, achieving high precision with White Light Interferometry, to delivering depth-resolved images with Confocal Microscopy. These methods enable the extraction of unique surface signatures necessary for the authentication of 3D-printed objects at a microscale, underscoring the critical role of advanced imaging techniques in modern manufacturing and quality assurance processes.

Table 4: Rough example specifications of range imaging systems suited for microvision (Hügli and Mure-Dubois, 2006)

Method	Multi-focus 3D microscopy	White light interferometry	Confocal microscopy
z-accuracy	2 µm	0.01-10 µm	0.05-1 µm
x-field of view	1 mm	0.2-2 µm	0.2-40 µm

Macro-scale

Stereo Vision: Stereo Vision involves using two or more cameras to capture the same scene from slightly different angles. The differences between these images are used to reconstruct a 3D scene by identifying corresponding points between the images. The z-accuracy of Stereo Vision systems varies with the square of the distance to the object (z^2), offering a field of view typically between 0.1 to 10 meters. This method is highly versatile and can be adapted to a wide range of applications, from industrial inspection to virtual reality(HP Labs, 2017).

Structured Light (SL): Structured Light systems project a known pattern onto the surface of an object. By observing the deformation of this pattern from a different angle, the system can calculate the 3D shape of the object. The accuracy of SL systems can reach 0.1 to 10 mm in the z-direction, with a field of view similar to that of stereo vision systems. SL is particularly effective for detailed and complex surfaces, providing high-resolution data suitable for quality control and reverse engineering applications (Rubinsztein-Dunlop *et al.*, 2017).

Photometric Stereo: Photometric Stereo estimates the surface normals of objects by observing the changes in appearance under different lighting conditions. This method can infer detailed surface textures and shapes, offering variable z-accuracy that depends on the distance squared (z^2). With a field of view ranging from 1 to 10 meters, Photometric Stereo excels in capturing subtle surface details across a wide area, making it invaluable for texture analysis and material identification(Woodham, 1978).

Each macro-scale non-contact capture method offers unique advantages, with Stereo Vision providing broad applicability, Structured Light delivering high-resolution details, and Photometric Stereo excelling in surface texture analysis. The selection of a specific technique depends on the requirements of the application, considering factors such as the desired level of detail, the complexity of the surface, and the size of the object to be scanned. These methods, summarized in **Error! Reference source not found.**, represent the forefront of macro-scale 3D data capture, facilitating accurate and detailed analysis for authentication and other applications.

Table 5: Rough example specifications of range imaging systems suited for macrovision (Hügli and Mure-Dubois, 2006)

Method	Stereo Vision	Structured Light (SL)	Photometric Stereo
z-accuracy	Varies with z^2	0.1-10 mm	Varies with z^2
x-field of view	0.1-10 m	0.1-10 m	1-10m

3.2.2. Contact Methods

Touch Probe Scanning: Touch Probe Scanning involves physically touching the object's surface with a probe to measure its geometry. This method, known for its high accuracy, is widely used in manufacturing for quality control and inspection. However, it can be time-consuming and may not be suitable for delicate or highly detailed surfaces due to the risk of damaging the object(Leach *et al.*, 2017).

Atomic Force Microscopy (AFM): Atomic Force Microscopy offers unparalleled resolution by scanning a surface with a fine-tipped probe. AFM is indispensable for nanoscale surface analysis, providing critical insights into material properties, molecular arrangements, and surface irregularities. Although it offers exceptional resolution, AFM is limited by slow scanning speeds and small coverage areas, making it less practical for large-scale or rapid authentication processes(Myshkin *et al.*, 2003).

3.2.3. Technological Limitations and Breakthroughs

The quest for accurate surface data capture in 3D-printed object authentication has led to the exploration of both contact and non-contact methods. Recent studies have highlighted the importance of considering local surface roughness variability, as stated by Pérez et al. (2018), which presents both challenges and opportunities in producing unique surface signatures for authentication.

There have been significant advances in non-contact methods. Yu and (2013) demonstrated the use of a structured light system (SL) with grey code and phase-shifting techniques to achieve a resolution of 100 µm (Yu and Wang, 2013). Yin et al. (2015) furthered this approach with a 3D microscopic SL system capable of similar resolution (Yin *et al.*, 2015). However, the work by Li et al. (2016) pointed out challenges in capturing microscale data using photometric stereo, particularly with reflective surfaces (Li *et al.*, 2016). These advancements underscore the importance of choosing the right non-contact method based on the specific requirements of surface texture and geometry.

For contact methods, technological limitations and breakthroughs are equally crucial. Touch Probe Scanning, while highly accurate, faces limitations in speed and potential surface damage. Atomic Force Microscopy (AFM) provides exceptional resolution but is hampered by slow scanning speeds and limited coverage areas. Recent innovations aim to address these limitations. High-speed AFM systems and more sensitive touch probes are being developed to enhance efficiency and applicability(Vora and Sanyal, 2020). The integration of automated scanning systems with adaptive force control is another promising advancement, potentially making Touch Probe Scanning suitable for a wider range of materials.

Adding to the advancements in contact methods, Ramya T. N and Veena M B (2020) explored Polynomial Coefficient-based authentication for 3D fingerprints, offering a dynamic matching rate and addressing some limitations of traditional contact-based recognition methods. This approach uses a 3D database and mathematical morphology for minutiae point extraction, providing a novel direction in the authentication of 3D-printed objects by leveraging unique fingerprint patterns (N and M B, 2020).

Furthermore, Lishchenko et al. (2022) conducted a study comparing contact (R130 roughness tester) and non-contact (LJ-8020 laser profiler) methods for determining surface irregularities on 3D printed parts. Their research highlights

the efficiency of online monitoring for 3D printing quality and suggests diagnostic features for identifying defects, indicating the importance of precise surface quality assessment in authentication processes(Lishchenko, Piteľ and Larshin, 2022).

Time-of-flight cameras, commonly used in 3D computer vision, traditionally exhibit lower accuracy, ranging from 1mm to 1cm, which is often inadequate for detailed authentication purposes. However, recent breakthroughs in computational imaging, such as the implementation of deep learning-based systems with time-of-flight cameras (Suo et al., 2021), offer new possibilities for capturing high-resolution 3D data.

In summary, the dynamic field of 3D data capture is experiencing rapid advancements in both contact and non-contact methods. The ongoing development of these technologies is enhancing their accuracy, efficiency, and applicability, thereby potentially improving the authentication process's performance for 3D-printed objects. As these technologies continue to evolve, they promise to provide more reliable solutions for capturing the unique surface signatures essential for effective authentication.

Summary

The exploration of capture methods for authenticating 3D-printed objects emphasizes the essential role of non-contact technologies in achieving precise and unintrusive surface data acquisition. These methodologies are especially conducive for this research, highlighting their effectiveness in capturing detailed structural and geometric characteristics without compromising the object's integrity. Non-contact methods, including Multi-focus 3D Microscopy, White Light Interferometry, Confocal Microscopy for micro-scale, and Stereo Vision, Structured Light (SL), Photometric Stereo for macro-scale analysis, stand out for their ability to accurately record the complex surface textures necessary for robust authentication processes.

According to Straub (2018), using surface data, which includes both inherent and intentionally introduced properties, serves as a foundation for extracting and analysing unique features required for authentication. This approach emphasises the importance of comprehensive surface characterization in developing effective authentication frameworks for 3D-printed objects.

Furthermore, advances in computational imaging technologies, such as deep learning applications in time-of-flight cameras, point to potential improvements in the efficiency and accuracy of non-contact capture techniques. This is

supported by contributions from researchers such as Pérez et al. (2018), Yu and Wang (2013), Yin et al. (2015), Li et al. (2016), and Suo et al. (2021), who collectively shed light on the dynamic evolution of 3D data capture technology and its critical application in 3D-printed object authentication.

In conclusion, non-contact methods are deemed most suitable for this research due to their non-invasive nature and ability to deliver the high-resolution data required for analysing and interpreting surface textures and features for authentication. This selection leverages surface data's rich structural and geometric attributes, whether naturally occurring or deliberately introduced, to establish a sound basis for developing a robust authentication framework for 3D-printed objects. The ongoing advancements in non-contact capture technologies not only aim to refine the authentication process's precision and efficiency but also highlight the critical role of innovation in advancing the fields of 3D printing and object authentication.

3.3. Surface Feature Extraction and Texture Analysis

This research aims at identifying reliable and repeatable surface features that occur during the AM processes. These surface features need to be invariant to translation and rotation and skewness. Studies specific to AM authentication will be discussed in Section 4. In this section, we review recent advances in surface texture analysis methods. The technique must be robust enough to identify anomalies that form the watermark on the surface and characterise the surface including the glyph to derive a unique signature of the surface. There are four major issues in texture analysis (Materka and Strzelecki, 1998):

1) Feature extraction: to compute a characteristic of a digital image able to numerically describe its texture properties.
2) Texture discrimination: to partition a textured image into regions, each corresponding to a perceptually homogeneous texture (leads to image segmentation).
3) Texture classification: to determine to which of a finite number of physically defined classes (such as normal and abnormal texture) a homogeneous texture region belongs.
4) Shape from texture: to reconstruct 3D surface geometry from texture information.

Feature extraction is the first stage of texture analysis followed by watermark identification. Watermark identification using texture analysis can be categorised into three different approaches: Statistical; Structural; and Filter-based. Below is a critical evaluation of each of these approaches in recovering the surface:

3.3.1. Structural Approach

Structural approaches represent texture by characterising texture elements, this is done with the detection and composition of several simpler texture structures at the microscale.

Early studies by Tuceryan and Jain (1993) proposed a structural approach to identify anomalies in textile images. The study used a histogram analysis to threshold the captured image and then a data structure was mapped which represented the skeleton structure of the texture. It used the texture of a known good surface to compare with the captured image to detect anomalies. This method is slow and computationally expensive as compared to a new system configuration proposed by Abouelela *et al.* that detected structural anomalies by implementing simple

statistical features (mean, variance, median) to 3D depth data (Abouelela *et al.*, 2005). The results indicate that the system can detect flaws which vary drastically in physical dimension and nature with a very low false detection rate.

Structural approaches are only reliable in segmenting anomalies from texture whose pattern is very regular. This method could be useful to obtain a geometrical fingerprint of the surface. Often these methods are used in conjunction with statistical approaches.

3.3.2. Statistical Approaches

In contrast to structural methods, statistical approaches do not attempt to understand explicitly the hierarchical structure of the texture. Instead, they represent the texture indirectly by the non-deterministic properties that govern the distributions and relationships between pixel values.

Histogram statistics of these distributions are the most used in this approach. Despite their simplicity, histogram techniques have proved their worth as a low computational cost, low-level approach in various applications (Madrigal *et al.*, 2017; Hou *et al.*, 2015; Chen and Bhanu, 2007; Wang, Zha and Cipolla, 2006). They are also invariant to translation and rotation. Commonly used histogram statistics include range, mean, geometric mean, harmonic mean, standard deviation, variance, and median. However, the reliability of these methods is low in characterising the surface uniquely (Hanbay, Talu and Özgüven, 2016).

3.3.1. Filter-Based Approach

Filter-based approaches are implemented by applying filter banks on the image and computing the intensity of the filter responses. The methods can be divided into time domain and frequency domain.

In the time domain, the images are usually filtered by gradient filters to extract edges, lines, isolated dots, etc. Sobel, Canny, and Laplacian filters have been routinely used as a precursor to measure edge density. (Kumar and Pang, 2002) used linear finite impulse response (FIR) filters to detect anomalies in fabric by comparing the filter responses from regions with anomalies to anomaly-free regions. Following the trend of combining two different approaches, (Zhao et.al., 2008) presented an extension to Local Binary Pattern (LBP) by enhancing images by using a Sobel filter(Sobel and Feldman, 1990). Whilst these techniques can still be useful, on complex, irregular textures, the textures are often too noisy to discern anything of use without using techniques to remove unwanted high-frequency features.

In the frequency domain, the image is transformed into the Fourier domain, multiplied with the filter function, and then re-transformed into the spatial domain saving on the spatial convolution operation. Ring and wedge filters are some of the most used frequency domain filters (Xie, 2008). A ring filter, being a symmetric band-pass filter, can reveal the distribution of texture's energy across the frequency domain and measure its roughness. A wedge filter can help evaluate the directionality of the image. In the original study presented in 1985, seven dyadically spaced ring filters and four wedge-shaped orientation filters for feature extraction (Coggins and Jain, 1985). Also, in studies by (Ferez, Silvestre and Munoz, 2004; Chiu *et al.*, 2002), although they used frequency domain to successfully defect anomalies, no evidence was provided for the reliability of the methods. But as the Fourier domain is only affected by the change in the structure of the surface, it is very suitable for real-time or high-speed applications (Hanbay, Talu and Özgüven, 2016).

Since the Fourier coefficients are depending on the entire image, the Fourier transform is not able to localise the defective regions in the time domain. The classical way of introducing time dependency into Fourier analysis is through the windowed Fourier transform. Gabor filters are used to detect anomalies using this principle. Gabor filters are used to analyse textures in both time and frequency domain (Tong, Wong and Kwong, 2016; Chen and Chen, 1999; Randen and Husøy, 1999). This method obtained a high true detection rate for surface anomalies. It can extract the outstanding features of all anomalies when tuned properly. However, since the Gabor filters are rotation-based filters, they are vulnerable to the rotational transforms of the images.

Summary

The surface characterisation is a crucial step in this research to obtain a unique signature. As observed in this section, every approach has certain drawbacks. And most of the implementations mentioned are a combination of at least two approaches. The main purpose of implementing these approaches is to be able to minimise the computational complexity and increase the rate of anomaly detection. The statistical approaches will be tested to obtain surface texture while the structural approach would be tested to obtain a geometrical fingerprint of the surface. This allows us to obtain a PUF of the surface. Findings from these tests would help develop a novel approach to authenticate 3D-printed parts using the derived unique signature obtain from the glyph and the watermark surrounding it.

4. Security in AM and Authentication of 3D-printed surfaces

Additive manufacturing (AM) or 3D printing is especially vulnerable to cyberattacks due to its reliance on digital files and connectivity. This impacts multiple parties throughout the supply chain. There is still no universal solution to solve all cyber security issues in AM industry. Cyber and cyber-physical attacks on the AM process can happen at any point in the process. So far, the three major categories of attack identified in AM are (Yampolskiy *et al.*, 2018):

- Theft of technical data
- Part sabotage
- Illegal part manufacturing.

Figure 20 illustrates the possible targets of AM sabotage, which include the manufactured object, the AM equipment, and the environment. It also shows various attack methods and their feasibility, with a focus on how part sabotage and illegal part manufacturing can affect each component of the AM process.

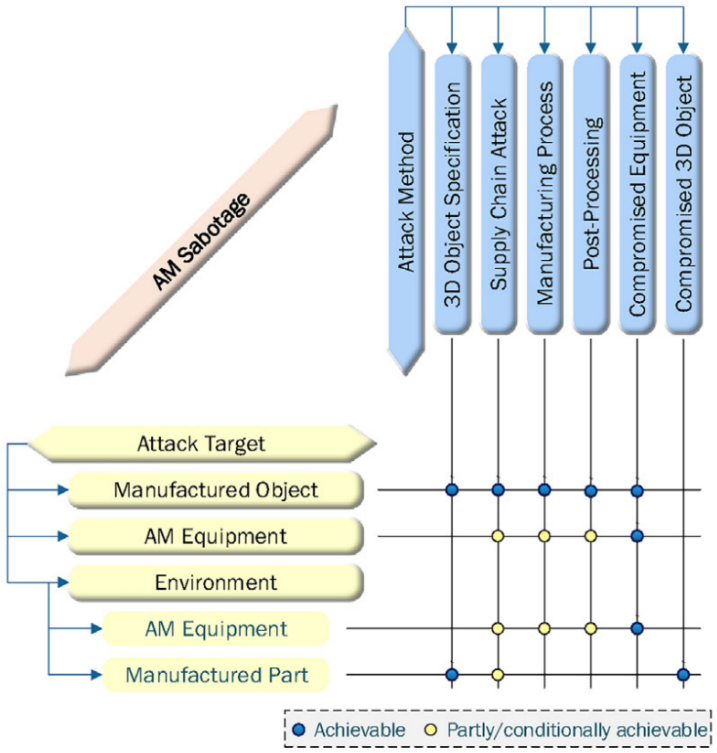

Figure 20: AM sabotage, correlation between attack methods and attack targets (Yampolskiy et al.*, 2018)*

Under the scope of this research, we would be concentrating only towards the countermeasures for part sabotage and illegal part manufacturing postproduction. Part sabotaging target's part manufacturing by either reducing the mechanical strength or the fatigue life of the part. Whereas illegal part manufacturers would attempt to replicate

the part by scanning, which can indirectly present similar issues as part sabotage. Then these parts enter the supply chain due to a break in custody and end up with the customer (Figure 21).

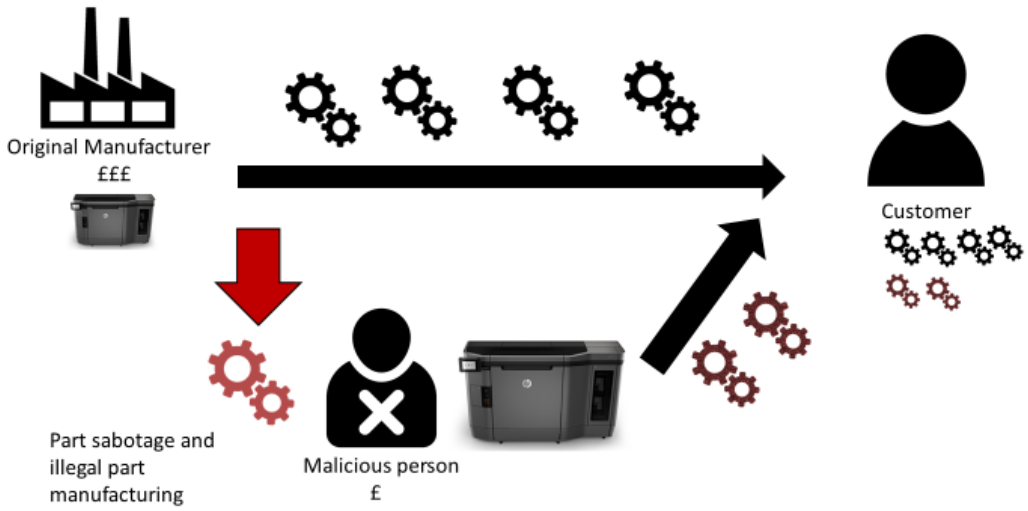

Figure 21: Adulterated AM supply chain

To countermeasure these adverse scenarios, several authentication methods for 3D-printed objects have been presented in recent times. Most 3D-printed authentication methods currently published have accomplished this by relying completely on certain specific additional information added to the part during manufacturing. These methods can be classified into two categories: Watermarking-based (Peng, Yang and Long, 2019; Straub, 2015, 2017, 2018; Chen, Mac and Gupta, 2017; Hou, Kim and Lee, 2017; Zeltmann *et al.*, 2016; Hou *et al.*, 2015) and Special material-based authentication.

4.1. Authentication Methods in Additive Manufacturing

This section will address the principal categories of authentication systems, defining their general principles and highlighting the differences between them.

There are two broad classifications for 3D-printed object authentication methods:

- **Watermarking-based strategies**: During the manufacturing process, these strategies entail embedding secret information or patterns within the 3D-printed object. This concealed information can be extracted for authentication purposes in the future. Blind (uninformed), non-blind (informed), and side-informed detection approaches differ in the quantity and type of information necessary for authentication.

- **Material-based approaches**: These methods involve the incorporation of materials or substances into the 3D-printed object, so establishing a unique, difficult-to-replicate signature. Incorporating quantum dots or chemical fingerprints into an artefact are examples of material-based techniques. For authentication, these approaches frequently require specialist equipment or procedures, such as spectrometry.

Each of these categories has advantages and disadvantages, and the choice of authentication technique may rely on the specific security requirements of the AM application, the complexity of the 3D-printed object, and the availability of authentication resources (e.g., specialised equipment or software). By studying the various approaches to AM authentication, researchers may better identify research gaps and develop new, more effective techniques for ensuring the security and integrity of 3D-printed parts.

With this overview in mind, the next sections will address the advantages, shortcomings, and future research possibilities of watermarking-based (Section 4.1.1) and material-based (Section 4.1.2) authentication approaches.

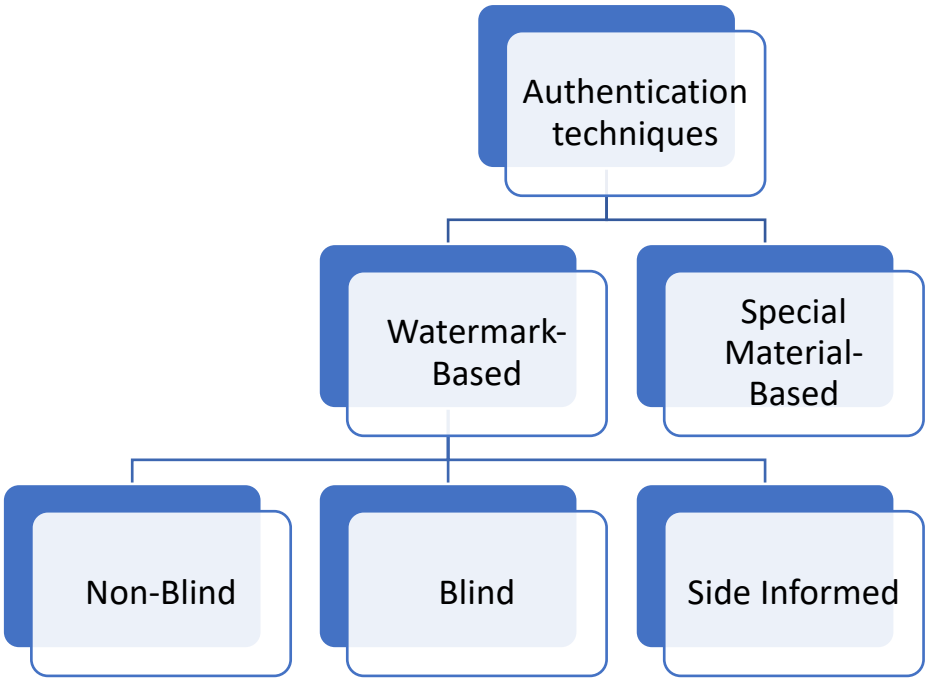

4.1.1. Watermarking-Based

Watermarking is the process of secretly embedding information. Authentication is done by retrieving this secret information using various means. This can be further distinguished between three categories (Macq, Alface and Montanola, 2015)

1) Blind (uninformed authentication): The watermark is decoded without the need for the original model. The watermark contains all the information required.
2) Non-Blind (informed authentication): The knowledge or the embedded algorithm to retrieve the watermark is not enough information. Prior knowledge of the original model is required to complete authentication.
3) Side-informed: Side-informed detection is a stage between the blind and the non-blind scenarios, where the original shape of the object is not needed on detection but only some information related to it.

Blind detection

Hou et al. (2017) proposed an improved blind 3D model watermarking system that is both robust to the 3D printing process, and invariant to the object itself (Hou et. al., 2017). The system relies on a z-axis-invariant watermarking algorithm and a print-axis estimator (Figure 22). The watermark is formed by distorting the model along the z-axis and printing the distorted model. The watermark is then retrieved from the surface on the same axis. The authors tested the robustness of the system against a variety of deformations, including noise introduced as a normal part of printing and scanning objects, and common post-processing steps such as painting or sanding. Across three printers and multiple models, the scheme produced varied results. The author observed that the model characteristics such as size and scaling could reduce detection accuracy, as could higher-resolution printing. Moreover, it does not work well with 3D models featuring complex surfaces, sharp edges, and piecewise planar portions.

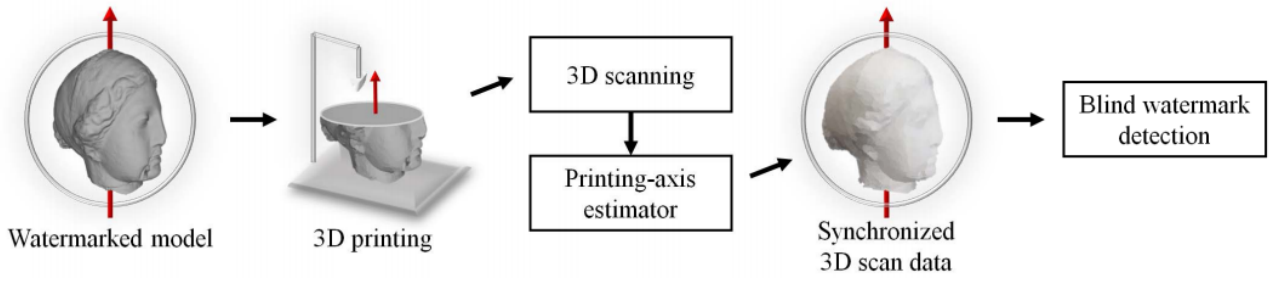

Figure 22 Blind watermarking for FDM printing (Hou et al., 2017)

Chen,et. al. (2017) and Zeltmann et al., (2016), proposed to incorporate into the design file some physical features that, if processed and printed with a specific combination of parameters, will result in a high-quality part; any other combination of parameters will result in a defective part or of inferior quality that can even lead to a failure in part. Another benefit to this protection method is that it does not leave a visible mark on the part.

Straub (2015, 2017, 2018) explored image-based fault detection and security for FDM 3D printing by comparing pixel values from images captured at five different angles to track the progress during printing. Even though it is a very good inspection system, the author admits, its manual operation means that it is not a very robust authentication system as it relied on human intervention to identify issues in those images that are flagged by the system. Also, this technique can only provide security during the print process. It doesn't provide any means to prevent illegal parts from entering the supply chain.

And Wu et al., (2017) proposed to use a combination of feature extraction techniques on 3D grayscale images. For each section of captured images, the following features are extracted using a stereovision camera: the mean of grayscale, the standard deviation of grayscale, and the number of pixels whose grayscale is larger than 120. To detect an attack on the part, the authors evaluate machine learning algorithms: k-Nearest Neighbor (kNN) and random forest. Using just a static camera, the author was able to achieve 96.1% accuracy for authentication using anomaly detection. But this method is not robust as it is only able to achieve that accuracy if there is no variation in skewness or changes to scale.

Pham et al., (2018) proposed a watermarking technique using Menger facet curvature and K-means clustering. The facets of the model clustered into groups based on the Menger curvature. The Menger curvature of each group is then used to compute the embedded watermark (Figure 23).

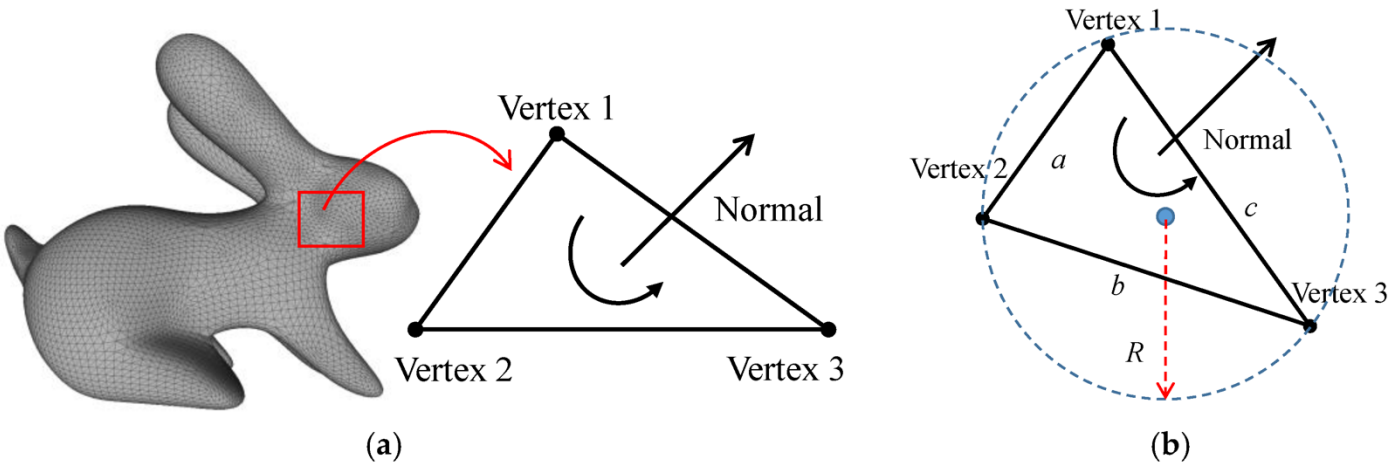

*Figure 23 Watermarking using Menger facet curvature (*Pham et al., 2018)

Taking a different approach, (Suzuki *et al.*, 2015, 2017; Silapasuphakornwong *et al.*, 2016) through a series of publications, proposed various methods to embed a watermark just below the top surface by forming fine cavities. The variation between all the approaches proposed is the authentication technique. Various non-destructive

extraction techniques are proposed to read the watermark namely, thermal photography(Suzuki *et al.*, 2015, 2017), thermal videography and Near-infrared.

To make the process a bit more difficult to replicate, Chen et al. (2019) implemented a QR code embedded within the layers of the part. This exploded view of the watermark was much harder to replicate as it would only decode when viewed from the correct angle. The information stored in the QR code can only be retrieved by using a CT image of the layers to retrieve information making it unfeasible for mass production use (Figure 24).

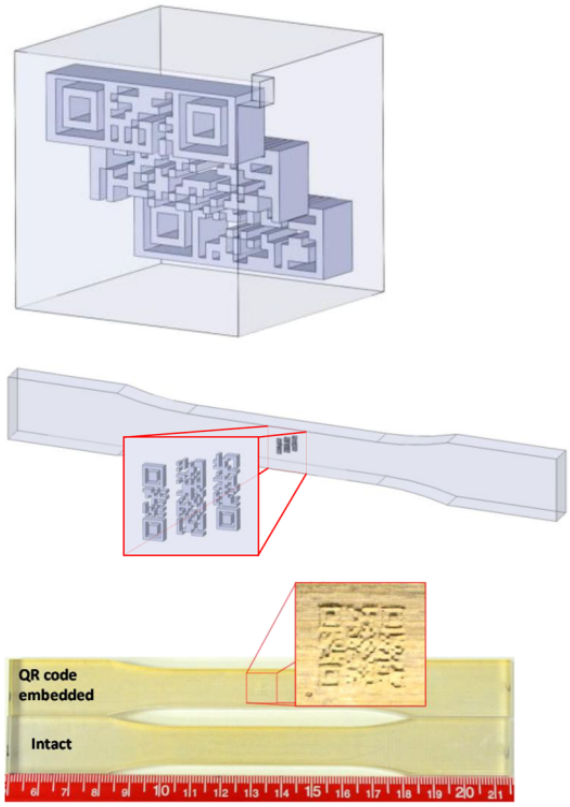

Figure 24: Embedded QR code(Chen et al.*, 2019)*

Blind watermarking has various practical advantages over non-blind approaches, as it is not necessary to know every 3D-printed object's corresponding key. These approaches are also simple to build and robust in detection; however, blind detection poses a greater challenge to the watermarking scheme and reduces its resilience relative to non-blind methods when features are not maintained. Furthermore, because these watermarks are static for all printed goods, an attacker can readily acquire and copy them.

Lastly, Liu et al., (2021) proposed a watermarking scheme based on wavelet transform, which can be embedded in 3D-printed objects without affecting their visual appearance. The authors employed the lifting wavelet transform

and singular value decomposition techniques to incorporate a watermark into the 3D model. The method that has been put forward exhibits' resilience against a range of attacks, including but not limited to the addition of noise, mesh simplification, and mesh smoothing. Nevertheless, this approach exhibits limitations in its ability to address intricate forms of attacks such as remeshing and object cutting.

In conclusion, blind detection watermarking techniques provide a level of security for 3D-printed things by embedding secret data within the product without requiring the original model. Although these approaches can be robust and simple to deploy, their resilience is compromised when characteristics are not preserved, and the watermark's static nature makes it susceptible to reproduction by attackers. In order to increase the security and authentication of 3D-printed products, researchers continue to investigate and create innovative watermarking techniques.

Non-Blind Detection

Peng et. al., (2019), proposed a method to model the observational and printing noise of an authentication mark printed on the surface to generate a digital signature at the microscale (Figure 25). The signature is captured and saved as a private key during the registration and later a public key is shared with the clients for verification. The method claims an accuracy of 100% but shows vulnerability to post-processing attacks such as polishing because it analyses and detects the markers in a 2D image.

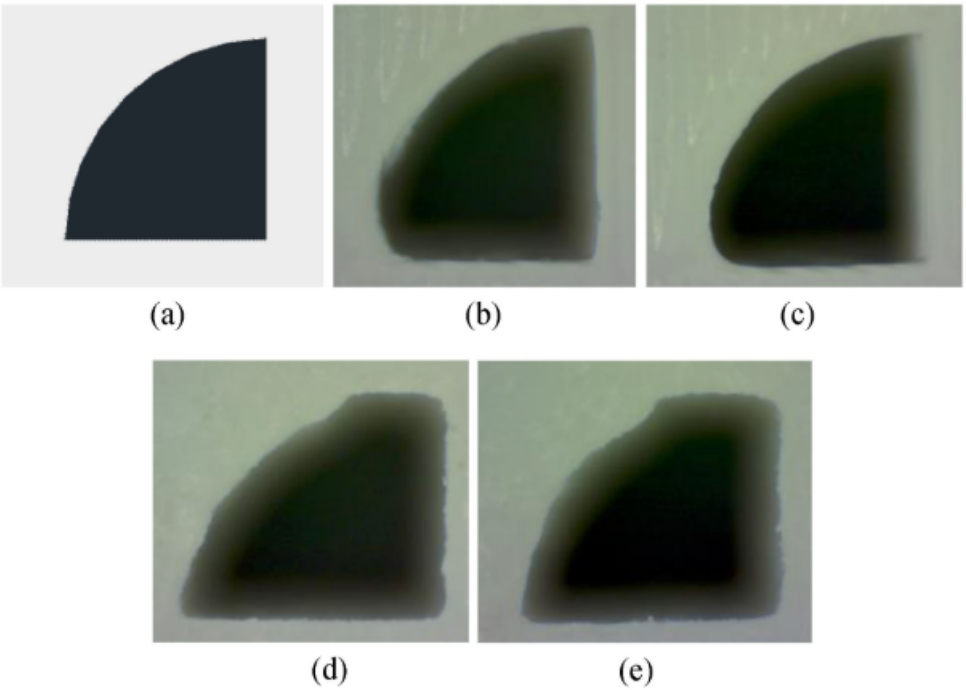

Figure 25 (a) Designed authentication mark. (b) One captured mark was printed by a FDM printer. (c) Another captured mark was printed by UnionTech RSPro 600. (d)One captured mark was printed by UnionTech Lite 600. (e) Another captured mark printed by UnionTech Lite 600
(Peng, Yang and Long, 2019)

Hou et al. (2015) presented a watermarking method that can survive the 3D printing and 3D re-scanning process. A normal vector in the x-y plane of each layer of the model mesh is modified to a reference pattern which has been rotated by some degree around the object. The verification of this watermark is done by scanning the surface of the model which results in a histogram of the features. That histogram is then compared with the reference pattern for authentication. However, this method has some limitations. The author concluded by mentioning how changing the print orientation will skew the authentication watermark and prevent the algorithm from verifying the required information.

Yamazaki et al., (2014) proposed one of the first authentication methods for 3D-printed objects. A watermark is embedded in the spectral domain of the 3D CAD using an informed algorithm based on the spread spectrum technique. The paper focused on the extraction technique of this embedded watermark and mentioned that the technique proposed is encoding agnostic. The watermark extraction is done by reconstructing the 3D surface mesh from the object and matching the surface to the model.

The authors of the study (Gao *et al.*, 2021) introduced a non-blind watermarking technique for 3D-printed objects that relies on Laplacian mesh optimisation. The technique incorporates the watermark into the high-frequency

elements of the Laplacian mesh, which exhibit reduced susceptibility to prevalent forms of tampering such as mesh simplification, smoothing, and noise injection. The approach additionally exhibits significant resilience to 3D printing and scanning procedures. Nonetheless, it is possible that the system may not possess the capability to effectively manage intricate forms of attacks such as remeshing and object cutting.

Since these methods are non-blind, both the embedding and extracting steps can only be performed by the owner of the original 3D mesh with complete access to the secret data. This allows each part printed to have a unique watermark/identifier. Non-blind detection methods offer increased security compared to blind detection methods because of the need for the original model and secret data for watermark extraction. However, these methods can also be more complex to implement and may still have vulnerabilities, such as susceptibility to post-processing attacks. Researchers are continually working on developing and refining non-blind detection methods to improve the security of 3D-printed objects.

4.1.2. Material-Based

Besides watermarking 3D-printed objects, the use of special or blended materials into 3D-printed objects is another method to prevent counterfeiting[2]. Quantum Materials Corporation (QMC) announced that they have patented the process of embedding quantum dots into 3D objects to detect counterfeit parts. The quantum dots are embedded in such a way that they create an unclonable signature (Heidi, 2014; Clare, 2016).

Also, InfraTrac developed a process to embed a unique chemical fingerprint into 3D-printed objects (Michael, 2023). The technology allows for products to be marked in a way that is nearly impossible to fake so that they can be authenticated at any time with a simple spectrometer. Both these methods are prohibitively expensive to be implemented on a mass scale.

By embedding unique materials or substances, such as quantum dots or chemical fingerprints, within the product, material-based authentication methods offer an alternative method for protecting 3D-printed items. This provides a signature that is unique and difficult to copy, which can be used for authentication. The primary disadvantage of these technologies, however, is their high cost, which makes them unfeasible for widespread use in mass-produced

[2] https://3dprint.com/7701/quantum-dots-3d-print/

items. Despite the cost, material-based authentication approaches continue to be investigated as a potential alternative to watermarking schemes, and academics are attempting to identify more cost-effective material-based ways for protecting 3D-printed products.

Summary

Authentication in AM is still a very developing field, but we see from this section that none of the authentication methods so far have used any 3D depth data to authenticate except for the study done by (Hou et al., (2015). Even this had a lot of limitations. Wu et al., (2017) does implement the use of anomalies but only uses 2D vision approaches to authenticate. There has not been any research so far that implements any 3D capture methods reliably for authentication and none that implements 3D capture methods at the microscale for authentication purposes.

2D extraction of surface features extraction approach requires robust feature extraction from micro textured surfaces and accurate 2D-3D registration for mapping that is practically impossible for non-blinded approaches (Yamazaki et al., 2014).

Most of the techniques mentioned above have tried to avoid using a 3D scanning tool for authentication. In theory, a 3D capture from an inexpensive 3D capture system would be sufficient to recover a watermark when using watermarking techniques such as Peng et al., (2019) or Pham et al. (2018) Even though both methods present very high robustness, and it is difficult to speculate on the impact of a 3D capture system on these methods. A 3D capture of the surface would have provided a lot more detailed surface representation with higher efficiency as seen in (Pollard *et al.*, 2018). Also, the method proposed in this study i.e., the use of glyphs and watermarks along with the intrinsic surface characteristics to derive a unique signature of the surface, using combined data captured at macro and micro scale can further help with the accuracy of authentication. Further investigation would be carried out in this research to prove this.

4.2. Limitations and Gaps

Many constraints and gaps remain unsolved, despite the several authentication methods covered in this chapter. This section intends to highlight these shortcomings and identify research opportunities in AM security and authentication.

- **Dependence on 2D data**: The majority of current authentication techniques rely on 2D surface data or pictures, which may not capture the entire complexity and distinctive properties of 3D-printed components. This reduces the precision and resiliency of these methods, making them subject to forgery and sabotage.
- **Inadequate use of 3D capture methods**: While several studies (e.g., Hou et al., 2015) have attempted to employ 3D depth data for authentication, there is a dearth of studies on the reliable application of 3D capture methods, particularly at the microscale. Creating novel authentication methods that utilise 3D capture techniques may improve the precision and robustness of part authentication.
- **Vulnerability to post-processing attacks**: Several authentication systems, including the one presented by Peng et al. (2019), are vulnerable to post-processing assaults, such as polishing and sanding. This vulnerability could jeopardise the authenticity of authenticated components and open the door to counterfeiting and sabotage.
- **Limited application to intricate geometries**: Certain authentication methods have difficulty with 3D models with complicated surfaces, sharp edges, and piecewise planar parts. Future research should investigate approaches that may effectively authenticate complex part geometries, hence boosting the security of a broader range of AM applications.

By addressing these limitations and gaps identified, this study aims at developing more robust and effective authentication methods for AM, ultimately enhancing the security of the AM process, and protecting the integrity of 3D-printed parts.

5. Surface Fingerprinting Techniques

This section provides a comprehensive review of various surface fingerprinting techniques used for the authentication and identification of objects. These techniques can be broadly categorised into three sections: 2D, 3D, and statistical approaches. Each of these categories focuses on different aspects of surface features and leverages various methodologies to achieve accurate and robust surface fingerprinting.

5.1. 2D Surface Fingerprinting Techniques

2D surface fingerprinting techniques involve the extraction and analysis of 2D features from a two-dimensional representation of an object's appearance, such as may be captured by images. These techniques can be categorised

into three main sections: **Edge Detection** and **Texture Analysis** for feature extraction, and **Pattern Matching** techniques for representing or modelling the extracted features. In this context, Edge Detection and Texture Analysis are used to extract distinctive features from the surface of a 3D-printed object, while Pattern Matching techniques serve to model and represent the extracted features for identification and authentication purposes.

5.1.1. Image-based Techniques

Image-based techniques focus on analysing the visual information of an object captured in 2D images. They can be used to identify the overall appearance, shape, structure, and texture of the object, making them useful for authentication purposes.

Edge Detection: Edge detection techniques, such as Canny edge detection or Sobel operators, identify the boundaries between different regions of intensity in an image. The extracted edges can then be used to identify the presence of coded patterns or markers. However, these methods may be sensitive to noise and require careful parameter tuning to achieve optimal results. Edge detection techniques like the Hough Transform (Hough, 1962) and Contour Tracing can also be used to identify and extract more elaborate geometrical features, such as lines, circles, or other parametrised shapes. These methods can provide valuable information about an object's geometry, but their performance may be affected by the presence of noise and clutter in the image.

Elaborate geometrical features: Techniques such as Local Binary Patterns (LBP) (Shi et. al., 2020; Ahonen et. al., 2006; Ojala et al., 2002) and Gabor filters (Wang et. al., 2005) can be used to capture more complex local intensity variations and edge-like structures in the image. These methods can help in understanding an object's elaborate geometrical texture and surface characteristics but may require extensive feature selection and parameter optimization to achieve optimal results.

5.1.2. Texture-based

Texture analysis techniques focus on extracting and characterising repetitive patterns of features describing the surface properties of an object.

Glyph-based techniques: In the context of glyph-based texture analysis, the extraction of coded patterns or markers can be achieved through techniques such as Template Matching (Brunelli, 2009) or Feature-based Matching (Lowe,

2004), which seek to identify the presence of specific texture patterns in the image. However, these methods may be sensitive to changes in scale, rotation, and illumination.

Elaborate geometrical features: Techniques like Co-occurrence Matrix-based methods and Local Ternary Patterns (LTP) (Tan and Triggs, 2010) can be employed to capture more elaborate geometrical features related to the object's texture. These methods can provide valuable information about the object's surface topographic properties but may require extensive feature selection and parameter optimization to achieve optimal results.

Intrinsic surface features: Methods such as Wavelet Transform and Fractal Dimension can be used to analyse the object's texture and surface properties at different scales and resolutions. These methods can help in understanding the object's intrinsic surface features but may be computationally expensive and require careful parameter selection.

5.1.3. Pattern Matching (Glyph-based)

Pattern matching techniques involve comparing the extracted features to a database of known features to identify and authenticate objects.

Glyph-based techniques: For glyph-based pattern matching, techniques such as Template Matching (Brunelli, 2009) or Feature-based Matching (Lowe, 2004) can be employed to compare the extracted coded patterns or markers against a database of known patterns. These methods can provide robust and reliable identification, but their performance may be affected by changes in scale, rotation, and illumination.

Elaborate geometrical features: Techniques like Shape Context (Belongie et al., 2002) and Scale-Invariant Feature Transform (SIFT) (Lowe, 2004) can be used for pattern matching based on the extracted elaborate geometrical features. These methods can provide robust and invariant matching performance, even in the presence of changes in scale, rotation, and illumination. However, they may require extensive feature extraction and matching procedures, which can be computationally expensive.

Intrinsic surface features: Methods such as Histogram of Oriented Gradients (HOG) (Dalal and Triggs, 2005) and Bag of Visual Words (BoVW) (de Lima *et al.*, 2019) can be employed for pattern matching based on the extracted intrinsic surface features. These techniques can offer a compact and discriminative representation of the object's texture and surface properties, enabling efficient and accurate matching against a database of known features. However, their

performance may be affected by the choice of feature extraction and quantization methods, as well as the size of the feature vocabulary.

In conclusion, 2D surface fingerprinting techniques can provide valuable information about the object's overall shape, structure, texture, and other surface properties, potentially enabling efficient and accurate identification and authentication. By combining different edge detection, texture analysis, and pattern matching techniques, a comprehensive and robust solution for 2D fingerprinting be developed, catering to a wide range of applications, such as security, forensics, and manufacturing.

5.2. 3D Surface Fingerprinting Techniques

The process of 3D surface fingerprinting encompasses the retrieval and evaluation of 3D characteristics from three-dimensional depictions of an entity. The aforementioned techniques are capable of capturing both local and global geometric features of an object's surface, thereby facilitating a more comprehensive representation of its structure. The subsequent sections will provide a critical analysis of different 3D fingerprinting methods that utilise mesh-based, point cloud-based, and occupancy grid-based approaches. These techniques will be evaluated in relation to the security feature outlined in Table 1.

5.2.1. Mesh-based Techniques

Mesh-based techniques are utilised to depict the surface of an object by means of a set of interconnected vertices, edges, and faces. The aforementioned depiction enables a condensed and readily available spatial configuration; however, it may pose certain difficulties in extracting characteristics and managing topological disturbances. Some examples of mesh-based techniques include the method proposed by Gumhold and Macleod (2001), which is effective for extracting robust features from 3D surfaces, and the methods by Li et al. (2021) and Zhang et al. (2022), which focus on extracting mesh parameters using local and global descriptors, respectively. These methods have shown promising results for extracting robust features from 3D surfaces, but they are not without their limitations.

Glyph-based techniques refer to methods that utilise visual symbols or glyphs to represent data or information. These techniques are commonly used in data visualisation and information design to convey complex information in a clear and concise manner(Sola *et al.*, 2022). Glyphs can be used to represent a wide range of data types, including numerical values, categorical variables, and textual information. By using glyphs, data can be presented in a way that

is easy to understand and interpret, allowing users to quickly identify patterns and trends in the data. The integration of coded patterns or markers in the mesh structure or texture can be achieved through the use of mesh-based glyph techniques. Nevertheless, there are difficulties associated with the modification of conventional feature-based matching methodologies, such as SIFT and SURF, to suit 3D mesh data. It is therefore helpful to investigate more recent techniques that are tailored for 3D data, such as 3D-SIFT (Scovanner et al., 2007) and 3D-SURF (Knopp *et al.*, 2010) while taking into account their computational intricacy and resilience to changes in scale, rotation, and lighting.

Intricate geometric characteristics: In order to derive intricate geometric characteristics from mesh structures, techniques such as the one introduced by Gumhold and Macleod (2001) have been employed. Figure 26 illustrates the process of feature extraction from mesh information. It demonstrates how interconnected vertices, edges, and faces represent an object's surface, enabling the extraction of various characteristics. The figure highlights the application of different techniques, such as mesh-based, glyph-based, and curvature-based methods, to derive surface features from the mesh structure. Nevertheless, these techniques frequently rely on particular mesh representations and could necessitate reparameterization or remeshing of the data, resulting in the possible forfeiture of geometric intricacy. It is imperative to conduct a thorough critical assessment of various mesh processing techniques, including mesh simplification, smoothing, and subdivision, to ascertain their influence on the extracted features and the overall performance of fingerprinting.

The intrinsic surface features are those characteristics that are inherent to the surface itself, without any external influence or modification. The utilisation of curvature-based techniques (Kazhdan, Funkhouser and Rusinkiewicz, 2003) and mesh parameterisation methods (Huang and Zhou, 2010; Reuter *et al.*, 2009; Li and Gu, 2004) have been employed to effectively capture the inherent characteristics of surfaces. Nonetheless, these techniques may exhibit susceptibility to noise and mesh resolution. Further exploration of advanced feature extraction techniques that are more resilient and adaptable, such as scale-invariant methods (Bronstein and Kokkinos, 2010) and diffusion-based methods (Yang *et al.*, 2023), could be beneficial in enhancing the dependability and precision of intrinsic surface feature extraction.

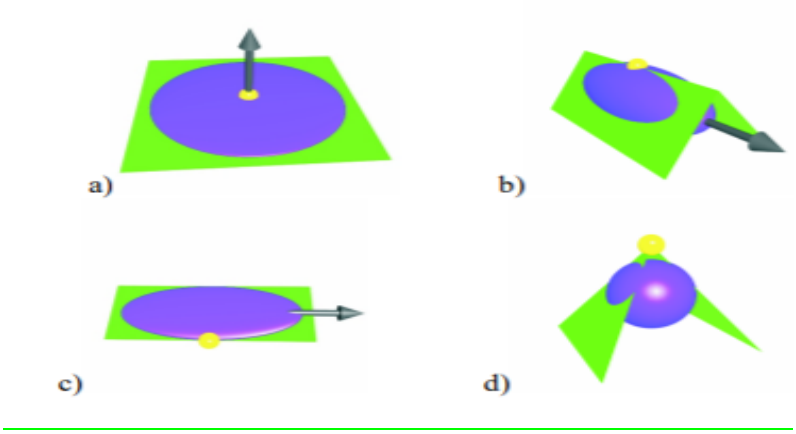

*Figure 26 Feature extraction using mesh information. (a): **Surface points**: Essential for understanding the general geometry of a 3D object, surface points can be extracted by analysing surface normals and curvatures in the mesh. (b): **Crease points**: Located along sharp edges where surfaces meet, crease points define boundaries between mesh regions and can be extracted by detecting surface normal discontinuities and dihedral angles. (c): **Border points**: Situated on the mesh boundary, border points provide valuable information about external features and interactions with surroundings and can be identified by detecting open edges. (d) **Corner points**: Representing junctions where multiple crease lines intersect, corner points define the overall mesh topology and offer insights into the object's complex geometry.*

5.2.2. Point Cloud-based Techniques

The utilisation of point cloud representation of object geometry is a prevalent technique for the creation of 3D fingerprinting. The process entails the extraction and manipulation of a vast collection of points situated in a three-dimensional space, each possessing distinct coordinate values (x, y, z), for the purpose of depicting the exterior of an entity. Point clouds can be obtained through diverse methods of data acquisition, including but not limited to laser scanning, structured light, or photogrammetry.

Qi et al. (2017) proposed the PointNet architecture, which is a deep learning methodology utilised for point cloud processing. The PointNet model exhibits the ability to extract advanced features from unprocessed point cloud data, thereby facilitating the categorization and partitioning of three-dimensional entities. The methodology involves the utilisation of symmetric functions and nonlinear transformations on the input point cloud, which effectively captures the local and global geometric features.

a) Local geometric features: The PointNet algorithm is designed to extract local geometric features from point clouds by examining the interrelationships among adjacent points. The process entails the computation of characteristics such as surface normals, curvature, and density, which facilitate comprehension of the regional structure and texture of the three-dimensional printed entity. The process of extracting said features is of utmost importance in order to create a distinct identification of an object's surface characteristics.

b) Global geometric features: By combining the local features throughout the entire point cloud, PointNet can also extract global geometric information. This is accomplished by a number of pooling procedures that compile the local data into a comprehensive understanding of the overall geometry of the 3D object. Global characteristics are crucial for identifying the object's larger-scale structure and can help create its distinctive fingerprint.

Although PointNet has exhibited remarkable efficacy in diverse 3D recognition assignments, it possesses certain constraints in encapsulating intricate details and conserving spatial correlations among points. Qi et al. (2018) presented PointNet++, an enhanced iteration of PointNet, which employs a hierarchical neural network architecture to tackle the aforementioned concerns. The integration of PointNet++ with additional methodologies such as mesh parameters and adaptive occupancy grids can yield a more comprehensive and resilient 3D fingerprinting approach. This can result in enhanced security and dependability when verifying the authenticity of 3D-printed items.

The utilisation of point cloud-based methodologies entails the derivation and manipulation of characteristics from an extensive collection of points situated within a three-dimensional spatial environment. Although point cloud data is known for its versatility and reduced susceptibility to topological noise, its processing can be computationally demanding and may necessitate supplementary pre-processing measures, such as denoising, downsampling, and registration.

Glyph-based: The process of integrating coded patterns or markers as unique geometric structures or spatial arrangements of points is necessary when applying glyph-based methods to point cloud data. The presence of sparsity and irregularity in point cloud data may pose difficulties in the implementation of conventional feature-based matching methods. Researchers have investigated techniques tailored for point cloud data, such as the 3D Hough Transform (Borrmann *et al.*, 2011) focusing on computational efficiency and resistance to noise and occlusions.

Elaborate geometrical features: Point clouds have been analysed using deep learning techniques, specifically PointNet (Qi *et al.*, 2017a) and PointNet++ (Qi *et al.*, 2017b), to extract geometrical features. Nonetheless, these techniques may necessitate substantial training datasets and may incur significant computational costs. Researchers have also compared alternative techniques, such as graph-based methodologies (Niepert, Ahmad and Kutzkov,

2016a) and spectral techniques (Ovsjanikovs, 2011) with regard to their computational demands, precision, and applicability to diverse object categories and datasets.

Intrinsic surface features: The process of identifying inherent surface characteristics from point cloud data can pose difficulties owing to the irregularity and noise that is inherent in the data. Various techniques such as normal estimation, curvature estimation, and density-based methods can be utilised. However, it is imperative to thoroughly assess their sensitivity to noise and parameter selection.

5.2.3. Occupancy Grid-based Techniques

Occupancy grids provide a structured and uniform way to represent 3D objects by discretising the space into a regular grid structure. They have been used in conjunction with glyph-based techniques, elaborate geometrical features, and intrinsic surface features to provide a comprehensive fingerprinting solution for 3D objects. However, they may face challenges in terms of computational complexity, data storage, and resolution limitations.

Glyph-based techniques in occupancy grids involve embedding coded patterns or markers as distinct patterns of occupied and unoccupied cells. 3D convolutional neural networks (Maturana and Scherer, 2015) and 3D grid-based matching algorithms (Sünderhauf *et al.*, 2015) have been proposed for occupancy grid data, but their computational complexity, resolution sensitivity, and robustness to noise and occlusions should be carefully considered.

Elaborate geometrical features can be extracted using adaptive and hierarchical grid representations, such as OctoMap, the work of Hornung et al. (2013) and Choy et al. (2019). The choice of grid resolution and the underlying hierarchical data structure should be thoroughly investigated to optimise the performance of geometrical feature extraction(Santos et al., 2013).

Intrinsic surface features can be extracted using methods like Minkowski Convolutional Neural Networks (Choy, Gwak and Savarese, 2019) and 3D ShapeNets (Wu *et al.*, 2014), which may require large training datasets and be computationally expensive. Alternative techniques, such as statistical methods (Rusu and Cousins, 2011) and graph-based approaches (Niepert, Ahmad and Kutzkov, 2016) should be explored to improve the efficiency and reliability of intrinsic surface feature extraction.

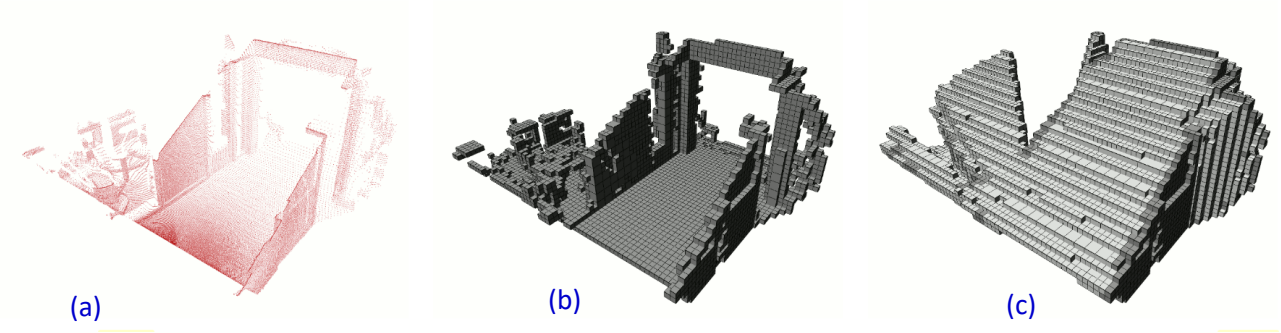

Figure 27: An octree map generated from example data. (a): Point cloud recorded in a corridor with a tilting laser range finder. (b): Octree generated from the data, showing occupied voxels only. (c): Visualization of the octree showing occupied voxels (dark) and free voxels (white). The free areas are obtained by clearing the space on a ray from the sensor origin to each endpoint. Lossless pruning results in leaf nodes of different sizes, mostly visible in the free areas on the right.

5.3. Statistical Fingerprinting Techniques

Statistical fingerprinting techniques involve the extraction and analysis of features from the spatial or frequency distribution of surface properties. These techniques can provide insights into an object's texture and global characteristics, which can be valuable for authentication and identification purposes. This section reviews several state-of-the-art statistical fingerprinting techniques, including the Gray-Level Co-occurrence Matrix (GLCM), Local Binary Patterns (LBP), and Gaussian Mixture Models (GMM).

5.3.1. Gray-Level Co-occurrence Matrix (GLCM)

GLCM is a widely used texture analysis method that captures the spatial distribution of gray levels in an image. GLCM computes a matrix that represents the frequency of co-occurring pixel intensities at a specific spatial relationship. Various features can be derived from the GLCM, such as contrast, correlation, energy, and homogeneity, which provide valuable information about an object's texture and surface properties (Dhruv, Mittal and Modi, 2018). However, GLCM can be sensitive to image rotation and scale, which might limit its robustness in certain applications. Recent research has focused on improving GLCM's invariance properties through multi-resolution and multi-orientation approaches (Khan and Professor, 2020).

5.3.2. Gaussian Mixture Models (GMM)

The Gaussian Mixture Model (GMM) is a probabilistic model that is generative in nature. It is designed to represent data as a combination of multiple Gaussian distributions, where each distribution is weighted according to its contribution to the overall data set. The Gaussian Mixture Model (GMM) has been employed in the realm of texture analysis and surface fingerprinting through the utilisation of local features, such as gradients or patches, in either an

image or 3D data. This approach has been documented by Zhang et al. (2021). The Gaussian Mixture Model (GMM) has the ability to effectively capture intricate probability distributions and offer a versatile depiction of surface characteristics. Nevertheless, Gaussian Mixture Model (GMM) may necessitate a substantial quantity of parameters and may incur high computational costs. Contemporary studies have been directed towards the enhancement of GMM-based techniques, including variational GMM (Xu *et al.*, 2020) and sparse GMM (Ravishankar et al., 2010), with the aim of diminishing computational intricacy.

The utilisation of GLCM and LBP could prove to be advantageous in capturing intrinsic surface features, given the contextual framework of a Glyph, the elaborate geometrical features, and Intrinsic surface features. These methods are particularly adept at identifying texture and local structures within the data. The Gaussian Mixture Model (GMM) has the ability to effectively represent complex geometric characteristics through the utilisation of local feature distribution modelling in both image and 3D model data. The integration of statistical fingerprinting techniques with the aforementioned 2D and 3D methods has the potential to yield a more exhaustive and resilient fingerprinting approach, thereby enhancing the level of security and dependability in the verification of entities.

Summary

In summary, this section gave a thorough review of the many methods used to authenticate and fingerprint 3D-printed objects. Three basic categories—2D approaches, 3D techniques, and statistical techniques—were used to group the methods under discussion.

A basic level of authentication can be provided by 2D approaches, such as image-based, texture-based, and glyph-based ones, although they are typically less successful at capturing the distinctive, intrinsic surface properties of 3D-printed items. Additionally, they are more sensitive to ambient noise, occlusion, and lighting.

A more thorough understanding of the geometry, topology, and distinguishing surface properties of 3D-printed items is possible thanks to 3D techniques, which include mesh-based, point cloud-based, and occupancy grid-based approaches. These methods could, however, run into issues with computing complexity, resolution restrictions, and noise sensitivity.

For finding hidden patterns and connections between extracted characteristics, statistical techniques like multivariate analysis, machine learning-based methodologies, and feature distribution analysis are helpful. Nevertheless, they might need sizable training datasets and can be costly computationally.

The methodologies that combine the benefits of 3D and statistical techniques are the most promising when considering the drawbacks of each technique. Occupancy grid-based approaches, like OctoMap, and point cloud-based algorithms, such PointNet and PointNet++, have demonstrated potential for extracting distinctive and trustworthy properties from 3D-printed objects. These methods have the potential to produce a reliable and complete fingerprinting solution for 3D object authentication when combined with cutting-edge statistical techniques and machine learning technologies.

6. Methodology

This section sets out how we propose to undertake the research. Based on the literature review, this study proposes to add an additional phase for watermark registration to implement a non-blind authentication method that will be developed in this research to register and uniquely identify each 3D-printed part produced by the AM process (

Figure 28). The features extracted fro **QR CODE** and/or **WATERMARK FORMATION** encrypted and stored digitally. Once registered, the object is then released to the supply chain. At the customer end, during the verification process, the same watermark is scanned, and features are extracted. These features are then compared with the features extracted during registration for authentication. If the features match, the object is believed to be of genuine origin (Figure 29).

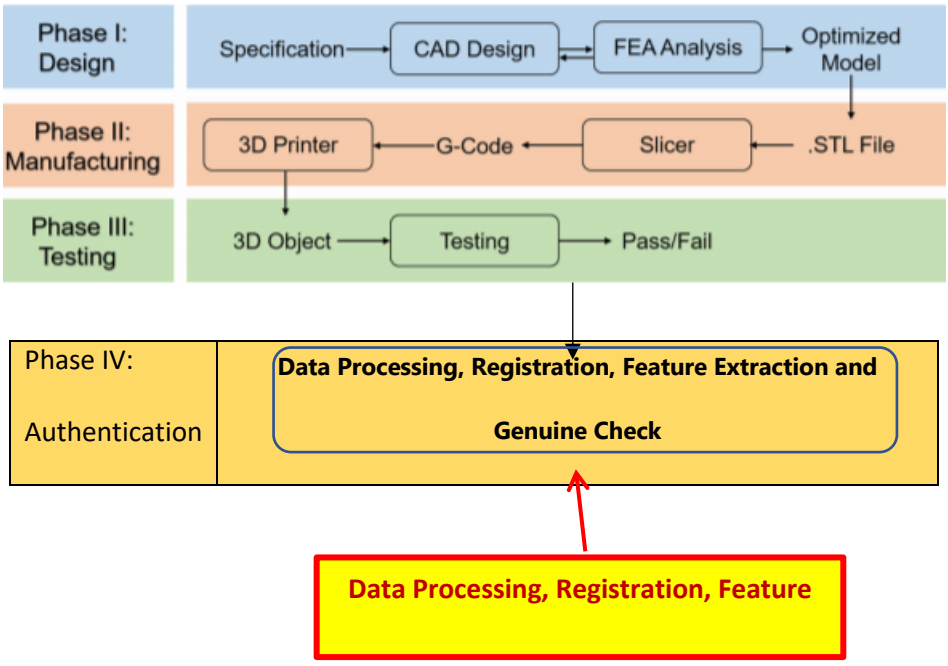

Figure 28: A typical process chain of Additive Manufacturing with the additional proposed phase IV of authentication

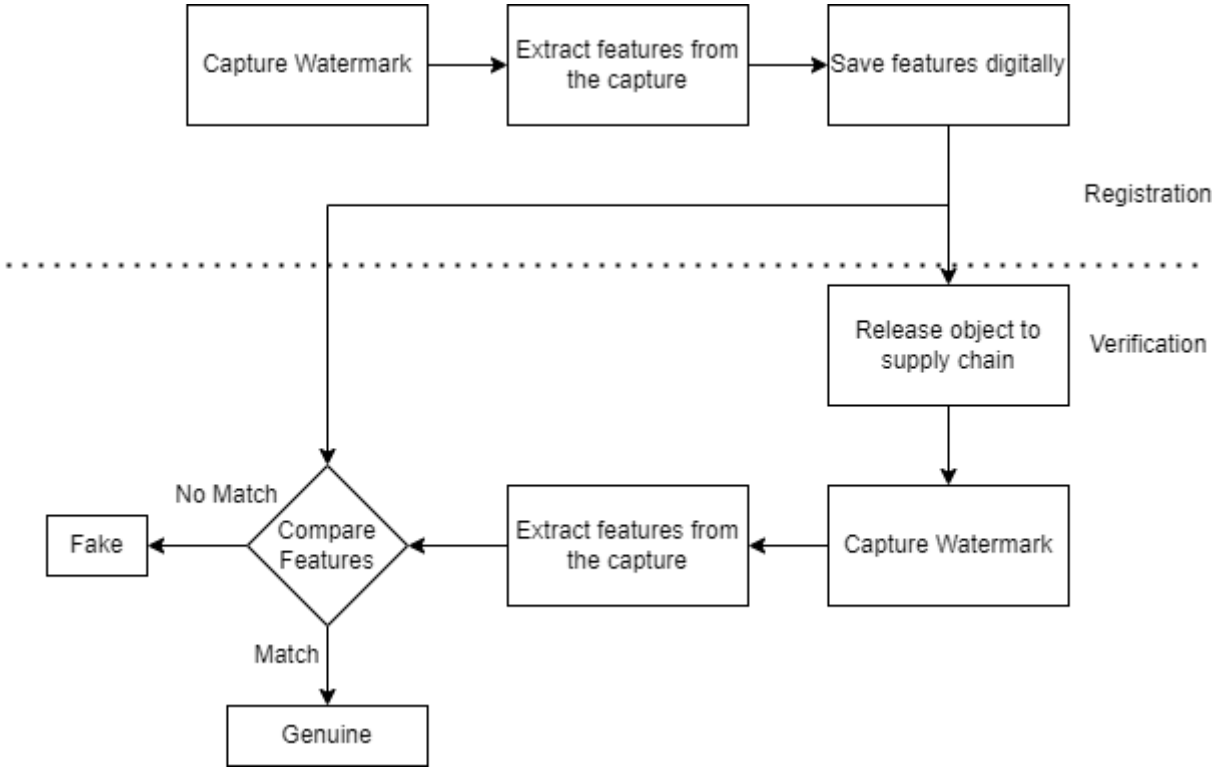

Figure 29:Authentication framework

The development of this non-blind authentication technique will follow the methodology provided in Figure 30, which serves as a comprehensive workflow diagram that encapsulates the research tools, both software and hardware, materials, and methods employed throughout the project. This diagram systematically integrates the processes and phases detailed in Figures 27, 28, and 29, ensuring a clear visual representation of the project's implementation strategy. This can be divided into 4 stages:

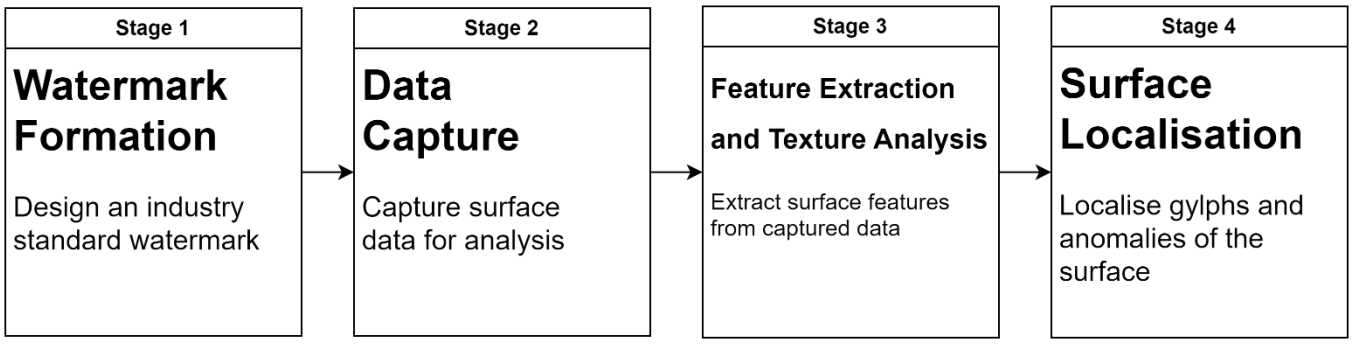

Figure 30: Overview of Methodology

- At Stage 1, in order to achieve the goals of this research, we would first need to build a dataset. This dataset is built by printing numerous objects with glyphs and anomalies from all the identified printing techniques.

This is the stage where the 3 layers (glyph-based features, elaborate geometrical features, and intrinsic surface features) of features have been defined that form the signature of the object.

- In Stage 2, the surface data from the 3D printed objects would then be captured for analysis. The ground truth data needs to be validated to ensure the captured data is consistent. Leading to the development and testing of a new capture device.
- Next, at Stage 3, the captured data would then be used to investigate feature extraction and texture analysis approaches to obtain a unique signature.
- Lastly, at Stage 4, the positional information of the QR code and watermark would be obtained to provide additional robustness to the authentication process.

6.1. Watermark Formation

The dataset required for this research is not currently available, therefore the required dataset needs to be generated for testing. In order to create a dataset for capture, we 3D print objects with anomalies discussed in Section 3.1.7. As this research would only be investigating plastic-based materials, we only use the following materials for each of the printing methods:

DLP

- Plastic-based photopolymer resin

SLS and MJF

- **Multijet Fusion PA12.** PA12 used is a strong thermoplastic.

Revisiting the table introduced in Section 1.1 (Table 1: Taxonomy of printed object security features), we propose a three-layered approach to forming the watermark based on the increasing level of difficulty to replicate:

- Level 1 – Glyph Verification: A 3D QR code is used as a glyph. The size and pattern would be used for authentication. Since the pattern is predetermined and easier to identify, the glyph provides the least security but is a good visual indicator (fiducial) to indicate the registration area used for authentication. This can also carry embedded information.

- Level 2 – Elaborate geometrical features: The location and shape of these elaborate geometrical features are used for authentication. These features offer a middle level of security because they were purposefully included in the design and integration of the object. Incorporating a suite of geometrically complex designs that include chamfered edges, Voronoi patterns, and noise textures, these features are strategically embossed or debossed around the glyph to enhance security. Each feature, such as a triangular wave pattern or a cube block, is meticulously crafted to be distinct and challenging to replicate, ensuring a robust middle layer of security. Although they are more difficult to imitate than glyphs, they can still be faked if the manufacturing process or the design of the item are sufficiently understood.
- Level 3 – Naturally occurring surface texture: Uses the printing techniques' intrinsic surface characteristics that are completely random and unique to each 3D printed object or part. Since this can't be replicated, it provides the highest level of security.

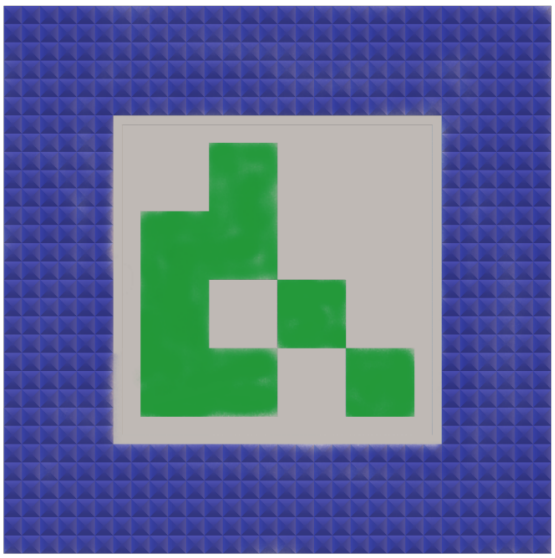

Figure 31: Whole artefact, elaborate geometrical feature (Blue) and QR code (Green)

A macroscopic glyph on the surface of a 3D-printed part, for the sole purpose of part verification, can be easily observed and replicated by an adversary, thus providing the least difficulty to counterfeit. Elaborate geometric features during manufacturing that mimic naturally occurring anomalies or specialised surface textures that are uniquely designed for authentication are harder to identify on the surface as they could be considered to be part of the design or mistaken as print defects. However, advanced knowledge of the manufacturing process or access to the original design files can provide the insight the adversary needs to counterfeit the 3D-printed parts. To ensure each object carries a unique signature, the methodology involves a detailed approach to the design and integration

of these features. By systematically altering the CAD files, we introduce variations in the geometrical patterns that are both intricate and unique to each printed object. This process not only requires a deep understanding of the 3D printing technology and material behaviour but also leverages software capabilities for precision design beyond conventional manufacturing limitations.

All these 3 Levels together provide the unique signature for the authentication of each object. Each of these test objects would have elaborate geometrical features added that are less than 500 µm around the glyph (larger than 1mm). The size of these anomalies is based on the minimum resolutions of various printing techniques. With the understanding of how anomalies occur on a 3D-printed surface, we attempt to replicate them by systematically modifying the CAD file to introduce controlled anomalies. This multi-layered approach ensures robust authentication, as each level contributes to the overall security, making it increasingly difficult for adversaries to successfully counterfeit the object.

6.2. Data Capture

To capture the watermark, based on our literature review, we select the industry-leading capture methods to capture the 3D-printed surface. The three methods are (1) Multi-focus 3D microscopy, (2) Photometric Stereo and (3) Structured Light. These methods have been selected based on their high-resolution output, speed, cost and their ability to span across multiscale except multi-focus 3D microscopy. However, the Multi-focus 3D microscopy software allows multiple microscale data capture to be stitched together to obtain the necessary capture size.

Multi-focus 3D microscopy provides the highest resolution at the microscale making it ideal to capture ground truth data.

6.3. Surface Feature Extraction and Texture Analysis

A systematic experimental method will be used to test the existing surface characterisation algorithms at micro and macroscales. The algorithms will be tested for speed and accuracy. The results from these tests will help derive unique features for the glyphs and watermarks on the surface. Successful features derived in this way will serve to help us build new characterisation techniques resulting in a novel approach specifically tailored for 3D-printed objects. Successful techniques should be able to characterise unique signatures based on viewpoint invariant features for authentication.

An algorithm based on the features extracted will also be developed that can identify and characterise the unique signatures of the glyphs and watermarks on the surface of the object. These features will be extracted using a combination of 2D and 3D image processing techniques as well as statistical modelling on the captured data. Some of the key expected outcomes are:

- Identifying the optimum feature extraction technique for authentication.
- Identifying unique fingerprint to a particular printing process.
- Highlighting the similarities on the surface of the printing process.

A comparison between the three features type (2D, 3D and statistical) is presented in the table below (Table 6). The processing techniques are classed against the three levels of authentication previously presented.

Table 6: Fingerprinting strategy

	2D	3D	Statistical
Level 1- QR code verification	• Easy translation to ArUco marker dictionary • Direct libraries available for quick implementation	• Additional complexity as the QR doesn't contain extra information	• Shape and size • Measurements of the QR code
Level 2- Elaborate geometrical feature	• Ray tracing • Texture pattern classification	• Point cloud classification • Classify all 8 patterns	• Statistical analysis of the surface • Each pattern printed will have a unique texture
Level 3- Intrinsic texture	• Microscopic structures might not be distinguishable	• Point cloud classification • Identify printing technique	• Statistical analysis of the surface • The surface profile of every printed object will be unique

Following the comparison in Table 6, an exploration into the authentication process across all three levels is presented:

Level 1 - QR Code Verification: The initial stage utilizes ArUco markers, an established and universally recognized 2D barcode system, for embedding essential authentication information within 3D-printed objects. These markers offer

a reliable method for quick identification and decoding, proving to be particularly effective for Level 1 authentication due to their adaptability to various lighting conditions and angles of view (OpenCV, 2023).

Level 2 - Elaborate geometrical feature: At this stage, the focus shifts to more sophisticated surface details, such as elaborate geometric patterns and textures that are challenging to replicate. The combination of ray tracing and texture pattern classification techniques is employed to analyze these complex features, enhancing the object's security by adding a layer of difficulty for counterfeiters.

Level 3 - Intrinsic Texture: The highest level of authentication examines the intrinsic surface texture of the 3D-printed object, which includes microscopic structures unique to each print. This level leverages advanced point cloud classification and statistical analysis to identify the unique "fingerprint" of each object, offering the most detailed and secure form of authentication.

This tiered approach to authentication, from the easily accessible ArUco markers to the in-depth analysis of intrinsic textures, creates a robust framework for verifying the authenticity of 3D-printed objects.

Summary

A research methodology is suggested along with the authentication framework for this study after reviewing the literature and the research questions. The proposed layers of security—Glyph Verification, Elaborate Geometrical Features, and Intrinsic Surface Features—will together create a watermark on the surface that will yield an individual signature that can be extracted. A capture method that will provide the ground truth data was chosen from among those mentioned in the literature review.

The validated ground truth data can then be used for more in-depth analysis. The new capture method that is being developed and tested will use it as a benchmark or reference dataset. The same dataset can also be used for improved surface feature extraction and texture analysis research and development. A combination of 2D, 3D, and statistical models will be used for feature extraction and texture analysis.

The validated ground truth data can then be used for more in-depth analysis. The new capture method that is being developed and tested will use it as a benchmark or reference dataset. The same dataset can also be used for improved surface feature extraction and texture analysis research and development. A combination of 2D, 3D, and statistical models will be used for feature extraction and texture analysis.

The methodology was created to provide an iterative improvement and integration of new knowledge as it emerges, allowing for an agile research approach. The research will be able to adjust to improvements in 3D printing technology and authentication methods thanks to its adaptability, ensuring that the findings will still be useful in a field that is developing quickly.

7. Experiments

In this section, several experiments are presented that are based on the research methodology presented above. This will lead to the development of the authentication framework presented previously. Firstly, the capture methods are tested for their capture resolution (micro and macro) and then the selected capture method is validated for its repeatability. The development of the watermark design is also described in this section. Once the capture method has been validated, the required dataset from the watermark developed is captured. This is then followed by the development of feature extraction and data augmentation techniques to achieve the desired authentication results. Finally, experimentation is presented that shows the effectiveness of the proposed authentication framework in securing 3D-printed objects and preventing counterfeiting.

7.1. Test Object

Industry-standard for authentication, as seen in Section 4, have predominantly been using watermarks. But there has not been a standard benchmark object that is used to establish the robustness of these authentication techniques. Thus, as part of this research, a test artefact refers to a specifically designed portion of the benchmark object, which is used for evaluating the effectiveness of the watermarking techniques. Each test artefact represents a distinct set of features and challenges, allowing for a comprehensive assessment of the authentication process across different scenarios. This benchmark object will also serve to evaluate the effectiveness of the three levels of security described in Section 2.1.

The 3D CAD model of the benchmark object was generated using the following 3D CAD and Design for Additive Manufacturing software: Fusion 360 and nTop (Autodesk, 2023; nTopology, 2023). The test object is split into 8 quadrants. Each quadrant consists of an embossed QR code that is surrounded by an elaborate surface feature, which refers to intricate, distinctive patterns or structures on the surface of the object. The QR codes were generated using a 4x4 ArUco marker dictionary (OpenCV, 2023). Some elaborate features were geometrically created, and others were randomly generated. The total object dimensions are 45x45x4mm and each test artefact is 15x15mm. Figure 32 shows the test artefact and

provides a short description of the geometrical features added around the QR code along with the ArUco marker ID.

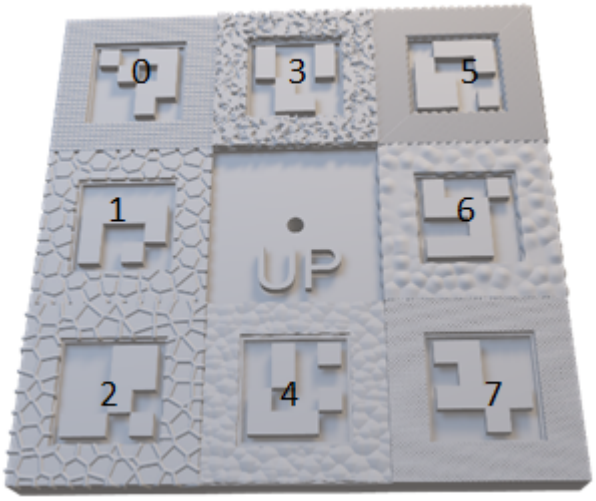

Figure 32: The test object with 7 test artefacts in which the geometrical features of each test artefact are added around the QR code that is well-aligned with the ArUco marker ID.

Table 7: The description of 7 test artefacts in which the geometrical features of each test artefact are added around the QR code that is well-aligned with the ArUco marker ID.

ArUco Marker ID	Elaborate geometrical features
0	0.5mm chamfered edges
1	Voronoi Deboss
2	Voronoi Emboss
3	Simplex Noise Deboss
4	Cellular Noise Deboss
5	45deg Triangular Wave Pattern
6	Voronoi Bubble
7	0.5mm Cube Block

Table 8: Technical Specifications of AM Systems Used in Fabrication of Test Objects

AM System (3D Printer)	XY Resolution	Z Resolution (Layer Thickness)	Materials	Max Printing Volume (X, Y, Z)
DLP	130 microns	25 microns	Standard photopolymer resin	128 x 128 x 200 mm
SLS	200 microns	100 microns	Nylon 12 (PA12)	165 x 165 x 320 mm
MJF	1200 dpi (approx. 21 microns)	80 microns	HP 3D High Reusability PA 12	380 x 284 x 380 mm

The benchmark objects are printed in 3-4 orientations, depending on the 3D printing technique as shown in Figure 33. The typical orientations are (1) Horizontal face down (2) Horizontal face up (3) Vertical and (4) 45-degree angle.

The printing techniques are chosen based on their relevance in the industry to mass produce and prototype detailed 3D-printed parts. The 3D printing techniques that were used for fabricating the test objects include DLP (Digital Light Processing), SLS (Selective laser sintering) and MJF (Multi Jet Fusion), as outlined in Table 8 for detailed technical specifications of each printing system. DLP printers have a resolution of 100 microns whereas MJF and SLS are 500 and 750 microns respectively. But the MJF and SLS see more industrial use due to their print volume, speed, and material choices. All these benchmark objects are printed using the most used printing materials used by each of these techniques identified above. That is a polymer resin for DLP and Nylon for SLS and MJF. No further processing was done on the surface.

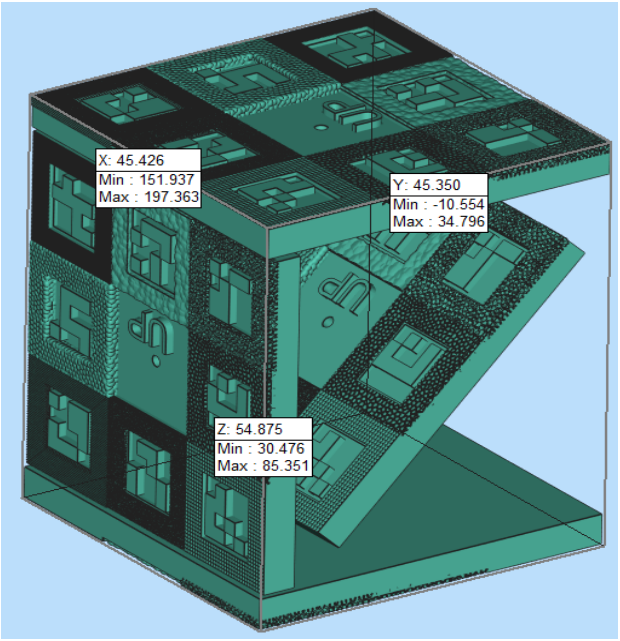

Figure 33: Four orientations of the benchmark object for 3D printing. It is noted that, each benchmark object has 8 quadrants which are 8 test artefacts.

7.1.1. Data capture

The scanning was done using an Alicona InfiniteFocusSL (Alicona, 2023) camera. It uses a multi-focus 3D microscopy technique. For this data capture, we used a 5x zoom lens that provided a claimed vertical resolution of 460nm, which is considerably higher than the print resolution. Each quadrant is individually scanned in a single shot. The scanned surface is segmented into three sections as shown in Figure 33: (1) The whole quadrant. It provides size and orientation information; (2) The elaborate geometrical feature. This can be uniquely generated for each print; and (3) The flat surfaces in and around the QR code present the intrinsic texture of the surface that is unique to the

printing technique. A total of 33 samples were used in the study. These samples were derived from different printing materials and orientations, and a total of 273 scans were performed to capture the necessary data.

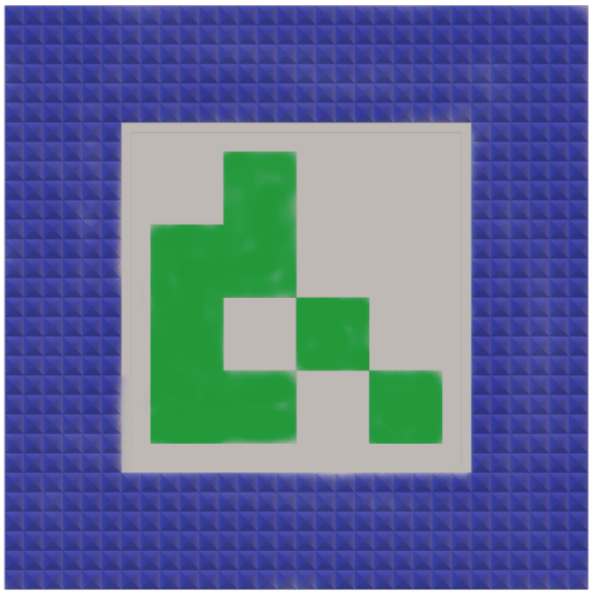

Figure 34: Three segmented sections of the 3D scanned surface of one test artefact: (1) the whole artefact which provides size and orientation information; (2) the geometrical feature (Blue) which is uniquely generated for each 3D printed artefact; and (3) the QR code (Green) that presents the intrinsic texture of the surface of the 3D printed artefact.

7.1.2. Results

The results presented here are based on the data capture process described in Section 4, focusing on watermark authentication as the industry standard. Despite watermarking being a prevalent method, it's noteworthy that there has been no established standard benchmark object for evaluating the robustness of watermarking techniques. In this research, we introduce new test artifacts designed to serve as benchmark objects. These artifacts are specifically created to assess the effectiveness of various watermarking techniques across the three security levels detailed in Table 1 of Section 1.1.

Each test artifact measures 15x15mm, contributing to the total dimensions of the benchmark object, which are 45x45x4mm. Figure 32 visually represents these test artifacts, while Table 8 provides detailed descriptions of the elaborated geometrical features surrounding the QR codes and their associated ArUco marker IDs.

The Alicona InfiniteFocusSL camera was used for data capture, with the collected data segmented into three distinct sections for comprehensive analysis. The evaluation criteria and methods applied to these printed objects are aligned with the procedures outlined in Sections 3.1 and 3.2. Table 9 compiles the number of test objects printed for this

study, alongside the total number of individual scans executed to gather the necessary data for our analysis. The classification of the captured data, based on these criteria, is shown in Figure 34.

Table 9: The total number of benchmark objects that were 3D printed and the number of individual 3D scans that were conducted for data collection and processing to assess the security levels and authentication of 3D printed parts.

The benchmark objects that were 3D printed				
Material	Resolution	Total benchmark objects	Number of orientations of each benchmark object	Total number of benchmark objects that were 3D printed
MJF	500 microns	3	4	12
SLS	750 microns	3	4	12
DLP	100 microns	3	3	9
Total				33
Individual 3D scans that were conducted for data collection and processing				
Material	Total benchmark objects	Total quadrants (test artefacts) to scan per benchmark object		Total number of 3D scans
MJF	12	8		96
SLS	12	8		96
DLP	9	8		81
Total				273

Analysis of the results revealed that the surface roughness varied among the printing techniques tested. The average roughness (Ra) and the maximum peak-to-valley height (Rz) were both significantly different for the horizontal face-down and face-up MJF parts. However, these amplitude parameters did not fully characterize the surface.

Below are some of the results that show the deviation analysis between two orientations of print in MJF (Figure 35). The scale bar shows the deviation analysis of the figure. And Table 10 shows the deviation values of the orientations, where:

- D_{neg}: Max. deviation below the reference surface
- D_{pos}: Max. deviation above the reference surface
- D_{mean}: Mean deviation

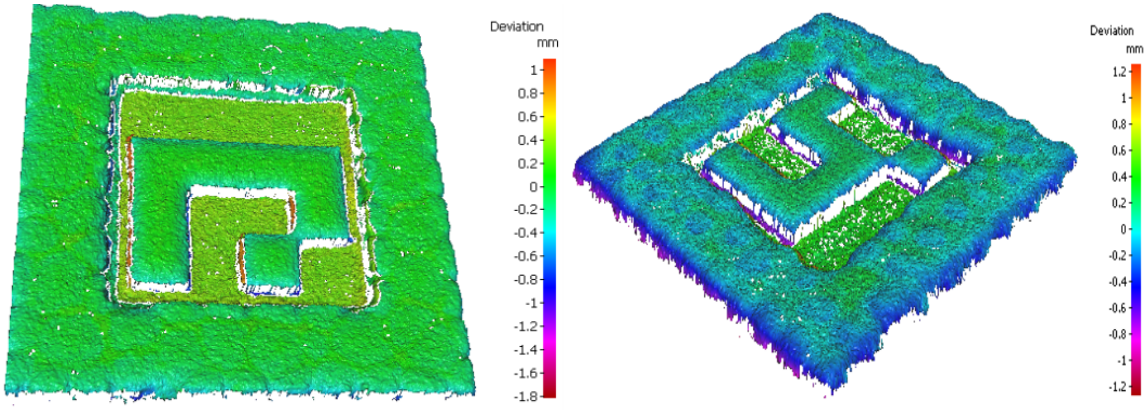

Figure 35: The error maps that show the difference between two 3D scanned surfaces of Marker ID 2 (left) and Marker ID 7 (right) that were 3D printed with two orientations of 0 deg and 45 deg using MJF.

Table 10: The deviation values in millimeters of two orientations of 3D prints using MJF, which were measured by comparing the scanned surfaces of two different 3D print orientations. The maximum deviation below and above the reference surface, as well as the mean deviation were calculated. Dneg stands for Max. deviation below the reference surface. Dpos stands for Max. deviation above the reference surface. Dmean stands for Mean deviation.

Marker ID	Dneg	Dpos	Dmean
2	1.812	1.093	0.035
7	1.273	1.258	0.045

By considering these deviation values and the methodology used to measure them within the context of this study, a better understanding of the surface roughness and its relationship with the printing techniques and orientations can be achieved. This knowledge can further inform the development and evaluation of authentication techniques for 3D-printed parts, as explored in this thesis.

Figure 36 provides a graph that shows the Ra value of the full characteristic of the surfaces of the QR codes; sampling each of the printing methods.

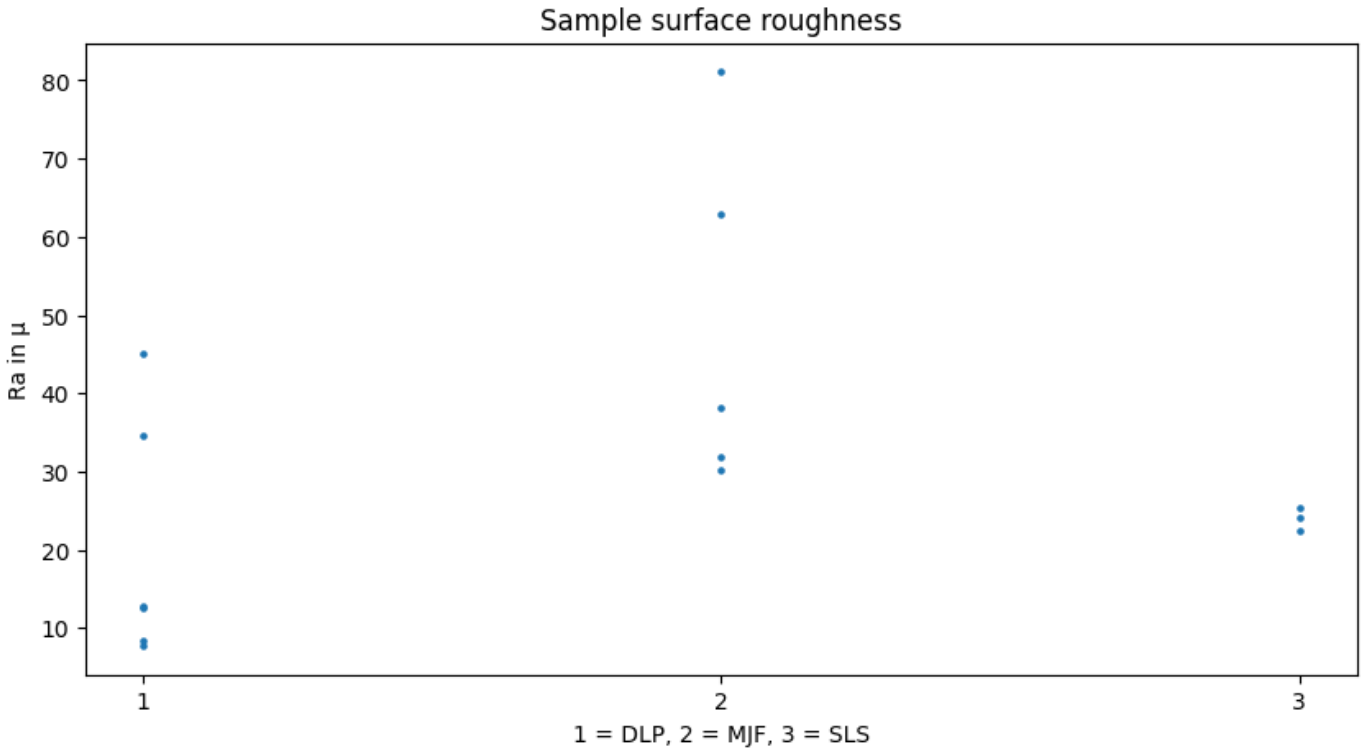

Figure 36: The surface roughness of the surfaces of the QR codes of the 3D printed benchmark objects using different AM processes. DLP stands for Digital Light Processing. SLS stands for Selective laser sintering. MJF stands for Multi Jet Fusion.

Each feature around the QR code produces a unique roughness signature. The average roughness, Ra, and the maximum peak-to-valley height, Rz, are both significantly different for the horizontal face-down and face-up MJF parts. However, these amplitude parameters do not fully characterise the surface. In order to enhance understanding of surface texture, an additional approach involves the analysis of root mean square roughness, Rq, which constitutes a significant parameter in the characterization of surface roughness. The parameter denoted as Rq in surface metrology refers to the mathematical operation of taking the square root of the mean value of the squared surface profile heights measured over a specified evaluation length. The utilisation of this method yields a heightened level of precision in assessing the comprehensive roughness, as it factors in both upward and downward deviations from the mean line. This can prove to be particularly advantageous in discerning disparities among the various printing methodologies and orientations.

The roughness profiles for MJF Marker ID 2 in horizontal face-down and horizontal face-up orientations are depicted in Figure 37 and Figure 38, respectively. The aforementioned images serve to illustrate the discrepancies in surface texture observed between the aforementioned pair of orientations.

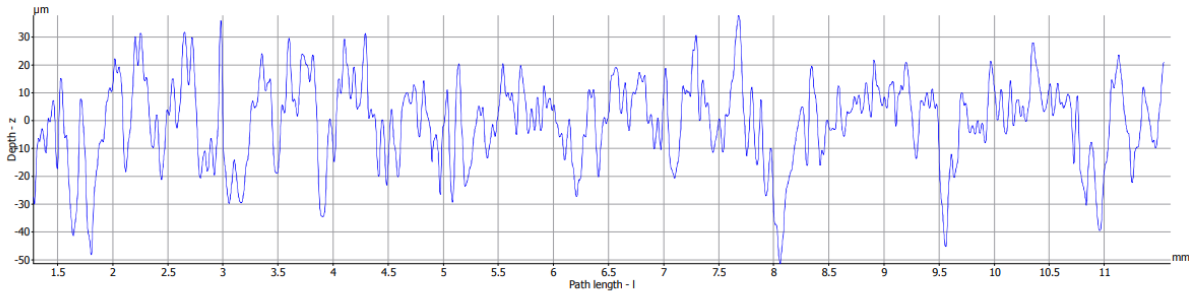

Ra: 11.849µm
Rq: 15.086µm
Rz: 73.973µm

Figure 37: Roughness profile for MJF Marker ID 2 horizontal face down

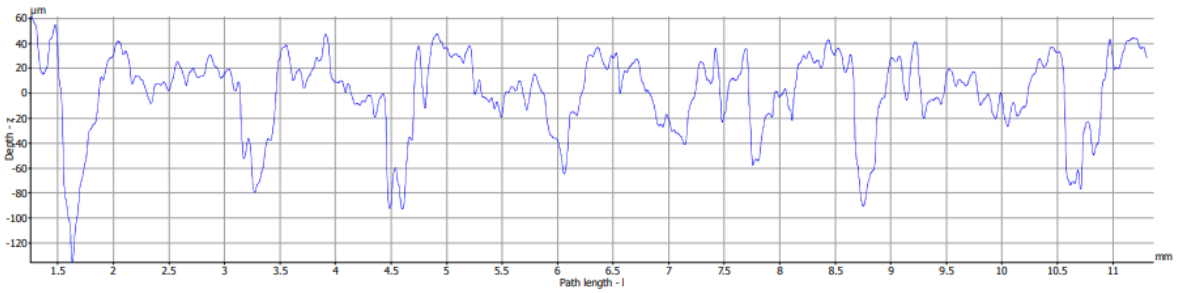

Ra: 25.167µm
Rq: 32.708µm
Rz: 138.577µm

Figure 38: Roughness profile for MJF Marker ID 2 horizontal face up

By examining the roughness profiles in Figure 37 and Figure 38, it becomes evident that there is a significant difference in Rq values between the two orientations. This information can be used to better understand the impact of different printing techniques and orientations on the surface roughness of 3D-printed parts, ultimately informing the development and evaluation of authentication techniques for these parts.

Summary

In summary, the artefacts developed and designed for this research establish a benchmark for future studies to evaluate their authentication techniques, addressing a critical gap in the current understanding of 3D printing authentication. The comparative analysis of different additive manufacturing (AM) processes reveals that each process exhibits unique surface roughness characteristics, which are consistent within the same printing technique but distinctly vary across different techniques. This differentiation is crucial for the authentication process, as it allows for the unique identification of objects based on their surface texture—a key factor in the proposed authentication framework.

Digital Light Processing (DLP) excels in producing parts with high detail and excellent surface finish, making it ideal for objects requiring detailed watermarking features. Selective Laser Sintering (SLS) offers a balance between detail and structural integrity, suitable for objects that need to be durable yet possess moderate resolution. However, Multi Jet Fusion (MJF) stands out as the most suitable technique for creating benchmark objects for authentication studies. Its superior resolution, expansive print volume, and broad material versatility make it adept at accurately capturing the intricate details essential for effective authentication techniques. The captured dataset from these processes, particularly emphasizing the surface roughness captured through Ra and Rz values, provides invaluable data for feature extraction and augments the authentication process.

Table 11 does a comparative analysis for a detailed overview of the technical specifications of the AM processes (DLP, SLS, and MJF), which identifies MJF's suitability for detailed, durable, and scalable authentication applications in 3D printing. It is important to note, however, that while Ra and Rz values offer some insight into the surface roughness, a more comprehensive analysis is essential to fully understand the surface properties and their implications for authentication. This nuanced approach is critical for developing a robust and exhaustive solution for the authentication of 3D-printed objects, as outlined in this research.

Table 11: Comparative Analysis of AM Processes for Authentication Applications

Feature/AM Process	DLP (Digital Light Processing)	SLS (Selective Laser Sintering)	MJF (Multi Jet Fusion)
XY Resolution	High (130 microns)	Moderate (200 microns)	High (Approx. 21 microns, 1200 dpi)
Z Resolution (Layer Thickness)	Very Thin (25 microns)	Thicker (100 microns)	Thin (80 microns)
Materials	Standard photopolymer resin	Nylon 12 (PA12)	HP 3D High Reusability PA 12
Max Printing Volume (X, Y, Z)	Smaller (128 x 128 x 200 mm)	Moderate (165 x 165 x 320 mm)	Larger (380 x 284 x 380 mm)
Detail and Surface Finish	Excellent for intricate details and smooth surfaces. Ideal for creating detailed watermarking features necessary for authentication.	Good for complex geometries and stronger parts. Might not capture fine details as DLP but offers a balance between detail and structural integrity.	Excellent for fine details and smoother surfaces. Suited for authentication objects requiring high detail and quality.
Suitability for Authentication Objects	Highly suitable for small, detailed objects. The smaller printing volume may limit application for larger objects.	Suitable for objects requiring a balance of detail and structural integrity.	Optimal for creating benchmark objects for authentication studies due to high resolution, material versatility, and larger print volume.

7.2. Capture Method Testing

The aim of the experiment is to capture 3D surface texture and surface geometry information of printed objects at various scales (macro and micro) using different capture methods identified in Section 3.2

In order to effectively test the existing surface characterisation algorithms at micro and macroscales, this experiment requires data from various sources. As discussed above in Section 3.1 and Section 3.2, there are various 3D printing methods and capture methods for authentication currently being used in the industry currently.

For this testing, the 3D model used in this experiment is of an extruder bracket that has been printed by the HP Multi Jet Fusion (MJF) 3D printer in **PA12 material**. The experiments focus on capturing the surface topography of the authentication glyph (Figure 39) and evaluating the performance of different 3D scanners in capturing this information. By doing so, the best possible 3D scanner for authentication purposes can be identified.

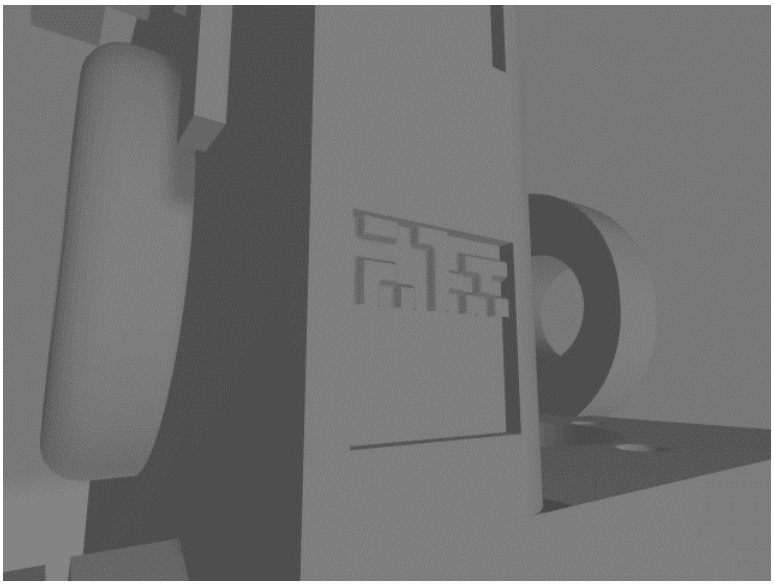

Figure 39: The authentication glyph printed on the extruder

7.2.1. Multi-focus 3D microscopy

The first surface dataset was captured at a microscale using Alicona InfiniteFocusSL (Figure 40). It uses a multi-focus 3D microscopy technique. For this data capture, a 5x zoom lens was utilised, achieving a vertical resolution of 460nm, significantly surpassing the layer height of the 3D-printed objects involved in this research. This makes this data capture method ideal to obtain ground truth data for future experiments.

In this technique, the depth of the surface is measured by finding the depth of field of the optics corresponding to the sharpness of the image captured. The optics are moved vertically along the optical axis varying the optical focus,

scanning the sharpness of the image captured under its small depth of field (Figure 41). A proprietary algorithm is then able to convert the captured data into 3D information with full depth of field and is stored as a STL file. It can provide a very high vertical resolution depending on the mounted lens. Figure 42 illustrates the output obtained. This method is not implemented in the AM industry for authentication due to its speed of capture[1] (30 seconds or higher, depending on resolution) and price, but it provides highly accurate surface data.

Figure 40: InfinitefocusSL (Alicona, 2023), the multi-focus 3D microscopy, which was used for 3D scanning of authentication artefacts of the 3D printed objects (Alicona, 2023).

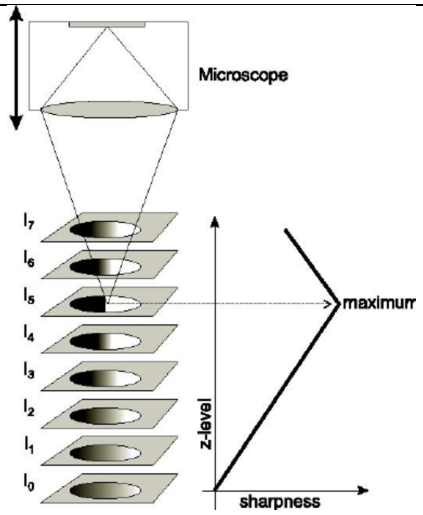

Figure 41: The schematic diagram of the multi-focus 3D microscopy (Zamofing and Hugli, 2004)

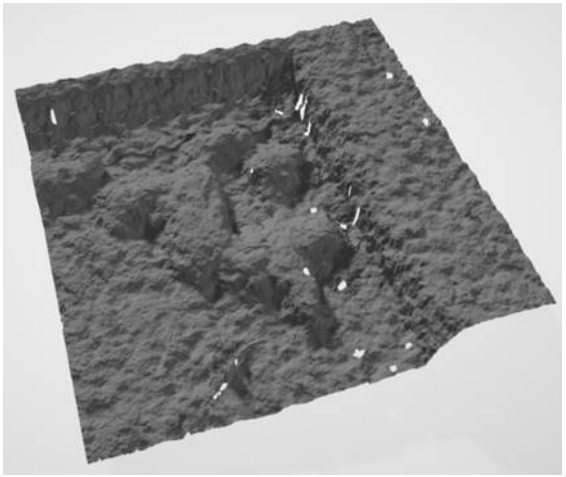

Figure 42: An example of the 3D reconstructed surface in the form of the STL format which was produced from the 3D scanned data by the 3D measurement system: InfiniteFocusSL

Observation

As seen in Figure 43, there are some missing patches in the surface data captured. These could be due to specular dust particles on the apparatus or on the object.

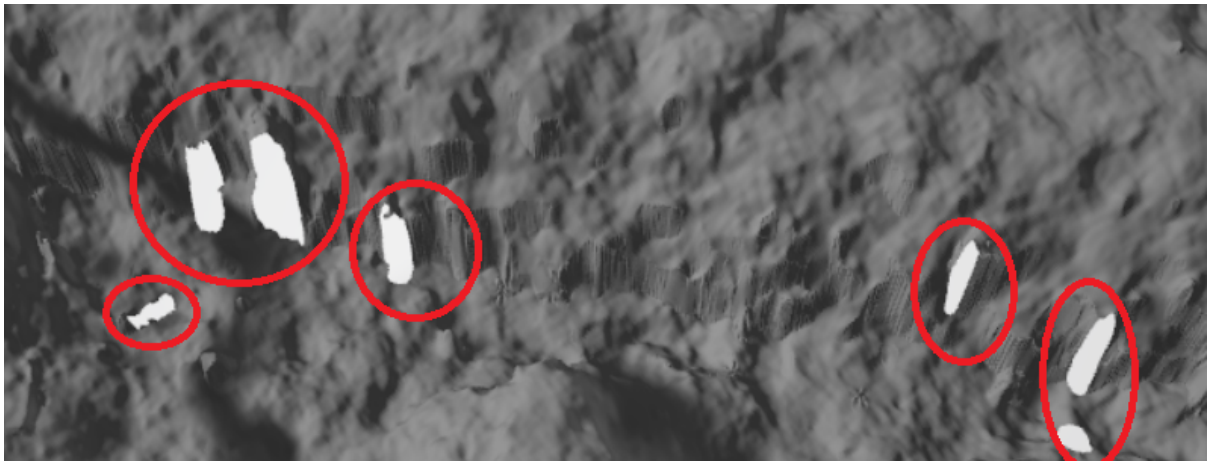

Figure 43: Holes in data captured (marked in red)

Some of the missing surface data is due to the angle of capture. The camera could not focus on the edge. As per the specification sheet for the system, the camera is unable to detect edges steeper than 87° from the horizontal surface.

7.2.2. Photometric Stereo at microscale

First implemented by Woodham in 1980, photometric stereo estimates the surface normals of a surface based on images captured from a fixed source with varying angles of light (Figure 44). Each pixel of the images captured corresponds to the same point on the object. The shading created by the varying light angles on the object is used to acquire the geometry.

To test photometric stereo at the microscale, the Alicona InfiniteFocusSL is used as a compound microscope. On a compound microscope, the image is formed between the objective and ocular lens (Figure 45). This image is then captured by the camera mounted behind the ocular lens at a fixed focus.

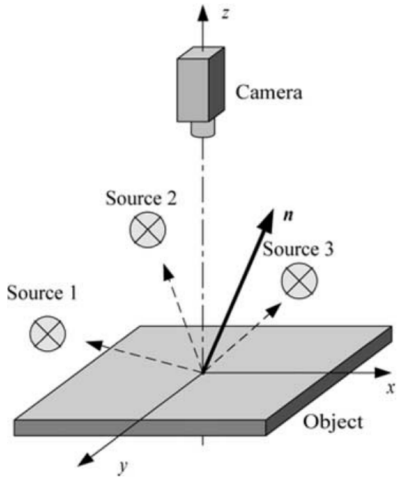

Figure 44: Principle of Photometric Stereo (Pernkopf and O'Leary, 2003)

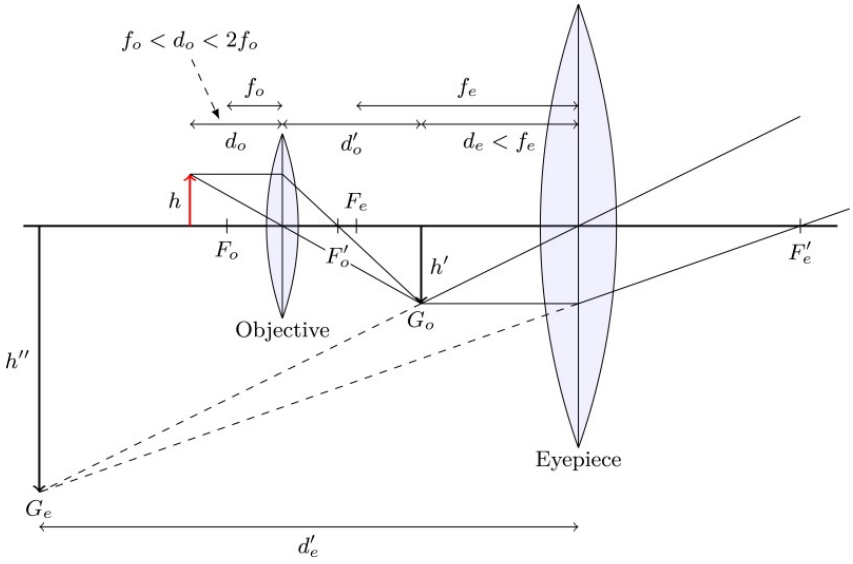

Figure 45: Image formation for a compound microscope (Cole, 2008)

Since the Alicona InfiniteFocusSL has a very shallow field of focus, the Alicona capture software can capture multiple images along the z-axis and merge them into a single 2D sharp image. The object is illuminated using an array of 16 lights mounted around the lens placed inside a diffuser. Each light was individually controlled to capture 16 different images with very low exposure (Figure 46). The combination of those images provided the output obtained in Figure 47.

In this setup, we are capturing 16 images for 16 different light positions. This method is based on the approach proposed by Li et al. (2016) but at a much smaller field of view.

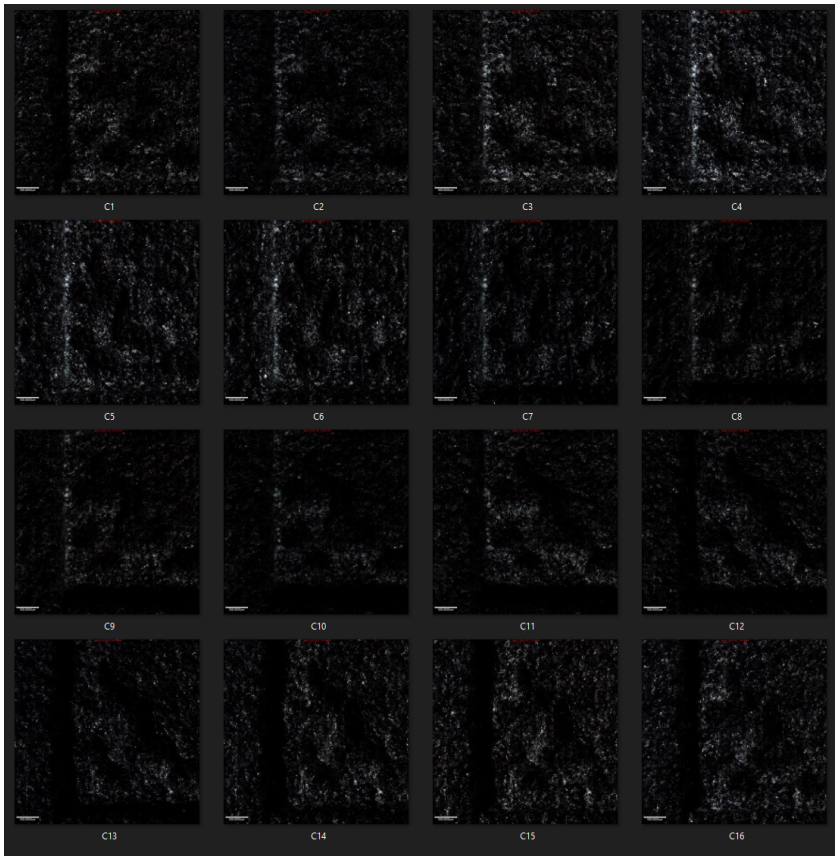

Figure 46: 16 images obtained using each rotating light source

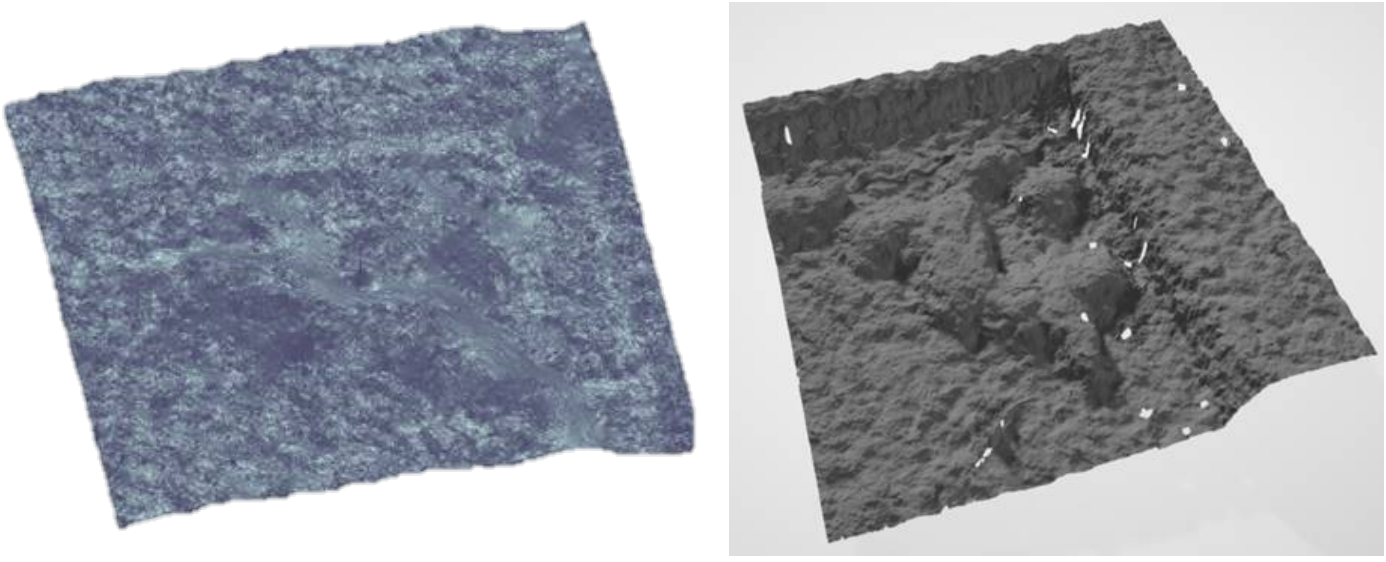

(A) *(B)*

Figure 47: Photometric Stereo output (A) compared to Output from Alicona camera (B)

Observation

The light was rotated around the object to capture the images as seen in Figure 46. As compared to the ground truth in Figure 47, the image does not seem to have captured the topography at a high resolution. The camera was

orthogonal to the object. The resultant image does not seem to capture the topography of the test object at a similar resolution as compared to the multi-focus capture method and has a lot of noise. This could be due to the incident lights being diffused causing infinite points of source illumination. Due to this, it is difficult to determine a precise illumination direction. The noise could also occur if the specular components in certain images were not able to overlap with all the images due to a lack of structure at that capture scale.

7.2.3. Structured Lighting (SL)

In a structured light 3D scanner, a projector is used to project a known narrow fringe pattern onto a 3D object. The illumination appears distorted from a slightly offset angle as compared to the projector. The camera mounted at that slightly offset angle from the projector, captures the distortion of the pattern on the surface of the object to calculate the depth and surface information of the object (Figure 48). To capture the overall geometry of the object, HP Structured Light Scanner Pro S3 (Figure 49) was used with a 2-camera setup. This allows the system to capture surface data as a stereo vision setup without the need to calibrate the projector position. The camera positions are calibrated using a 90-degree V-plate calibration target (Figure 50). The HP system can get a resolution of up to 0.05mm. The object is placed on a turn table and the scan is repeated 16 times at 22.5° rotations to capture all sides of the object. This system can produce up to 32 different patterns and can also capture the colour information of the object.

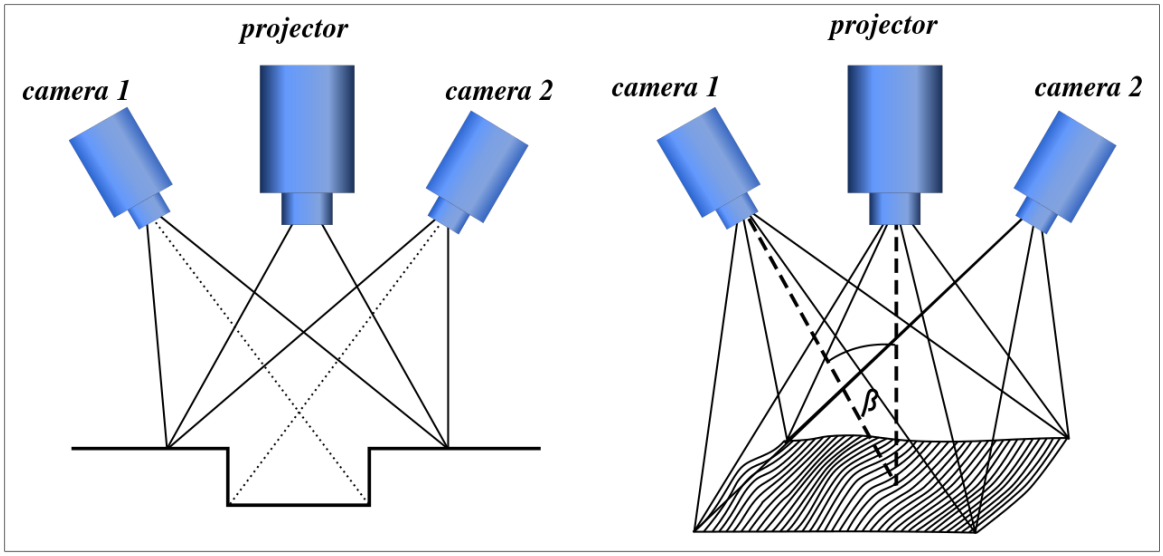

Figure 48: Working of Structured Light setup(Rubinsztein-Dunlop et al.*, 2017)*

Figure 49: HP Structured Light Scanner Pro S3 (HP, 2023), a structured light scanner that was used for 3D capturing of the 3D printed objects.

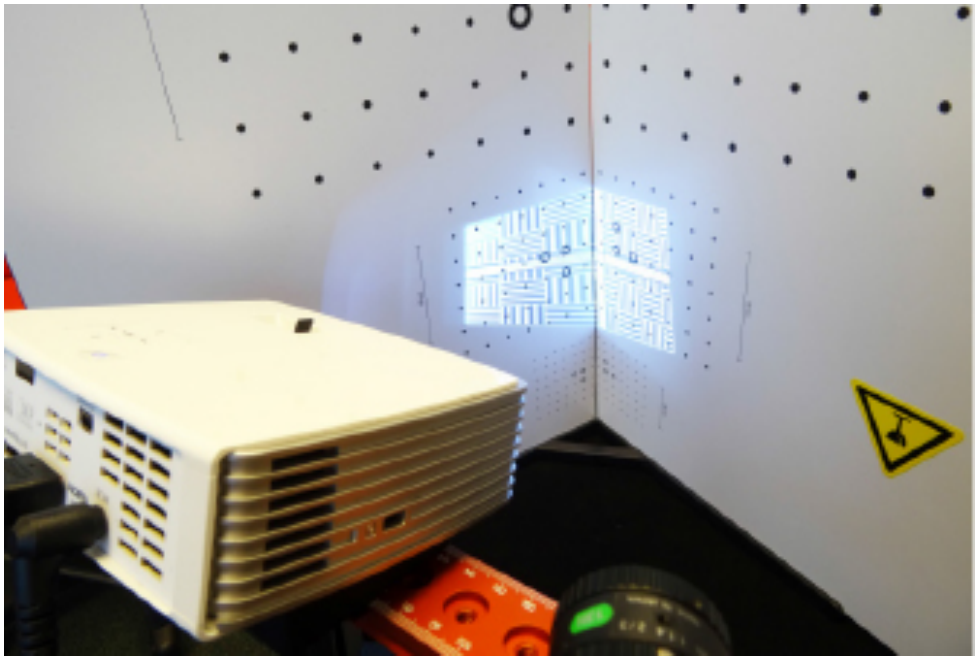

Figure 50: Calibration Target

Observation

Figure 51 shows data captured using the HP Structured Light Scanner Pro S3 system. We can observe that the system is unable to capture the 3D surface of the object in its entirety. Parts of the 3D surface are missing, which could be accounted for by the presence of shadows cast by the projector or the inclination of the surface. The system was used with its proprietary software called HP 3D Scan 5. It has an automatic function to align multiple scan surfaces to form one 3D object but was not very successful due to a lot of background noise. This background noise is caused by other surfaces captured in the background of the 3D object. This can be mitigated by manually cropping the background from the capture(Zhang, 2018).

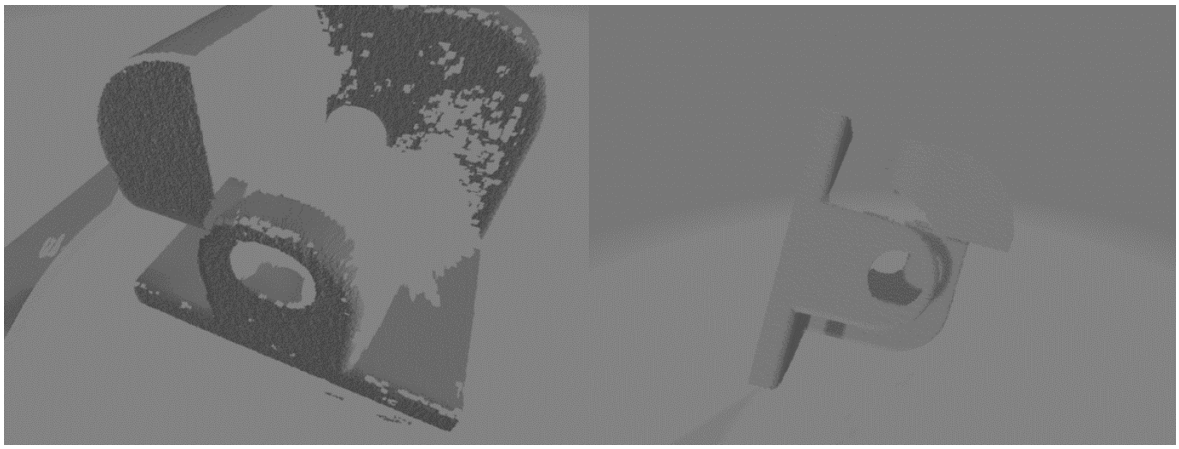

Figure 51: The scanned point cloud data from different scanning angles using HP Structured Light Scanner Pro S30

Summary

From the above experiments, it is observed that the Alicona InfiniteFocusSL provides the highest resolution of 3D data capture among the methods tested. With a minimum vertical resolution of 100nm at 10x magnification, it surpasses the resolution offered by other capture methods. Despite the capture area being limited to 2x2mm, the captured data can be stitched together to form a larger dataset. This capability makes the Alicona InfiniteFocusSL particularly valuable for applications requiring high-detail imaging over a relatively small area. Although this Multi-focus 3D microscope has been validated for accuracy by the manufacturer, additional testing is necessary to verify the manufacturer's claims thoroughly.

Adding to the context of 3D scanning technologies, the HP 3D Structured Light Scanner Pro S3 presents a different approach to data capture. It offers a resolution of up to 0.05% of the scan size, equating to a maximum of 0.05 mm

or 50 microns. This structured-light 3D scanner is notable for its ability to measure with an accuracy of up to ±0.05 mm, showcasing its proficiency in capturing detailed 3D models of larger objects where such precision is sufficient.

Moreover, with the Alicona InfiniteFocusSL camera using a 5x zoom lens, a vertical resolution of 460nm is achievable. This specification indicates that while the InfiniteFocusSL model provides superior resolution at higher magnifications, the InfiniteFocusSL offers a competitive resolution at a lower magnification, broadening the scope of applications for which Alicona's technology can be employed (Figure 52).

Objective name		4xAX	5xAX	10xAX	20xAX	50xSX
Working distance	mm	30	34	33.5	20	13
Lateral measurement area (X,Y) (X x Y)	mm m	4.87 23.72	3.61 13.03	2 4	1 1	0.4 0.16
Vertical resolution	nm	620	460	130	70	45
Height step accuracy (1 mm)	%	0.1	0.1	0.1	0.1	0.1
Max. measurable area	mm²	2500	2500	2500	2500	2500
Min. measurable roughness (Ra)	µm	n.a.	n.a.	0.45	0.25	0.15
Min. measurable roughness (Sa)	µm	n.a.	n.a.	0.25	0.1	0.08
Min. measurable radius	µm	12	10	5	3	2

Figure 52: Alicona InfiniteFocusSL lens specification with the selected lens highlighted (Alicona, 2023).

The comparative capabilities of the various scanning methods can be summarized in the following table:

Table 12: Comparative Scanning Capabilities

Method	Accuracy	Resolution	Speed (Points/second)	Suitable Scan Size	Colour Texture Capability
Triangulation	Moderate	High	High	Small to Medium	Yes
Structured Lights (HP S3)	High (up to ±0.05 mm)	High (up to 0.05mm)	Moderate	Medium to Large	Yes
Time of Flight	Low (1mm to 1cm)	Moderate	Very High	Large	No
Multi-focus 3D Microscopy (Alicona)	Very High (up to 460nm)	Very High	Low	Microscale	No
Photometric Stereo	Low to Moderate	Moderate	Moderate	Microscale	No

This table illustrates the distinctive strengths and limitations of each scanning technology in terms of accuracy, resolution, and scanning speed, highlighting the Multi-focus 3D Microscopy (Alicona) as particularly suited for capturing detailed images on the microscale. The choice of scanning method will depend on the specific requirements of the application, including the level of detail required and the scale of the object to be scanned.

7.3. Capture Method Validation

As the capture method to obtain the ground truth data has been identified, the device needs to be validated. This will also validate the accuracy and precision of the ground truth data that will be captured for this research. This is achieved by conducting two experiments to ascertain the repeatability of the device. First is by measuring deviation between multiple captures from the same position; Second is by measuring deviations between multiple captures at various angles.

The object that was scanned was a cube of 40x40x40mm dimensions 3D-printed in PLA using Alicona InfiniteFocusSL. Only the surface marked in green was captured repeatedly. The object was placed at the centre of a turntable. The capture size was 2.043 x 2.043 mm (2040x2040 pixels) with a vertical resolution of 1.02µm at 10x zoom.

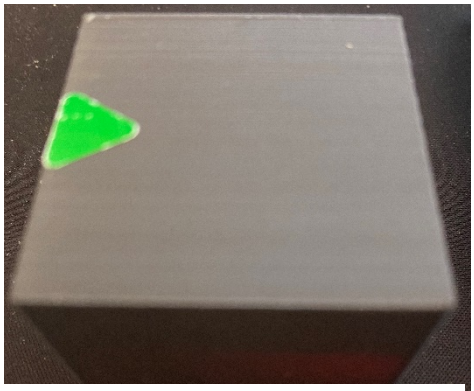

Figure 53: Test object with the scanned surface indicated in green

In the first experiment, the same area was captured three times without any changes to the setup. The multiple captures of data were plotted in 3D using MATLAB and overlayed on top of each other (Figure 54). The distance between each of the closest points was measured to calculate the root mean square (RMS) deviation in capture.

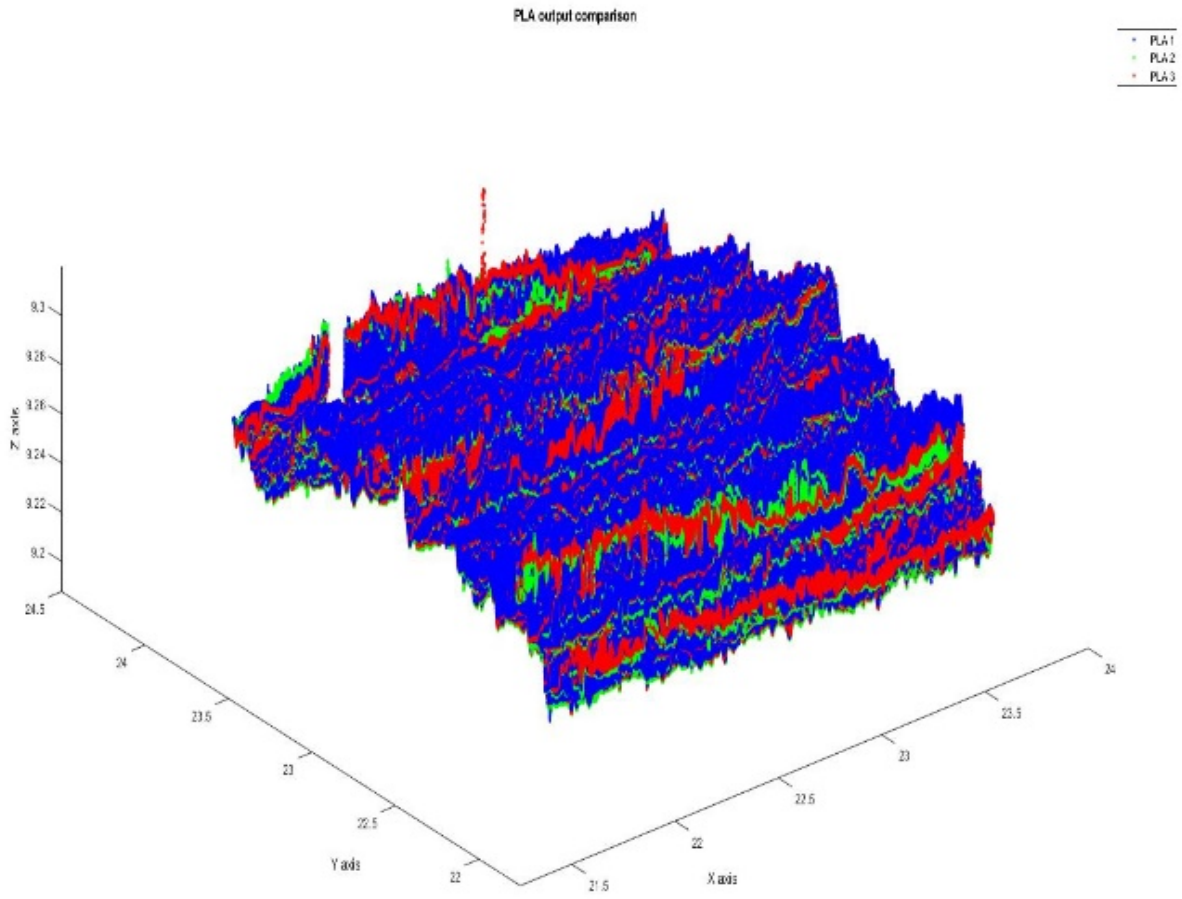

Figure 54: Captured surfaces overlayed on top of each other

In the second experiment, the same object, with the same surface capture was rotated clockwise about the z-axis, and the surface data was captured at 30-degree intervals. The captured data was then aligned using the iterative closest point (ICP) algorithm. ICP is used to minimise the difference between 3D datasets. This is done by keeping one dataset as the reference while transforming the other dataset to best match the reference. The mean deviation between the overlapping surface was measured to observe an error in capture.

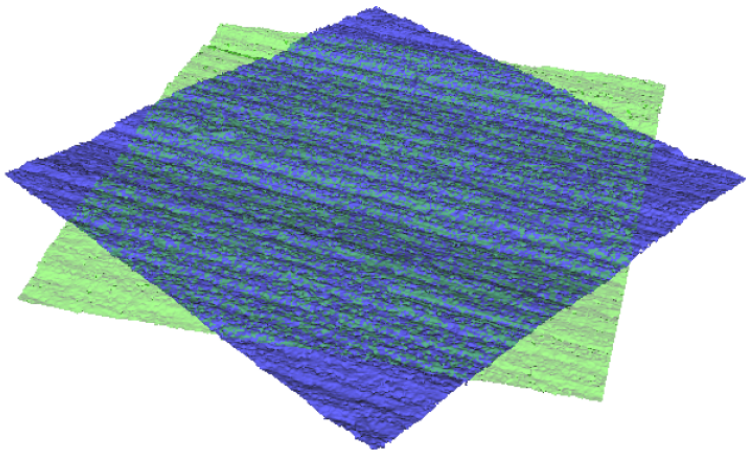

Figure 55: Captured surfaces aligned and overlayed

Observation

In the first experiment, a 0.04µm RMS between the 3 surfaces was observed. And the results for the second experiment are in Table 13. These values are within the manufacturing specification for the capture devices as well as the ISO standards for a metrological device.

This successfully validates the capture device's precision and repeatability. As for accuracy, although it is not directly addressed in these tests, the high repeatability of the data implies that the capture device can produce reliable measurements for this research.

Table 13: Mean deviation between two angles

Angles (deg)	Mean deviation (µm)
0-30	-0.028
0-90	0
0-180	0.015
30-60	0.005
30-90	0.013
90-120	0.034
90-180	0.030
120-150	-0.006
150-180	-0.001
180-210	-0.029
180-270	-0.028
210-240	-0.008
240-270	-0.002
270-0	0.009
270-300	0.003
300-330	0.005
330-0	-0.011

7.4. Data Augmentation

The amount of data required to perform feature extraction using deep learning may not be possible to obtain just by using the captured data. There needs to be a reliable method to augment data based on real data that is captured. Standard image augmentation techniques would not be sufficient as they may create bias in the dataset. To successfully model a 3D-printed surface, we would just need to model the surface texture of a particular printing technique (Figure 56).

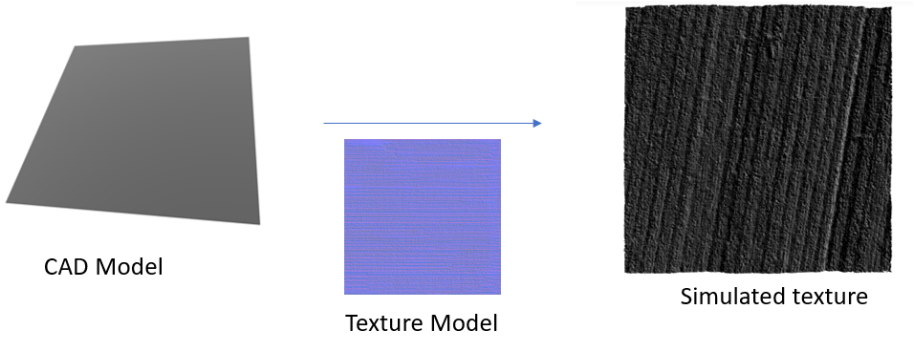

Figure 56: Surface augmentation

In order to generate the texture model, a Gaussian mixture modelling (GMM) is used to fit the surface topology of a real-world capture(Keselman and Hebert, 2019). A Gaussian mixture model is a probabilistic model in which all data points are assumed to be generated by a mixture of a finite number of Gaussian distributions with unknown parameters that form a cluster. In this case, the data points are the Z-axis distribution of the point cloud data and the number of GMM clusters is dynamically selected to best fit the surface topology based on the log-likelihood score for each cluster.

Mathematically, a Gaussian Mixture Model can be expressed as follows:

$$P(x) = \sum_{k=1}^{K} \pi_k N(x|\mu_k, \Sigma_k)$$

Where P(x) is the probability of a data point x, K is the number of Gaussian components, πk is the mixing coefficient of the kth Gaussian component, and N(x | μk, Σk) is the probability density function of the kth Gaussian distribution with mean μk and covariance matrix Σk. The Expectation-Maximization (EM) algorithm is typically used to estimate the parameters of the GMM, optimising the log-likelihood of the data.

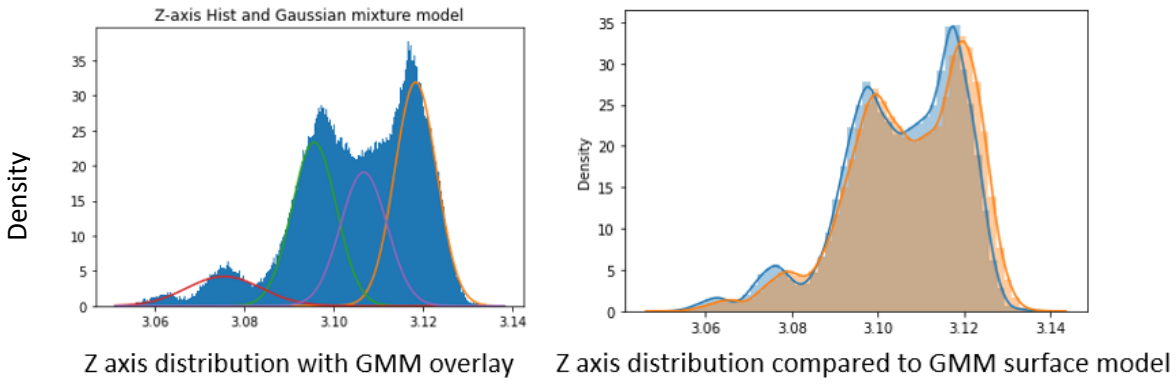

Figure 57: Z-axis distribution (a)with GMM clusters overlayed (left) (b) with GMM distribution (right)

Rather than using a generalised random noise to generate the surfaces, this GMM distribution is used to generate a one-dimensional Perlin noise model. Perlin noise is particularly appropriate for this application due to its several desirable properties: it produces smooth, continuous gradients, leading to realistic surface textures that appear natural and consistent; it exhibits self-similarity across different scales, ensuring that the noise patterns look similar when zoomed in or out, which is essential for modelling the surface texture of 3D-printed objects; it is computationally efficient, enabling quick generation for large-scale data augmentation processes; and it is easily customizable by adjusting parameters such as amplitude, frequency, and number of octaves to match the specific characteristics of the 3D-printed surface textures. These properties make Perlin noise an ideal choice for generating realistic surface texture models in the context of 3D-printed object authentication.

This noise model is then applied to normalised real-world surface data to generate the new augmented data. This will model the randomness of the surface texture. The noise function can be described as:

$$f(x) = \sum_{n=0}^{N} A_n \cdot g(B_n \cdot x)$$

Where f(x) is the Perlin noise function, N is the number of octaves, A_n is the amplitude for the nth octave, g(x) is a gradient noise function, and Bn is the frequency for the nth octave.

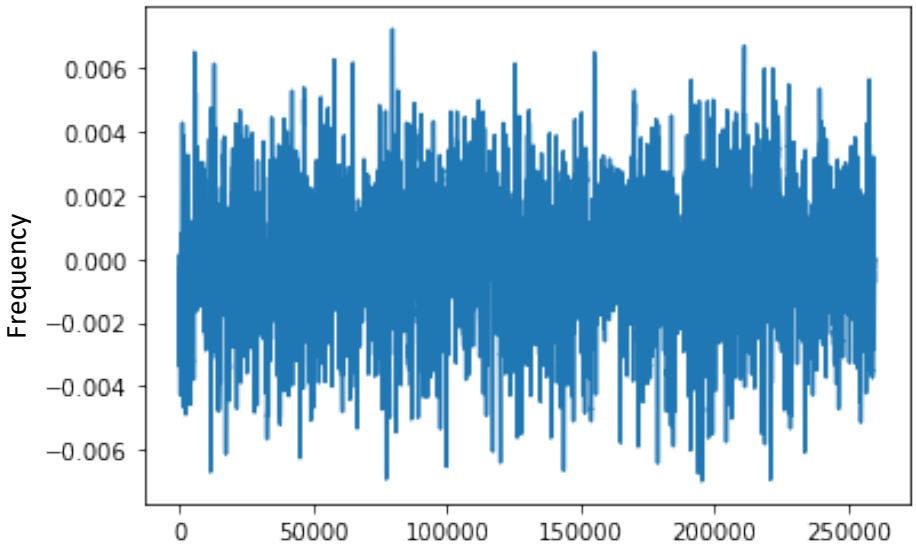

Figure 58: Perlin noise based on GMM

Summary

In this section, the reliable method to augment data based on the real data that is captured was summarised and discussed. The one-dimensional Perlin noise model, when applied to the normalised surface data, produces the simulated data successfully. Figure 59 demonstrates the resultant data and a comparison of the Z-axis distribution between the real-world data and the captured data. Figure 59 shows the resultant data and a comparison of the Z-axis distribution between real-world data and captured data. Augmented data is able to mimic the surface texture of real-world data. This will help in forming a substantial dataset for the feature extraction techniques to be trained and evaluated.

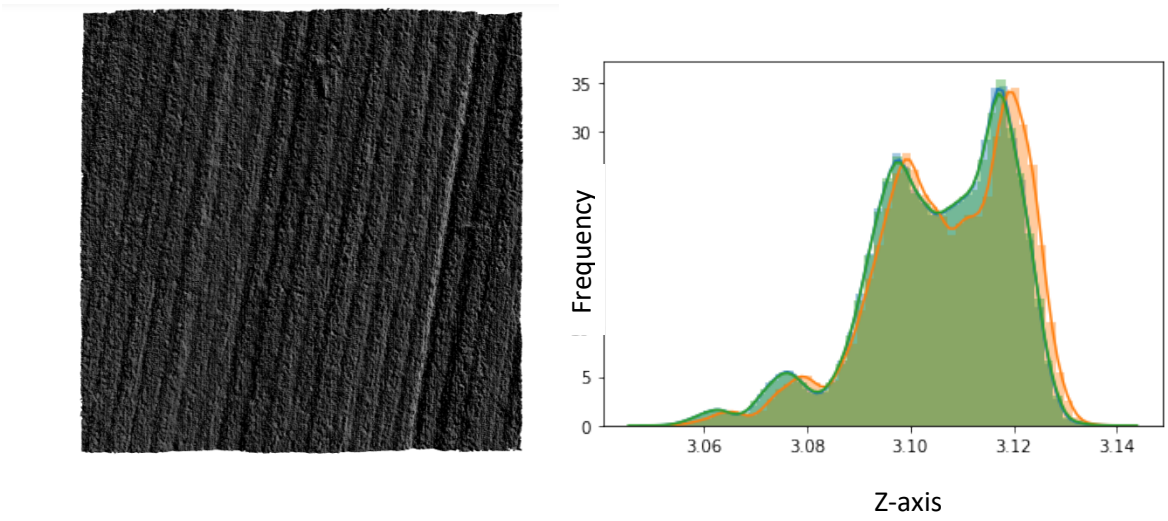

Figure 59: (left) Generated data (right) Z-axis distribution of real-world data (orange) compared to generated data (green)

7.5. Feature Extraction

The feature extraction techniques aim to successfully extract information at different levels of authentication as established in Section 6.1. These features are extracted using a combination of 2D and 3D analysis as described in Section 6.3.

7.5.1. 3D-2D conversion – Ray tracing

Section 6.3 highlights the rationale behind extracting features using different techniques. As the data captured is a 3D point cloud, it needs to be converted into 2D data for some levels of authentication. One method for performing this conversion is ray tracing, which can be used to generate a height map of the given point cloud data.

Ray tracing is a computer graphics technique that simulates the path of light rays through a 3D scene, enabling the creation of photorealistic images by accounting for shadows, reflections, and refractions. In the context of 3D-2D

conversion, ray tracing can be employed to generate a height map that represents the surface of the object, preserving the z-axis information of the original point cloud. This is achieved by directly mapping the projections of the point cloud on the ray-traced surface, as illustrated in Figure 60: Ray tracing.

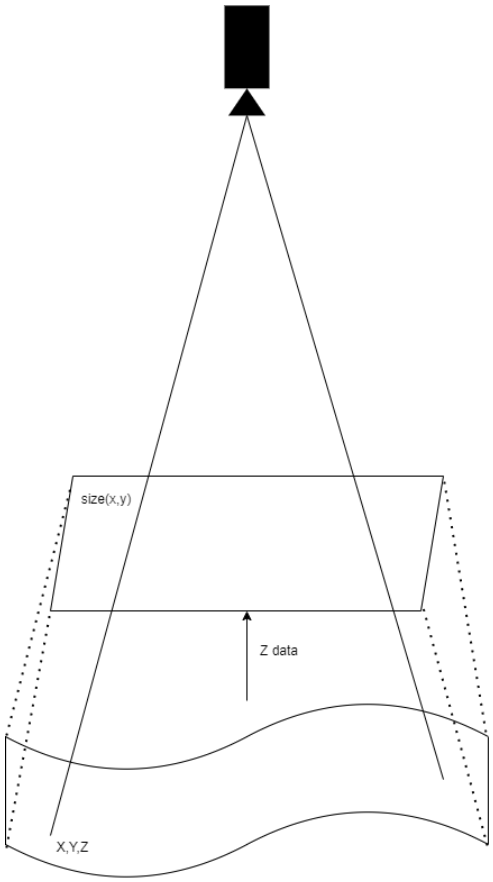

Figure 60: Ray tracing

Some of the results of this technique are in Figure 61.

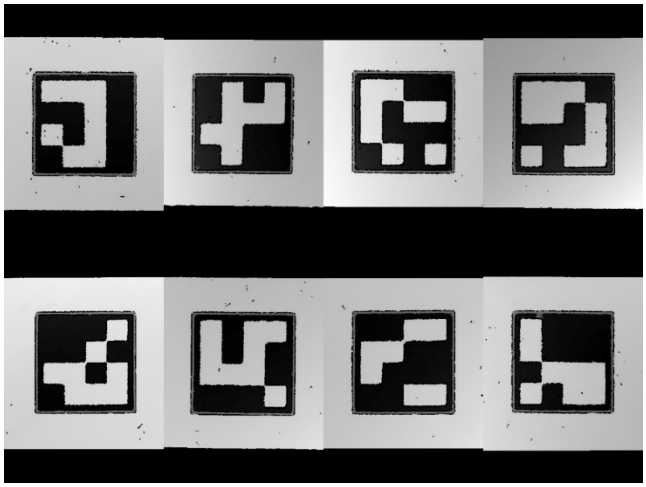

Figure 61: Ray-traced image of DLP test object

Using ray tracing for 3D-2D conversion offers several benefits. Firstly, it enables the whole surface to be resampled to the desired image size without losing any z-axis information. This is particularly important for maintaining the fidelity of surface features when converting from 3D to 2D representations. Secondly, ray tracing provides a means to incorporate realistic lighting and shading into the 2D image, which can further enhance the visibility of surface features and improve the overall quality of the resulting 2D representation.

However, it is important to note that ray tracing can be computationally expensive, particularly for high-resolution images and complex 3D scenes. As a result, efficient implementations of ray tracing algorithms, such as parallel processing and adaptive sampling, may be necessary to ensure reasonable processing times when converting 3D point clouds to 2D images for feature extraction and authentication purposes.

In terms of authentication, the ray-traced 2D images can provide different levels of information based on the resolution and quality of the generated height map:

Level 1 Authentication: At this level, the ray-traced 2D image can be used for basic pattern recognition and texture analysis, similar to the QR code verification example. It can also be utilised for simple feature extraction and comparison, allowing for a basic level of authentication and object identification.

Level 2 Authentication: At the second level, the ray-traced 2D image can provide more detailed information about the surface texture and complex patterns. The improved visibility of surface features, enabled by realistic lighting and shading, can enhance the authentication process by allowing for more sophisticated feature extraction and comparison techniques. This level of authentication can potentially identify specific printing techniques and materials used in the object's manufacturing process.

Level 3 Authentication: At the highest level of authentication, the ray-traced 2D image can reveal intricate details about the object's surface, including microscopic structures and unique surface profiles. By leveraging advanced feature extraction methods and statistical analysis techniques, this level of authentication can provide a higher degree of confidence in the identification and verification of 3D-printed objects.

In summary, ray tracing for 3D-2D conversion plays a crucial role in the authentication process by enabling the extraction of features from different levels of detail. This flexibility allows for a more comprehensive and robust authentication framework that can accommodate various applications and security requirements. Ray tracing can

produce 2D images that more accurately reproduce the surface characteristics of the 3D object due to the improved visibility of surface features made possible by realistic lighting and shading. Effective authentication requires an accurate representation of surface features like surface roughness, gradients, and subtle height variations. These features in the 2D image are highlighted by realistic lighting and shading, which helps to make them more noticeable and facilitates more precise feature extraction and comparison during the authentication process.

7.5.2. Level 1 Authentication: Basic Surface Patterns and Texture Analysis

2D Level 1 - 2D authentication based on detection of 2D ArUco QR code or embedded ArUco marker via the authentication information stored within the 3D QR code and embedded ArUco marker

At level 1, only the 3D QR code is scanned and verified for authentication. The information stored within the QR code can also be used to provide essential authentication information. In this case, as described in Section 7.1, ArUco numbers are encoded.

To implement the ArUco detection, a simple convolutional neural network (CNN) based AI is utilised in conjunction with the ArUco 4x4 dictionary. The CNN is designed to recognize and decode the ArUco markers embedded in the QR code. The architecture of the CNN consists of multiple convolutional layers, pooling layers, and fully connected layers, which are trained to detect the presence of the ArUco markers and classify them according to the 4x4 dictionary. To implement the ArUco detection, a simple convolutional neural network (CNN) based AI is utilised in conjunction with the ArUco 4x4 dictionary. The CNN is designed to recognise and decode the ArUco markers embedded in the QR code. The architecture of the CNN consists of multiple convolutional layers, pooling layers, and fully connected layers, which are trained to detect the presence of the ArUco markers and classify them according to the 4x4 dictionary.

CNN was implemented because standard ArUco detection algorithms were unable to decode the glyphs effectively. Template matching and other traditional algorithms were found to be less effective in our experiments, due to the blurred edges on the printed surfaces and the high level of noise in the captured data. This challenge is compounded by the intricate textures and complex patterns found in 3D-printed objects, which standard algorithms struggled to accurately interpret. As a result, a CNN was chosen due to its proven robustness and adaptability across a wide range of conditions, including lighting and occlusion variations, resulting in more reliable detection and decoding of the embedded ArUco markers.

The detection process begins by pre-processing the captured image to enhance the visibility of the ArUco markers. This may involve applying filters, such as Gaussian blur or contrast stretching, to improve the image quality. The pre-processed image is then fed into the CNN, which detects the presence of the ArUco markers and decodes their encoded information.

Upon successful detection of the Level 1 authentication markers, the CNN also provides additional information, such as the translation and angle of the scanned QR code. This information is crucial for Level 2 and 3 authentications, as it enables the system to accurately align and analyse the 3D surface data in subsequent stages.

The ArUco detection framework can be implemented using popular computer vision libraries, such as OpenCV or TensorFlow, which provide built-in functions for training and deploying CNN-based object detection models. By leveraging these libraries, the Level 1 authentication system can be efficiently designed, tested, and optimized to achieve robust and accurate ArUco marker detection.

Figure 62: The detection of 2D ArUco QR code or embedded ArUco marker using the custom trained convolutional neural network (CNN) model.

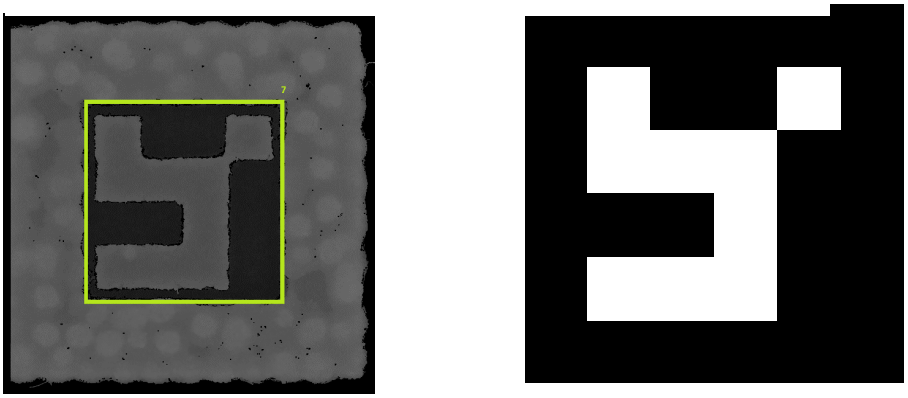

Figure 63: The detected ArUco marker on the 3D printed object (left) and the ArUco marker from the ArUco dictionary with the corresponding pattern - marker (right)

3D Level 1 - 3D authentication based on detection of the ArUco QR code via advanced geometrical features such as curvature and normal estimation stored within the ArUco QR code

At Level 1 authentication, the goal is to extract simple geometric features such as shape and size from the 3D object. As discussed in Section 6, in the case of ArUco QR codes, the additional complexity of extracting more advanced features does not provide extra useful information for authentication. This is because the ArUco QR codes themselves store the necessary authentication information in their encoded patterns. Extracting more advanced features (e.g., curvature, normal estimation) from the ArUco QR code may not add significant value to the authentication process, as the authentication information is already encoded in the QR code itself.

Therefore, for Level 1 authentication, focusing on simple geometric features is sufficient for ArUco QR codes. More advanced feature extraction methods may not provide additional benefits in this context, as the primary authentication information is contained in the encoded patterns of the QR codes.

Statistical Level 1 - Authentication based on detection of the ArUco QR code via the statistical information about shape, size, and orientation of the ArUco QR code

Using Python's OpenCV library to extract statistical information about an ArUco QR code's shape, size, and orientation can enhance Level 1 security. Using the 2D ArUco detection code used above, the input image containing the glyph is analysed. Next, the ArUco QR code detected in the image is used to compute its geometric features, such as size, orientation, and centroid.

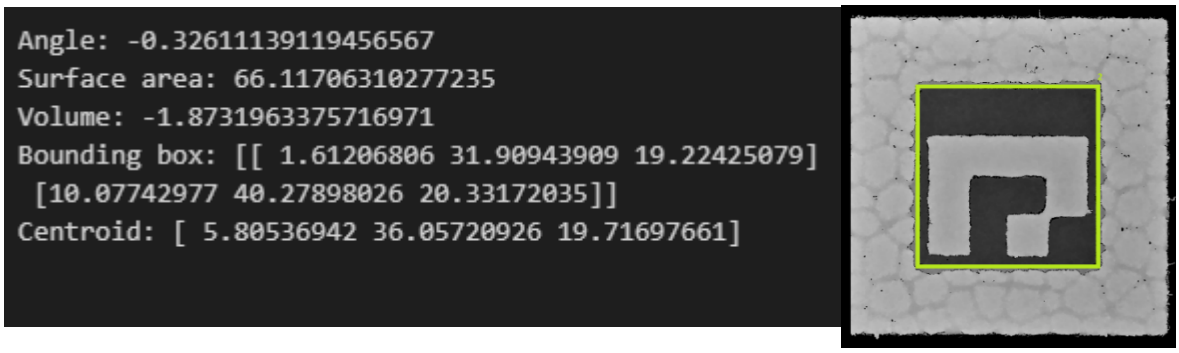

Figure 64: An example about the statistical information about the shape, size, and orientation of the ArUco QR code.

The size of the QR code can provide an estimate of its scale, while the orientation helps determine its rotation relative to the image plane. The centroid gives an indication of the QR code's position within the image.

The visual output highlights the detected ArUco QR code, its corners, and centroid. This visualization aids in understanding the code's orientation and position in the image, which can be useful for aligning and analysing the 3D surface data in subsequent authentication stages. Multiple runs of the code were performed on the same object with added noise to simulate realistic data capture conditions. The results demonstrated an accuracy of 87% in obtaining values within a 1% error margin. Furthermore, each scan during the data capture process produced unique results, showcasing the robustness of the method in extracting features from 3D objects under varying conditions. This highlights the potential of the proposed approach for use in practical authentication and identification applications.

Summary

In the Level 1 authentication stage, the research focused on extracting basic features from the ArUco QR code to provide essential information for object identification and verification. The experiment involved utilising Python and OpenCV to analyse the QR code's shape, size, and orientation. The detection and decoding of the ArUco QR code were facilitated by a Convolutional Neural Network (CNN) that effectively recognised and classified the markers embedded in the code. The computed geometric features enabled a better understanding of the QR code's scale, rotation, and position within the image.

The visual output generated in the experiment highlighted the detected ArUco QR code, its corners, and its centroid. This visualization provided valuable insights into the code's orientation and position in the image, which could be useful for aligning and analysing the 3D surface data in subsequent authentication stages. The successful extraction of basic features at Level 1 authentication laid the groundwork for more advanced feature extraction and comparison techniques at higher authentication levels.

Each scan during data capture produced different results, demonstrating the system's sensitivity to variations in the scanning environment and the object's placement. This variability underscores the robustness of the approach, as the system was still able to achieve an accuracy of 87% in identifying and decoding the ArUco QR codes, even with added noise simulating realistic conditions. This accuracy level within a 1% error margin indicates the method's reliability in extracting and processing features from 3D objects under varying conditions, showcasing its potential for practical authentication and identification applications.

Overall, the Level 1 authentication experiment demonstrated the feasibility of extracting essential geometric and statistical features from an ArUco QR code for basic authentication purposes. This approach contributes to the development of a comprehensive and robust authentication framework that can accommodate various applications and security requirements in the field of 3D printing and object identification.

7.5.3. Level 2 Authentication: Detailed Surface Texture and Complex Patterns

2D Level 2 - 2D authentication based on detailed surface texture and complex patterns, via analysis of the advanced texture patterns within the 2D representation of the object

At Level 2, advanced texture pattern classification methods, such as Local Binary Patterns (LBP) and Gabor filters, can be applied to the 2D representation of the object. These methods allow for more elaborate geometrical feature analysis and can provide insights into complex patterns and structures present on the surface.

The experiment involved applying the LBP method to analyse the local texture patterns within the 2D representation of the object. This approach compared the intensity of each pixel to its neighbouring pixels, producing binary patterns that served as texture descriptors.

The LBP features visualization highlighted the local structures and patterns within the 2D image, revealing intricate details that were not apparent in the original image. This enhanced texture representation allowed for more accurate classification and comparison of surface properties, contributing to a more reliable authentication process.

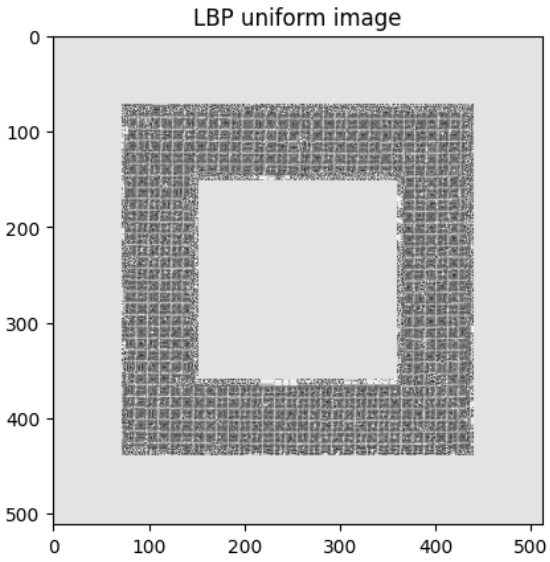

Figure 65: LBP uniform image

Another approach employed in the experiment was the use of Gabor filters to analyse the frequency and orientation information present in the 2D image. Gabor filters are a set of linear filters that can capture localised frequency information in different orientations.

The Gabor filters provided different views of the 2D image at various orientations, enabling a more comprehensive analysis of the texture and frequency information. By applying the Gabor filters, the resulting images are used for further analysis and comparison, allowing for the identification of similarities and differences in the texture and frequency information between captured data and ground truth. This multi-orientation approach contributed to a more robust authentication process by capturing a broader range of surface properties.

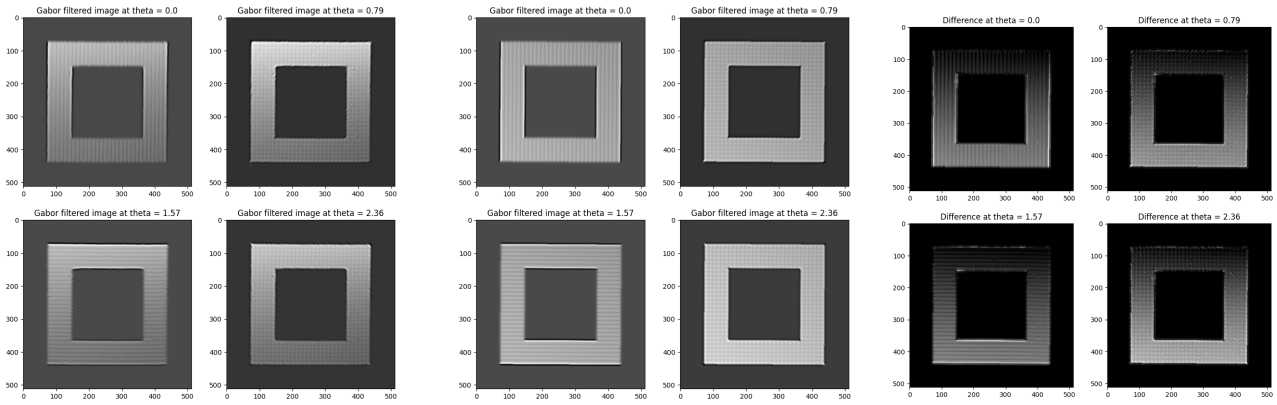

Figure 66: Gabor filter at various angles applied to captured data (left). Gabor filter at various angles applied to ground truth data (middle) Difference between filtered images (right)

The results of the Level 2 authentication experiments demonstrated the effectiveness of LBP and Gabor filters in extracting detailed texture and frequency information from the 2D representation of the object. The visual outputs generated by these methods revealed complex patterns and structures that were not evident in the original image, offering valuable insights for object authentication.

The successful application of these advanced texture pattern classification methods at Level 2 authentication reinforced the robustness of the proposed authentication framework. By incorporating both LBP and Gabor filters, the authentication process was able to capture a wider range of surface properties, leading to more accurate and reliable identification and verification of 3D-printed objects.

3D Level 2 - 3D Authentication based on 3D point cloud datasets and the deep learning architecture for point cloud classification and detection of geometrical features and patterns

For 3D data, point cloud classification techniques, such as PointNet and Normal Estimation, can be employed to analyse more detailed surface features. Advanced mesh parameter analysis can include crease points, border points, and curvature analysis, providing a deeper understanding of the object's 3D structure.

In the Level 2 authentication stage, the research investigated point cloud classification techniques, specifically PointNet and Normal Estimation, as well as advanced mesh parameter analysis methods, such as crease points, border points, and curvature analysis. These methods were applied to 3D data to extract and analyse more detailed surface features, providing a deeper understanding of the object's 3D structure and enhancing the authentication process.

PointNet

The experiment utilised PointNet, a deep learning architecture for point cloud classification, to analyse and classify the 3D point cloud data. PointNet has the ability to learn complex patterns and features within the point cloud data, providing valuable insights into the 3D structure.

The PointNet classification results provided valuable information on the 3D point cloud data, revealing complex patterns and features that contributed to a more accurate and reliable authentication process.

To provide a complete understanding of the PointNet classification process, it is essential to describe the training process of the PointNet model. In this experiment, we utilised the Keras deep learning library for training the PointNet model.

PointNet Training

Before applying the PointNet model to the classification task, it was necessary to train the model using a labelled dataset of 3D point clouds. In this experiment, we used the dataset created for Level 2 classification, which is the dataset comprising Elaborate geometrical features. The dataset contains 8 categories, with each scan represented by a point cloud.

During the training process, the PointNet model learns to recognise and classify the 8 elaborate geometrical features present on the captured dataset. The model's performance is monitored using the validation data, and the training

is stopped when the validation loss stops improving for 10 consecutive epochs. The best-performing model, as determined by the validation accuracy, is saved as a checkpoint.

Once the PointNet model is trained, it can be applied to the classification task as described in the previous section 6.3. The trained model is capable of recognising patterns and features within the 3D point cloud data with an accuracy of 91% (Figure 68: Training output), providing valuable insights into the 3D structure for Level 2 authentication.

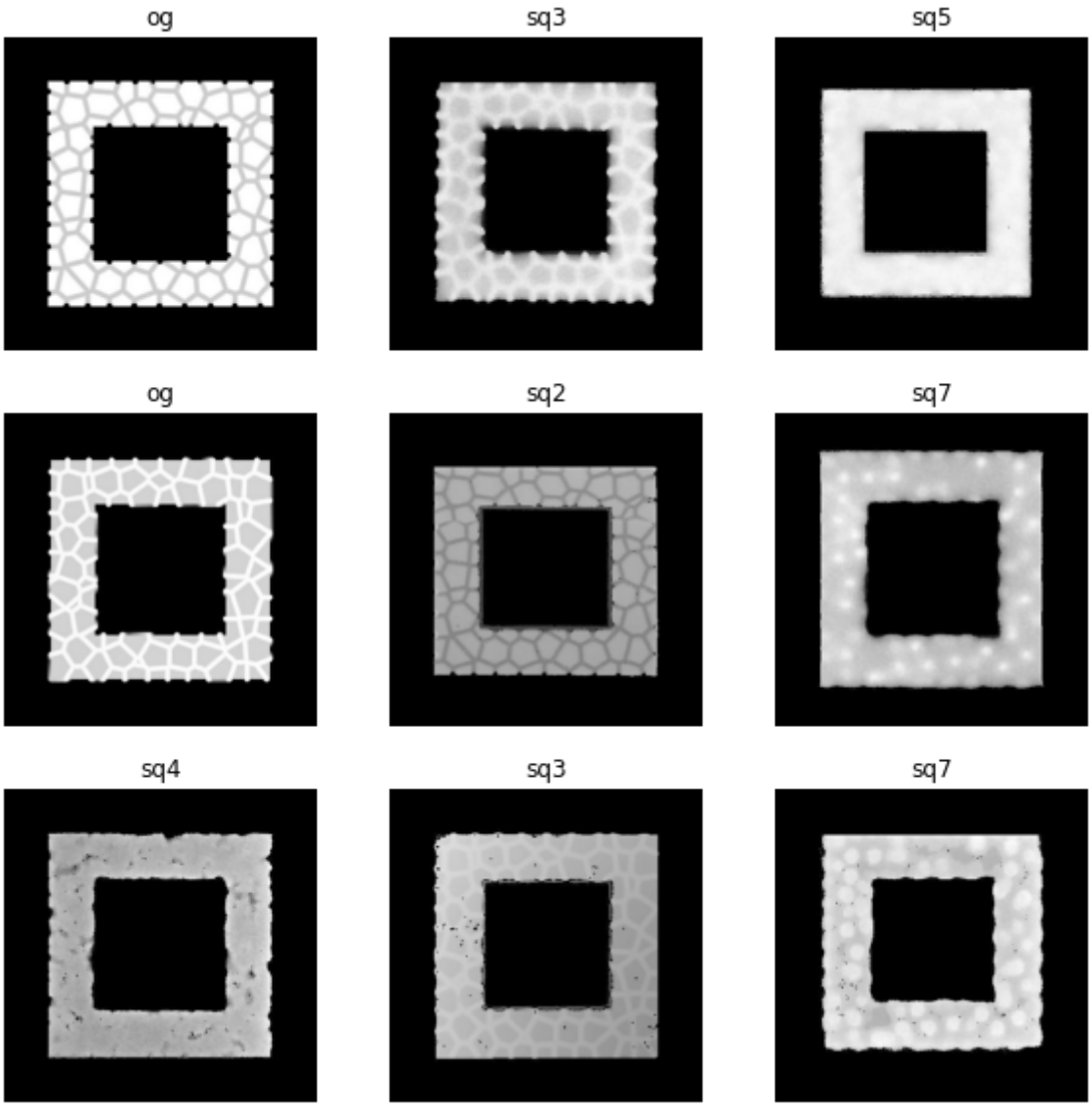

Figure 67: Sample results

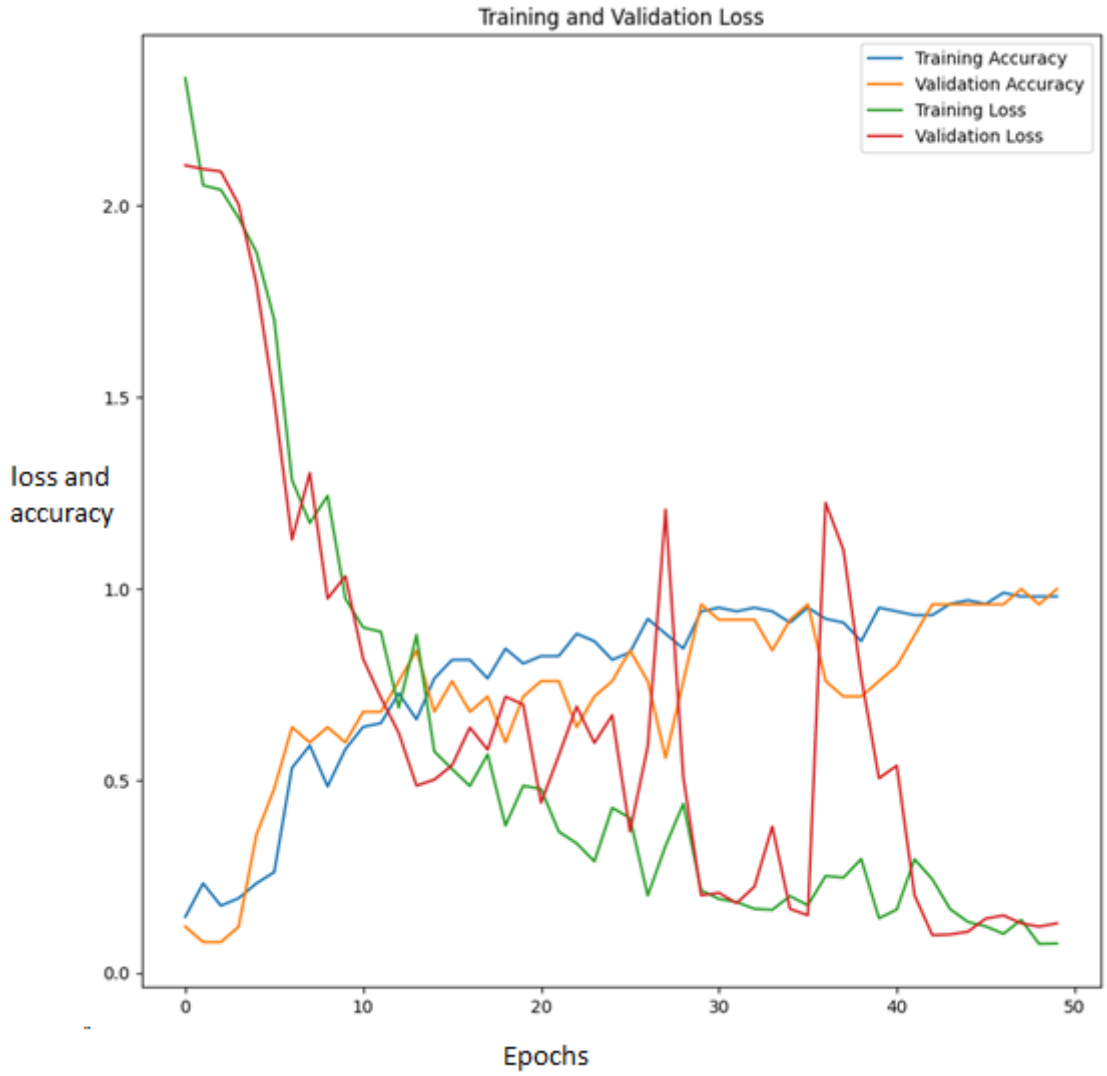

Figure 68: Training output for PointNet on classification of elaborate geometrical features

The classification results showed that the PointNet model was able to distinguish between various classes of objects, such as different types of geometric shapes or categories of manufacturing defects. Moreover, the model demonstrated a high level of precision in detecting minute differences in surface textures, capturing even subtle variations in the object's surface that may result from different manufacturing processes or materials. These insights into the 3D structure contribute to a more accurate and reliable authentication process.

In addition to the overall accuracy of 91%, the model's performance was further evaluated by examining the confusion matrix, which provided a detailed view of the classification results. The confusion matrix revealed that the model was able to correctly classify most objects, with only a few misclassifications occurring between objects with similar surface properties or structures. This analysis helped identify areas where the model could be further improved, such as fine-tuning the architecture or adjusting the training parameters.

Furthermore, the PointNet model's robustness was assessed by testing its performance on unseen data or objects with varying levels of noise. The model demonstrated its ability to maintain a high level of accuracy even under challenging conditions, highlighting its potential for use in real-world applications where data may be noisy or incomplete.

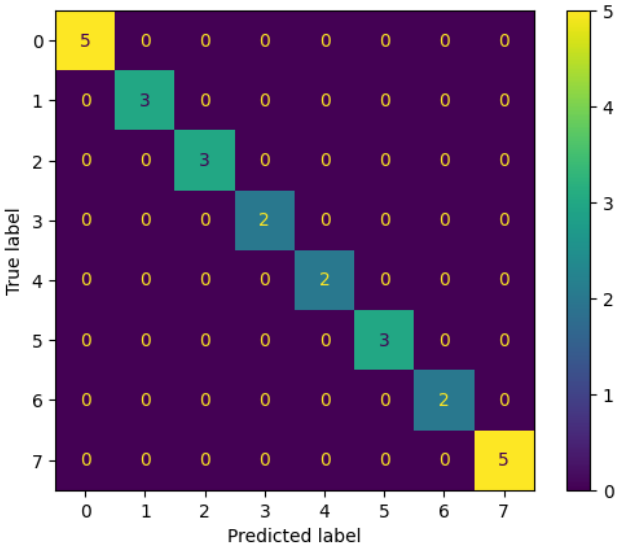

Figure 69: Confusion Matrix for Level 2 texture detection

In summary, the PointNet model's successful application in the classification task demonstrated its effectiveness in recognising patterns and features within the 3D point cloud data. The detailed results, such as the confusion matrix and robustness analysis, provided valuable insights into the model's performance, contributing to the development of a reliable Level 2 authentication process for 3D-printed objects.

Normal Estimation

Another approach employed in the experiment was normal estimation, a technique for estimating the normal vectors at each point within the point cloud. This information is crucial for advanced mesh parameter analysis and can provide insights into the surface properties and curvature of the 3D object.

The normal estimation results provided a detailed representation of the object's surface properties and curvature, contributing to a more in-depth analysis of the 3D structure.

The results of the Level 2 authentication experiments using PointNet, and normal estimation demonstrated their effectiveness in extracting and analysing complex patterns and features from the 3D point cloud data. The visual

outputs generated by these methods revealed intricate details of the object's 3D structure, providing valuable insights for object authentication.

The successful application of these point cloud classification techniques and advanced mesh parameter analysis methods at Level 2 authentication reinforced the robustness of the proposed authentication framework. By incorporating both PointNet and normal estimation, the authentication process was able to capture a wider range of 3D surface properties, leading to more accurate and reliable identification and verification of 3D-printed objects.

Statistical Level 2 - Authentication based on the statistical distribution of geometrical features on the 3D surface, and to identification of similarities and differences between the surface textures

At Level 2, the researchers employed Gaussian Mixture Models (GMM) to model the distribution of features on the object's surface. GMM is a probabilistic model that represents the distribution of data as a combination of multiple Gaussian distributions. By comparing the GMMs of different objects, the researchers were able to identify similarities and differences between their surface textures, providing more robust authentication results. Based on previously presented Gaussian Mixture Modelling (GMM) techniques for augmented surface generation in Section 7.4, a statistical model of the elaborate geometrical feature can be obtained. The GMMs obtained are all unique with slight variations between similar patterns. This is convincing evidence to support my hypothesis of all 3D-printed parts are unique.

The researchers analysed the GMMs of the surface features and found that they are unique with slight variations between similar patterns. Figures 68 and 69 show the GMM results and the GGM score of the entire dataset.

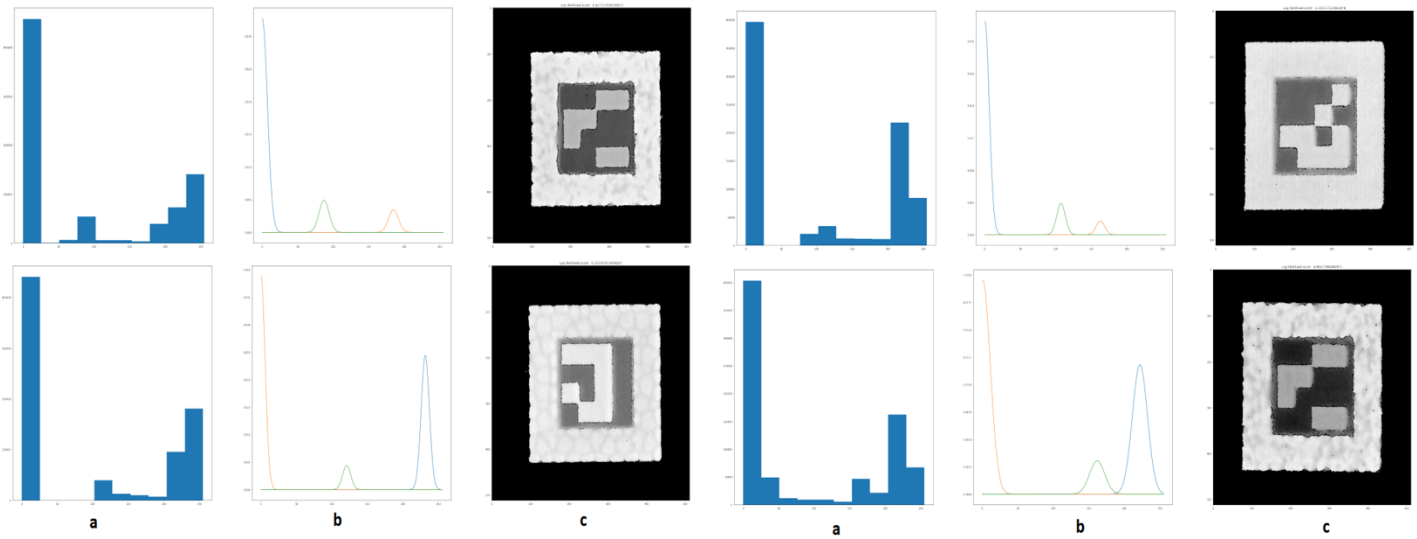

Figure 70: (a): Z-axis distribution of the elaborate geometrical feature (y-axis: frequency; x-axis: z-axis distribution of elaborate geometrical feature). (b): GMM (y-axis: frequency; x-axis: z-axis distribution of elaborate geometrical feature). (c) 2D raytracing of captured data.

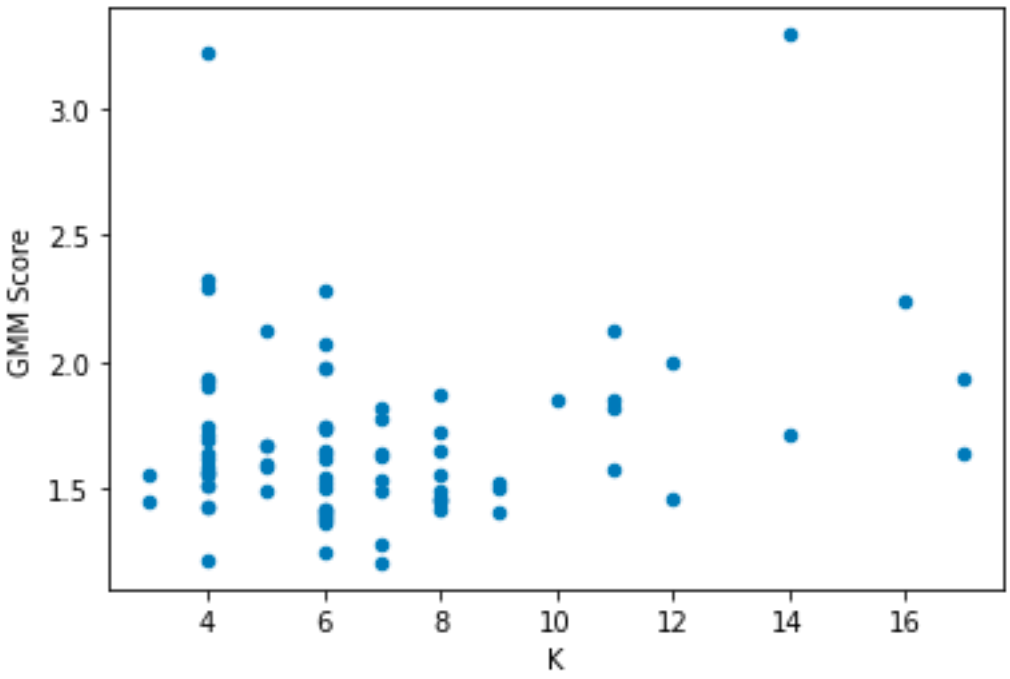

Figure 71: The GGM score of the entire dataset. It illustrates the GGM scores for all the objects in the dataset, with the y-axis representing the score and the x-axis representing the object index. The GGM scores provide a quantitative measure of similarity between the surface textures of the objects, with lower scores indicating greater similarity and higher scores indicating more significant differences. By observing the distribution of scores, researchers can gain insights into the degree of variation between objects and the effectiveness of GMM-based authentication.

By comparing the GMMs of different objects, the researchers can assess the similarities and differences between their surface textures, which can be used to improve the authentication process at Level 2. For example, if two objects have very similar GMMs, it might indicate that they share a common manufacturing process or material, making it more challenging to differentiate between them based on surface features alone.

On the other hand, if the GMMs of two objects are significantly different, it could suggest that they were produced using different techniques or materials, which could provide a basis for distinguishing between them and potentially enhancing the authentication process.

In conclusion, the use of Gaussian Mixture Models at Level 2 enables a more detailed analysis of the object's surface features, providing valuable insights into the patterns and structures present on the surface. This additional information can improve the robustness of the authentication process, allowing for a more accurate assessment of the object's identity and origin.

Summary

During the Level 2 authentication phase, the study investigated sophisticated techniques for classifying texture patterns in 2D data, such as Local Binary Patterns (LBP) and Gabor filters, as well as point cloud classification methods and advanced mesh parameter analysis techniques for 3D data, such as PointNet and normal estimation. These techniques proved to be efficacious in extracting intricate texture, frequency, and surface information from the object's representation, thereby exposing intricate patterns and structures that were not discernible in the original image or point cloud data.

The framework also includes a deeper analysis of the printing methods, as discussed in detail in Section 8, which allows for an enhanced understanding of the object's manufacturing process. This comprehensive approach to data analysis supports a robust authentication process by providing multiple layers of verification.

The robustness of the proposed authentication framework, as outlined in Section 8, is significantly enhanced by the effective utilization of LBP, Gabor filters, PointNet, and normal estimation during Level 2 authentication. The integration of these sophisticated methodologies has broadened the scope of authentication to include a wide range of surface characteristics, resulting in increased precision and reliability in the identification and verification of three-dimensional printed entities.

Moreover, Gaussian Mixture Models (GMM) were employed at Level 2 to model the distribution of surface characteristics, providing significant insights into the surface's patterns and structures. The comparison of GMMs among different objects aided in identifying both similarities and differences in surface textures, advancing the authentication process.

In addition to the modalities explored, the framework, as elaborated upon in Section 8, leverages machine learning classifiers to discern between the surface textures characteristic of different printing methods.

The experiments on Level 2 authentication have demonstrated the capability of sophisticated feature extraction and analysis techniques to reveal intricate details regarding the structure and surface properties of objects. This has greatly contributed to the formulation of a comprehensive and reliable authentication framework for the identification of 3D-printed objects, as thoroughly discussed in Section 8. The integration of these advanced

techniques into the framework solidifies its adaptability and scalability in response to the continuous advancements in printing technologies and authentication needs.

7.5.4. Level 3 Authentication: Microscopic Structures and Unique Surface Profiles

2D Level 3 - 2D authentication based on Microscopic Structures and Unique Surface Profiles of 3D printed objects such as those related to material properties and internal structures

At Level 3, advanced authentication techniques aim to capture microscopic details and unique surface profiles of the 3D-printed object. Intrinsic surface features, such as those related to material properties and internal structures, are particularly challenging to extract from 2D images due to their complexity and lack of explicit visual cues. Intrinsic features are often related to the shape and texture of the surface, which can only be properly captured in 3D space.

To demonstrate the difficulty of extracting intrinsic surface features using 2D features, a simple experiment can be conducted. A set of 2D images with varying resolutions is generated from a 3D object using ray tracing. The images are then processed using basic feature extraction techniques, such as LBP and Gabor filters, to extract texture and pattern information.

The results show that, while some surface features can be captured in the 2D images, the intrinsic details of the object are largely lost. Subtle variations in surface curvature and texture, which are important for identifying unique surface profiles, are not well-represented in the 2D features. This highlights the limitations of relying solely on 2D data for advanced authentication applications.

The visual output of the experiment clearly shows that while some texture and pattern information can be extracted from the 2D images, the subtle variations in surface curvature and texture, which are crucial for identifying unique surface profiles, are not well-captured. This highlights the limitations of relying solely on 2D data for advanced authentication applications, particularly when it comes to capturing intrinsic surface features.

3D Level 3 - 3D authentication based on Microscopic Structures and Unique Surface Profiles with feature extraction and classification, and computed surface normals from point cloud data

This section will delve into the experiments carried out at Level 3, with a particular emphasis on sophisticated 3D methodologies employed for the purpose of feature extraction and classification. The experimental techniques

employed in this study comprise Normal Estimation and Octrees. The procedural aspects of executing these methodologies will be expounded upon, accompanied by a delineation of the anticipated outcomes.

To obtain the surface normals from point cloud data, a numerical differentiation technique, such as the Principal Component Analysis (PCA), was applied. This technique was carefully implemented, and additional pre-processing steps, such as smoothing and outlier removal, were used to preserve the accuracy of the extracted normals.

Normal estimation is a computational method utilised to determine the normal vectors for individual points within a point cloud. These normal vectors are indicative of the surface orientation at each respective point. Normal vectors offer insights into the surface's local geometry and can be utilised for feature extraction and object authentication. Through the process of approximating the normal vectors of a three-dimensional printed entity, it is anticipated that valuable knowledge regarding the specific surface characteristics will be obtained. This knowledge can subsequently be utilised to differentiate between authentic and counterfeit objects.

As shown in Figure 70, Normal Estimation was applied to the entire test object, providing a visualization of the normal vectors for each point in the point cloud.

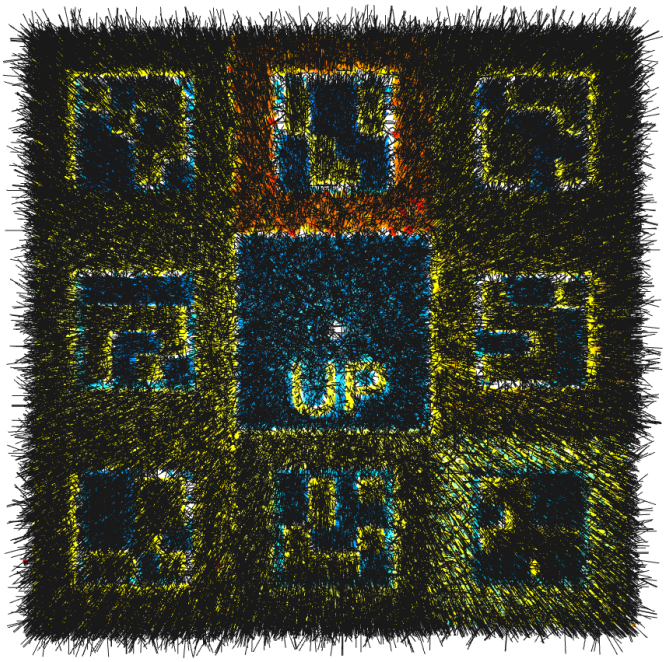

Figure 72: Normal Estimation of the whole test object

Octrees are a type of hierarchical data structure that is commonly employed for the purpose of efficiently representing point cloud data in three dimensions. The process involves partitioning the three-dimensional space

into octants, followed by iterative subdivision of these octants until the desired level of intricacy is attained. The utilisation of Octrees in feature extraction enables the effective processing and analysis of point cloud data of 3D-printed objects. It is anticipated that the utilisation of Octree representation will facilitate the identification of distinct spatial patterns within the object, thereby serving as a means of authentication.

As seen in Figure 71, the Octree output displays the hierarchical data structure representing the point cloud data of the 3D-printed object.

```
Octree with origin: [-1.02659, -1.0375, -2.85924], size: 46.2193, max_depth: 30
```

Figure 73: Octree output

By implementing sophisticated 3D methodologies, distinctive and intricate attributes can be derived from objects that have been printed in 3D. The aforementioned characteristics possess the potential to augment the process of authentication and furnish an elevated degree of assurance in discerning authentic entities.

Upon comparing the methodologies, it becomes evident that each approach presents distinct advantages and disadvantages. Normal Estimation is a technique that offers valuable insights into the local properties of a surface. This information can be utilised to distinguish between objects that exhibit different surface qualities or have been produced using distinct printing methods. Octrees provide a proficient approach for the processing and analysis of point cloud data, facilitating the detection of distinctive spatial patterns within the object.

The approach to ascertain the optimal authentication method for 3D-printed objects involves the utilisation of a blend of these techniques. Through the utilisation of the unique advantages offered by each individual method, it is possible to establish an authentication process that is both more resilient and all-encompassing in nature. The integration of Normal Estimation and Octrees has the potential to yield comprehensive insights into the object's local geometry and spatial arrangements, thereby enhancing the precision of the authentication procedure.

Statistical Level 3 - Authentication based on sophisticated statistical methodologies employed for feature extraction and classification

This section will delve into the experiments carried out at Level 3, with a particular emphasis on sophisticated statistical methodologies employed for feature extraction and classification. The experimental techniques employed in this study comprise Curvature Estimation, Signed Distance Function (SDF), Fast Point Feature Histogram (FPFH),

and Wavelet Transform. The present study aims to explicate the procedural aspects of executing the aforementioned methodologies, accompanied by a comprehensive elucidation of the anticipated outcomes.

The local curvature of each point on the surface of the three-dimensional printed object is determined using the curvature estimation method. In this study, the average curvature at each point was determined by calculating mean curvature, which produced a single scalar value. Curvature values were used to identify distinctive surface characteristics that are crucial to the authentication process. The estimation of an object's surface curvature provided important insights into the distinctive shape characteristics that separate genuine objects from counterfeit ones. As shown in Figure 72, the output of Curvature Estimation displays the calculated mean curvature values for the points on the object's surface.

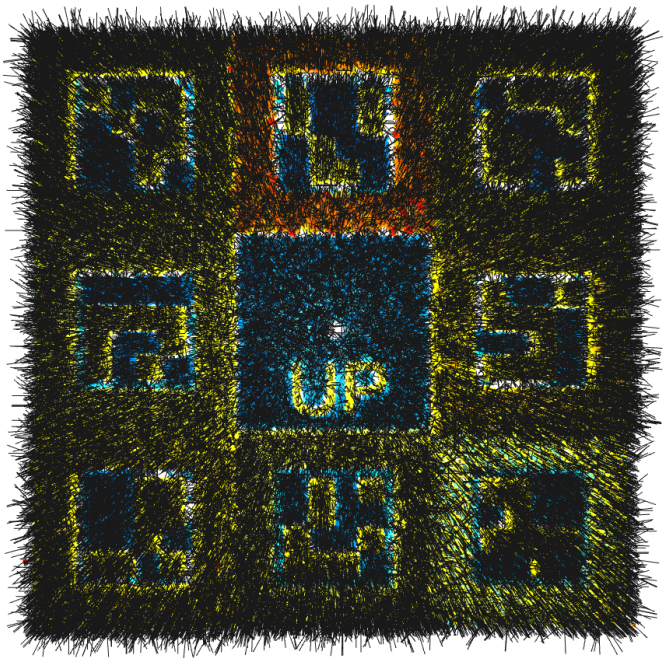

```
[2.9290968  2.46683347 2.53119056 ... 9.99303878 5.88614614 6.64378732]
```

Figure 74: Curvature Estimation Output

The Signed Distance Function (SDF) is a mathematical tool that calculates the distance between a reference plane and every point on the surface of an object. This method offers a concise way to represent the shape of the object. The aforementioned data may be utilised for the purpose of extracting features and authenticating objects. The

utilisation of the SDF is anticipated to yield a depiction of the comprehensive structure of the entity, which can be employed to distinguish and discriminate between authentic and fraudulent entities.

The Fast Point Feature Histogram (FPFH) is a technique utilised to extract the local geometric characteristics of a point cloud. This method is applicable in the fields of object recognition and authentication. The FPFH technique produces a histogram of geometric characteristics for individual points within a given point cloud. It is anticipated that these histograms will furnish an intricate depiction of the nearby geometry, which can be leveraged to recognise and verify 3D-printed items. By representing the Fast Point Feature Histogram (FPFH) characteristics as hues, one is effectively examining a three-dimensional (3D) entity's point cloud, wherein each point is chromatically differentiated according to its proximate geometric attributes. The FPFH characteristics extract data pertaining to the immediate geometry surrounding individual points within the point cloud, which is then depicted as a histogram.

Through the process of assigning a colour map to the FPFH features, it is possible to visually represent the variations of these features throughout the object's surface. Points that exhibit analogous Fast Point Feature Histogram (FPFH) characteristics will display comparable hues, thus signifying their akin local geometric attributes. Figure 73 presents the visualization of the Fast Point Feature Histogram, wherein the FPFH features are represented as hues in the 3D point cloud.

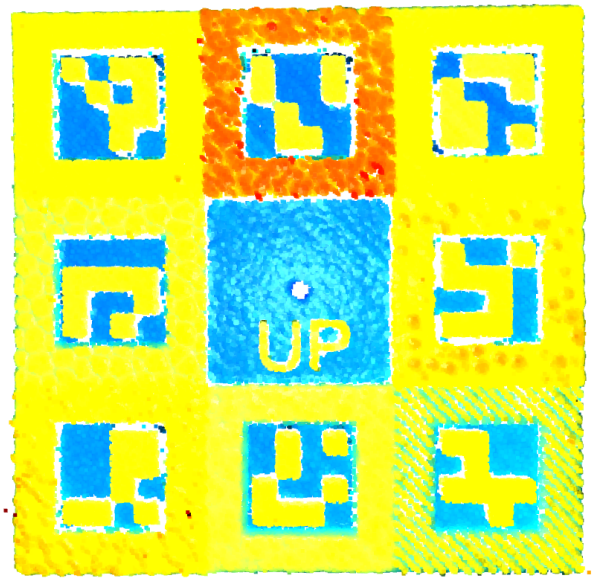

Figure 75: Fast Point Feature Histogram

The Wavelet Transform methodology can be utilised to analyse point clouds and extract features at multiple scales. This approach has potential applications in object authentication. The utilisation of wavelets to decompose point

cloud data into multiple frequency bands is anticipated to enable the capture of distinct shape characteristics of an object at varying scales. This approach is expected to yield a more comprehensive representation of the geometry of the object. Figure 74 displays the Wavelet Transform output, showcasing the extracted features at different scales.

```
Level 1 coefficients:
[[62.40693705 61.98504777 28.89565141]
 [62.27144943 62.14311261 28.83541716]
 [62.04564212 61.75924046 28.88407148]
 ...
 [38.85507175 46.6526258  27.98004248]
 [41.42929336 22.3330098  27.42698547]
 [25.50976781 39.49448327 27.33871176]]
Level 2 coefficients:
[[ 4.51598424e-02 -4.51598424e-02  1.11065375e-02]
 [-1.80647462e-01  2.25799212e-02  1.38808117e-02]
 [ 1.80644764e-01  4.51625398e-02  3.78310112e-03]
 ...
 [ 1.34807889e+01  8.51299444e+00  6.31781934e-01]
 [-1.60098506e+01  1.65292087e+01 -7.97121660e-02]
 [ 0.00000000e+00  0.00000000e+00  0.00000000e+00]]
```

Figure 76: Wavelet Transform Output

By utilising sophisticated statistical methodologies, it is possible to derive distinctive and intricate characteristics from three-dimensional printed artefacts. The aforementioned characteristics possess the potential to augment the process of authentication and furnish an elevated degree of assurance in discerning authentic entities.

Upon comparing the methodologies, it becomes evident that each approach presents distinct advantages and disadvantages. Curvature Estimation and the Signed Distance Function are two methods that respectively offer insights into local surface features and capture the overall shape of an object. The FPFH method presents an intricate account of the nearby geometry, while the Wavelet Transform provides multifaceted characteristics across various scales.

To ascertain the optimal approach for verifying the authenticity of 3D-printed items, a blend of these methodologies could be utilised. Through the integration of the unique advantages of each approach, a more resilient and all-encompassing authentication mechanism can be established. The utilisation of FPFH and Wavelet Transform in tandem has the potential to yield a comprehensive depiction of approximate geometry in conjunction with multi-scale attributes, thereby enhancing the precision of the authentication procedure.

Summary

In Level 3, the research centred on utilising advanced authentication techniques in both 2D and 3D spaces, along with sophisticated statistical methodologies, to capture microscopic details and unique surface profiles of 3D-printed objects. The experimental results utilising LBP and Gabor filters underscored the constraints of extracting intrinsic surface features in the 2D space using 2D features. The results underscore the significance of considering three-dimensional data for sophisticated authentication purposes.

The study mainly focused on two methods in the 3D space: Normal Estimation and Octrees. These methods significantly increased the precision of the verification process by revealing important information about the local surface properties and spatial configurations of the entities. The combination of these two methods produced a more thorough authentication procedure.

The study explored various statistical techniques such as Curvature Estimation, Signed Distance Function (SDF), Fast Point Feature Histogram (FPFH), and Wavelet Transform. Each methodology presented distinct benefits in capturing diverse facets of the object's geometry and surface characteristics. Through the combination of these approaches, a more robust and comprehensive authentication procedure was established.

The Level 3 authentication experiments exhibited the potential of sophisticated techniques and statistical methodologies in revealing intricate details pertaining to the structure and surface characteristics of 3D-printed entities. The acquisition of this knowledge facilitates the advancement of a thorough and dependable authentication framework for the purpose of identifying and verifying 3D-printed entities.

7.6. Printing Method Identification

This section outlines the experimental procedures employed to determine the printing methodology of 3D-printed objects utilising PointNet in conjunction with a triplet loss function. The objective of the experiments is to evaluate the efficacy of the model in categorising the print techniques by analysing the characteristics of the 3D-printed entities.

The dataset comprises of surfaces of 3D-printed objects that were captured previously. The dataset is partitioned into training and testing subsets utilising an 80-20 ratio. The objects produced through 3D printing are depicted by point clouds that have been extracted from the meshes of said objects. The point cloud is configured to contain a fixed number of 2048 points. The dataset is subject to augmentation through the implementation of random perturbations and permutations of the data points.

The PointNet framework has been instantiated through the utilisation of Keras in conjunction with TensorFlow. The utilised model employs input tensors with a shape of (NUM_POINTS, 3), whereby the value of NUM_POINTS has been predetermined to be 2048. The proposed model comprises a pair of T-Net transformations, succeeded by a sequence of convolutional and fully connected layers. The ultimate layer of output employs a SoftMax activation function in order to forecast the probabilities of the print method class. The quantity of courses has been established as three.

The Triplet Loss is a loss function used in deep learning for training neural networks. It is designed to learn embeddings of images or other data points in a way that maximises the distance between embeddings of different classes and minimises the distance between embeddings of the same class. This loss function is commonly used in tasks such as face recognition and image retrieval.

The utilisation of triplet loss is aimed at augmenting the model's capacity to discriminate among comparable and disparate entities. The dataset has undergone pre-processing to generate triplets that comprise anchor, positive, and negative images. The anchor and positive images are classified under the same category, whereas the negative image is categorised differently. The dataset is partitioned into training and validation sets and subsequently supplied to the model in batches.

Figure 77: Triplet Loss minimises the distance between anchor and positive and maximises the distance between anchor and negative

The optimisation algorithm utilised in the model is Adam, with a learning rate of 0.001 and the loss function employed is sparse categorical cross-entropy. The evaluation of the model's effectiveness is conducted through the utilisation of sparse categorical accuracy. The training of the model was conducted over a period of 20 epochs, utilising the train_dataset for this purpose. The test_dataset was employed for validation purposes during this process. The study determined that the approach exhibited an overall classification accuracy of 92%.

The evaluation of the model's performance is demonstrated through the utilisation of 3-dimensional scatter plots, which depict point clouds derived from a subset of the test data. The visual representations exhibit the anticipated category and factual classification for every entity. The evaluation of the model's performance can be conducted through both qualitative and quantitative methods. Qualitative assessment involves examining the scatter plots, while quantitative assessment involves reporting the evaluation metrics such as accuracy, precision, recall, and F1-score, which are obtained during the training and validation phases.

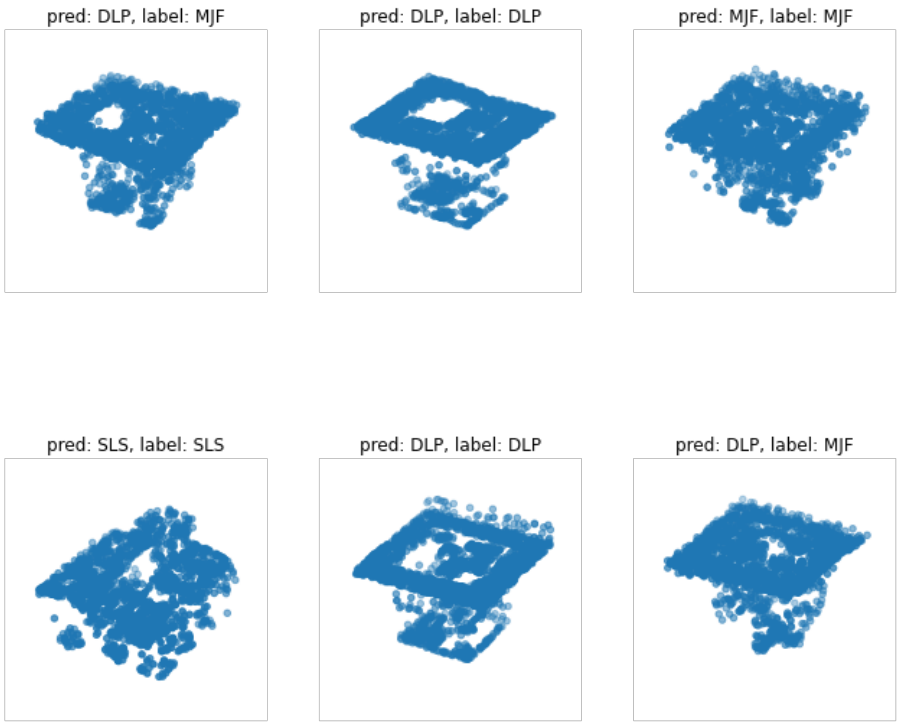

Figure 78: Print Method identification output

The conducted experiments provide evidence for the viability of utilising PointNet in conjunction with a triplet loss function for the purpose of identifying print methods in 3D-printed objects. The model exhibits the ability to acquire significant features from point clouds, which can be employed for the categorization of objects based on distinct printing techniques. The overall classification accuracy of the approach confirms its effectiveness in identifying printing methods.

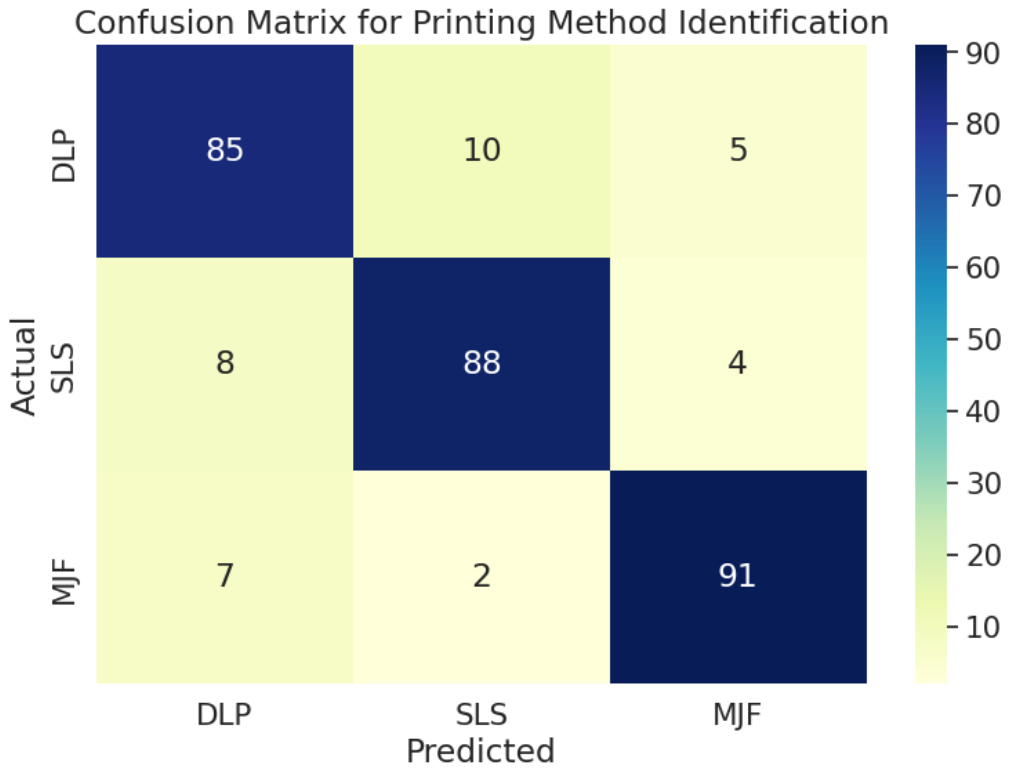

Figure 79: Confusion Matrix for Printing Method Identification

8. Authentication Framework

This chapter describes a comprehensive solution architecture that aims to enforce a strong, multi-layered authentication system for 3D-printed objects. The proposed architecture, which aims to protect the authenticity of these objects along the supply chain, systematically integrates three unique layers of authentication, makes use of a range of data capture technologies, and applies advanced algorithms for surface feature extraction and analysis. This methodical methodology ensures a rigorous and dependable process for certifying 3D-printed objects, ensuring their validity and quality from manufacturing to end-use.

The architecture is structured around four primary components, each playing a critical role in the authentication process. These components, along with their subcomponents, are designed to comprehensively address the multifaceted nature of 3D object authentication:

- Watermark Formation
- Data Capture
- Surface Feature Extraction and Texture Analysis
- Authentication Process

These components are further divided into various subcomponents to address different aspects of the authentication process.

8.1. Watermark Formation

The watermark formation process is a critical component of the security feature architecture for 3D-printed objects. It serves as the foundation of a multi-layered authentication system designed to secure the integrity of these objects throughout their lifecycle. This section delves into the intricacies of each level of authentication, explaining how they collectively forge a unique, indelible signature for every 3D-printed item.:

Level 1 - Glyph Verification (3D QR code)

The Glyph Verification process is a Level 1 authentication method that uses a 3D QR code as its primary means of authentication. This QR code is more than just a surface-level addition; it is intricately integrated into the 3D object's

design, ensuring that it is an inseparable part of the item throughout its life. The 3D QR code serves a variety of purposes:

Visual Indicator: It serves as a distinct, easily identifiable marker that denotes the specific area of the object designated for authentication checks. This ensures that the verification process is simple and effective.

Embedded Information: The QR code contains important information embedded within its pattern. This information can range from simple identification details to more complex data about the object's manufacturing process, origin, and intended use.

Ease of Access: While offering a significant level of security, the QR code remains accessible for scanning and verification with standard equipment, ensuring compatibility with existing infrastructure.

Level 2 - Elaborate geometrical features

Building on the foundational security provided by Glyph Verification, Level 2 adds Elaborate Geometrical Features to improve the authentication process. These features are meticulously designed and placed on the object to achieve two primary goals:

Increased Security: By incorporating specific shapes and patterns that are difficult to replicate or alter without a thorough understanding of the design process, this level significantly increases the barrier for potential counterfeiters.

Unique Identification: The elaborate geometrical features are chosen or designed to be unique to each object or batch, allowing for more precise authentication and traceability.

Level 3 - Naturally occurring surface texture

The use of naturally occurring surface texture as the ultimate authentication measure marks the pinnacle of the watermark formation process. This level capitalises on the inherent surface characteristics that emerge during the printing process, which include:

Unique to Each Print: The microscopic variations in texture that occur naturally during the 3D printing process give each item a distinct surface pattern, similar to a fingerprint.

Irreplicable: Due to the random and uncontrollable nature of these variations, replicating an object's exact surface texture is nearly impossible, providing the highest level of security.

Advanced Verification: Authenticating an object at this level necessitates sophisticated scanning and analysis technology capable of capturing and analysing minute details of the surface texture.

The combination of these three levels of authentication to the watermark formation process results in a comprehensive and resilient security system for 3D-printed objects. From simple glyph verification to in-depth analysis of naturally occurring surface textures, this multi-layered approach ensures that each 3D-printed object has a distinct, indelible signature. This not only prevents counterfeiting and unauthorised replication, but it also allows for a consistent method of verifying the authenticity and integrity of objects throughout their supply chain journey and lifecycle.

8.2. Data Capture

The 3D-printed objects' high-resolution surface data must be captured via the data collection component. Multi-focus 3D Microscopy has been chosen as the method for this application. This method was selected because of its accuracy, speed, affordability, and capacity to collect data at various scales.

The best resolution at the microscale level is provided by multi-focus 3D microscopy, enabling a thorough examination of the surface details. With this method, it is possible to stitch together many microscale data captures to create a thorough and precise depiction of the object's surface. The authentication process becomes more dependable by capturing high-resolution data, safeguarding the integrity of 3D-printed goods along the supply chain.

The effectiveness of the authentication system is considerably increased using multi-focus 3D microscopy. It ensures that the features that are extracted are precise and accurate in addition to capturing the fine details of the distinctive signature created during the watermark generation process. As a result, the authentication procedure becomes extremely dependable and solid, making it challenging for imitators to imitate the distinctive signatures and jeopardise the object's quality 3D printing process.

8.3. Surface Feature Extraction and Texture Analysis

The surface feature extraction and texture analysis component process the captured data to derive unique signatures for authentication. It employs a combination of 2D, 3D, and statistical models for characterising the surface features at various levels of authentication:

Level 1 - QR code verification

This first level uses advanced 2D image processing to authenticate the pattern encoded in the QR code. The QR code, a glyph embedded on the object's surface, acts as a gateway to critical information required for the authentication process. This stage leverages:

Advanced Pattern Recognition: Algorithms meticulously scan and decode the QR code, ensuring alignment with previously registered data, allowing for quick and efficient preliminary verification.

Geometric Analysis: Essential for confirming the QR code's adherence to predefined dimensional and orientational specifications, ensuring that the first layer of authentication is both rigorous and accurate.

Level 2 - Elaborate geometrical feature

This level delves into the object's surface, highlighting the elaborate geometrical features that enhance security. Extraction of these features involves:

Texture Pattern Classification: Using algorithms such as Local Binary Patterns (LBP) and Gabor filters, this process examines the surface to identify specific patterns that are naturally difficult to replicate.

Point Cloud Classification: Using point cloud models like PointNet, this method deciphers the 3D structure, identifying and categorising the elaborate geometrical features that contribute to the object's distinct identity.

Comprehensive Statistical Surface Analysis: This technique uses statistical analysis to dissect the surface's textural distribution, providing insights into the object's distinct topographical nuances.

Level 3 - Intrinsic texture

Level 3 makes use of the object's inherent, random surface characteristics—the unclonable signature created by the 3D printing process itself. This stage leverages:

Advanced Point Cloud Analysis: Goes deeper into the point cloud data to find unique, random surface characteristics that are hard to replicate.

Detailed Statistical Analysis: Looks at the statistical properties of the object's surface texture to identify features unique to each print.

By combining these methods, the system generates a comprehensive signature for each object, making authentication more precise and reliable. This method ensures that objects can be authenticated on multiple levels, ranging from easily visible QR codes to intricate surface textures unique to the printing process. This strong authentication framework improves security against counterfeiting and ensures the integrity of 3D-printed objects throughout their lifecycle.

8.4. Authentication Process

The authentication process is a critical phase in the proposed architecture that unifies the previously described components into a seamless, operational system for authenticating 3D-printed objects.

Registration

At the outset, the registration process establishes the object's identity by capturing and storing its unique fingerprint. This is achieved through a detailed scan of the object, which includes all three levels of the watermark:

- Level 1 captures the glyph verification using the 3D QR code.
- Level 2 captures the elaborate geometrical features added into the object's design.
- Level 3 captures the naturally occurring surface texture that is unique to each print.

The resulting composite signature is securely recorded and will serve as the baseline for all future authentication checks of that 3D printed object.

Verification

The verification stage is initiated whenever there is a need to authenticate an object, whether at the point of entry into the supply chain, during transit, or before final delivery to the consumer. A new scan of the object is performed to obtain real-time surface data, which is then meticulously processed to reconstruct the object's unique signature

as captured during the registration stage. This stage is critical as it must accommodate any natural variations in the object's surface that may occur over time without compromising the integrity of the authentication process.

Comparison

The comparison phase is where the authentication decision is made. The newly extracted signature from the verification scan is rigorously compared against the registered signature. This involves a detailed analysis across all three levels of authentication:

- Level 1 Comparison: Here, the system matches the QR code patterns, ensuring that the basic glyph information aligns with the registered data.
- Level 2 Comparison: At this intermediate level, the system delves deeper, comparing the detailed geometrical features to detect any discrepancies or alterations.
- Level 3 Comparison: This is the most granular level, where the intrinsic surface textures are matched. Due to the unique and random nature of these textures, this level provides the strongest assurance of authenticity.

If the comparison across all three levels affirms that the signatures are consistent, the object is authenticated as genuine. This layered approach to validation is designed to be highly reliable, akin to the authentication principles employed in advanced security systems, where multiple checks and balances are in place to verify identity.

The authentication process, as described in this section, forms the cornerstone of the proposed multi-layered authentication system. It ensures a robust and comprehensive method for verifying the authenticity of 3D-printed objects. The process is not only about confirming the identity but also about safeguarding the integrity and quality of these objects from the manufacturing stage through to the end-user. By meticulously detailing each stage of this process and ensuring that each level of authentication is clearly defined and implemented, the proposed architecture offers a robust framework for securing the supply chain of 3D-printed components (Figure 80).

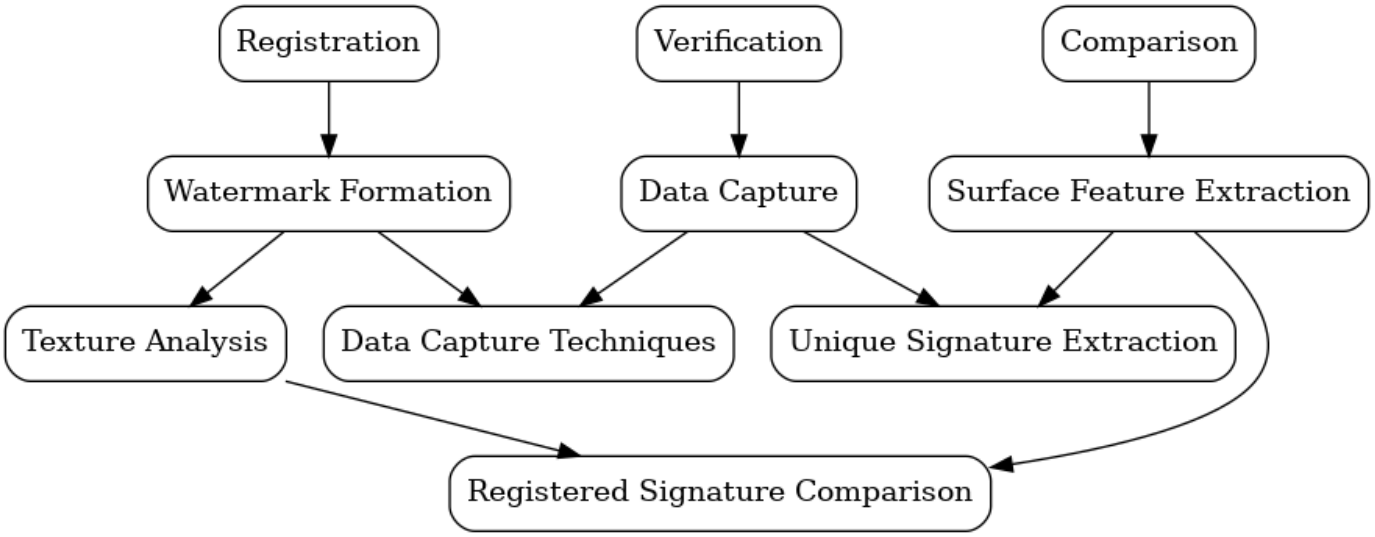

Figure 80: Proposed authentication framework for the identification of 3D-printed objects

9. Conclusion

This study provided a thorough analysis of surface fingerprinting methods for 3D-printed object identification and authentication. The study concentrated on the creation and assessment of various approaches to extract distinctive characteristics from the surfaces of 3D-printed items, enabling their trustworthy verification under varying levels of examination. The study was divided into three primary portions that dealt with distinct facets of the surface fingerprinting issue: 2D, 3D, and statistical techniques.

The 2D methodologies investigated in this study comprised advanced image processing algorithms, texture pattern categorization, and QR code verification. By examining the surface patterns and textures of the 3D-printed items, these techniques attempted to offer a fundamental level of verification.

Mesh parameter analysis, point cloud classification, and high-precision microscopic feature extraction were the 3D methods that were examined in this study. These techniques gave a deeper comprehension of the geometry, topology, and distinctive surface characteristics of the 3D-printed items, providing a better level of authentication.

The statistical techniques used in this study also included multivariate analysis, machine learning-based methodologies, and basic feature distribution analysis. To provide a thorough understanding of the surface characteristics of 3D-printed objects, these approaches sought to elucidate underlying patterns and correlations between the retrieved features.

The research hypothesis, which proposed that each manufactured 3D-printed object would present a unique signature on the surface that defines the PUF (Physically Unclonable Function) due to highly random microscale features, was successfully proven. Through the combination of 2D, 3D, and statistical techniques, this study demonstrated that these intrinsic surface characteristics can be used for reliable and repeatable identification of 3D-printed objects, making it extremely difficult to counterfeit them and thus providing the highest security.

9.1. Key Findings and Contributions

The key findings of this study can be summarised as follows:

- The integration of 2D, 3D, and statistical methods presents a robust and comprehensive solution for the surface profiling and authentication of 3D-printed objects. This multidimensional approach ensures a higher level of precision and security in identifying and authenticating 3D-printed items.
- The hierarchical approach to authentication, encompassing Level 1 (glyph verification), Level 2 (elaborate geometrical features), and Level 3 (naturally occurring surface texture), introduces a flexible and adaptable framework. This framework enhances the system's ability to accurately identify and secure objects against unauthorized replication and counterfeiting.
- A novel algorithm has been developed for identifying and characterizing the unique signatures of glyphs and watermarks on the surfaces of 3D-printed objects. This algorithm plays a crucial role in the detailed authentication process, significantly improving the accuracy of object identification.
- The study's exploration into precision surface analysis techniques at Level 3 authentication emphasizes the use of microscopic surface details. This method sets a new standard for security protocols in additive manufacturing by utilizing unique 'fingerprints' of each object for authentication.

The contributions of this study to the field of 3D printing and surface fingerprinting include:

- A comprehensive analysis of the latest techniques for surface profiling in the context of 3D-printed objects, highlighting the importance of integrating various methods for a more secure and reliable authentication process.
- The development of a hierarchical approach to authentication that incorporates multiple levels of scrutiny, enabling a more sophisticated and nuanced verification system capable of addressing the complexities inherent in 3D-printed objects.
- The introduction of innovative feature extraction techniques that enhance the process of authentication and identification. These techniques enable the detailed analysis of surface textures and geometries, providing a more accurate means of distinguishing between genuine and counterfeit objects.

State-of-the-Art Comparison:

Table 14 shows how this research, through its methodical examination of Level 1, Level 2, and Level 3 authentication methods, surpasses existing solutions in additive manufacturing security. This study stands out for its holistic and detailed approach to authentication, significantly advancing the field by offering:

- Defined additive manufacturing security protocols that incorporate both digital and physical aspects of object security, ensuring comprehensive protection across the supply chain.
- Precision surface analysis techniques that leverage microscopic details for authentication, offering an advanced method for verifying authenticity that is challenging for counterfeiters to bypass.
- A comprehensive approach to cyber-physical system security that integrates physical object authentication with cyber security measures to create a robust defence against various threats.
- An assessment of 3D print output quality that extends the study's relevance beyond security, ensuring that 3D-printed objects not only are secure but also meet high-quality standards.

By offering these advancements, the study contributes significantly to enhancing the trustworthiness, security, and quality assurance of 3D printing technologies.

Table 14: Comparative Analysis of State-of-the-Art Authentication Solutions in Additive Manufacturing

	State of the art and emerging research topics and challenges in the areas of Authentication Methods in Additive Manufacturing				
Authors & Research Groups	**SOTA Authentication Solutions**	**Define Additive Manufacturing Security Protocols**	**Precision Surface Analysis Techniques**	**Comprehensive Cyber-Physical System Security**	**Assessment of 3D Print Output Quality**
Belikovetsky et al. (2016)		X		X	
Chen et al. (2019)	X	X		X	
Cai et al. (2021)	X			X	X
Peng et al. (2019)	X	X			
Gao et al. (2021)	X	X		X	
Ahn et al. (2009)			X		X
Tey et al. (2021)					X
Suzuki et al. (2017)	X	X			
This Research	X	X	X	X	X

9.2. Limitations and Future Work

9.2.1. Limitations

Despite the comprehensive approach and rigorous methodology employed in this study, there are some limitations that should be acknowledged:

- **Material scope**: This may limit the applicability of the authentication system to other materials, such as metals and ceramics.
- **Data capture techniques**: The data collection methods used in this study were chosen based on their accuracy, speed, and cost; however, other emerging techniques could potentially enhance the authentication procedure.
- **Feature extraction and texture analysis algorithms**: The algorithms used for feature extraction and texture analysis are based on existing methods, and there may be space for improvement or more sophisticated algorithms that can improve the authentication process.
- **Printing techniques**: The study only addresses a limited number of 3D printing techniques, and the authentication system may need to be adapted for other printing techniques not covered by this study.
- **Adversarial attacks**: The authentication system is intended to prevent attempts at forgery; however, it is difficult to predict and account for all potential adversarial strategies, particularly as technology continues to advance.

9.2.2. Future Work

To address the limitations and build upon the foundation laid by this study, several avenues for future work are proposed:

- **Expand material scope**: Examine the applicability of the authentication system to other materials, such as metals and ceramics, to expand the range of 3D-printed objects that can be secured.
- **Explore emerging data capture techniques**: Continuously monitor and assess emerging data capture technologies that could potentially enhance the authentication process's precision, speed, or cost.
- **Improve feature extraction and texture analysis algorithms**: Develop new or refined algorithms for feature extraction and texture analysis to improve the efficacy and robustness of the authentication system.

- **Incorporate additional printing techniques**: Extend the research to include additional 3D printing techniques, adapting the authentication system as needed to accommodate a broader array of manufacturing techniques.
- **Address potential adversarial attacks**: Conduct in-depth analyses of potential adversarial attacks and develop countermeasures to bolster the authentication system against sophisticated attempts at forgery.
- **Evaluate real-world performance**: Assess the performance and efficacy of the authentication system in securing 3D-printed objects across various supply chains and industries using real-world scenarios.

By addressing these limitations and pursuing the proposed future work, the authentication system can continue to evolve, providing a robust and dependable solution to secure 3D-printed objects and prevent counterfeiting in a swiftly expanding industry.

This research has contributed to the development and comprehension of surface profiling techniques for 3D-printed objects. The findings and contributions of this research have the potential to have a significant impact on the security and authentication of 3D printing, paving the way for future solutions that are more reliable and robust.

10. References

Abouelela, A., Abbas, H.M., Eldeeb, H., Wahdan, A.A. and Nassar, S.M. (2005) Automated vision system for localizing structural defects in textile fabrics. *Pattern Recognition Letters* [online]. 26 (10), pp. 1435–1443.

Ahn, D., Kweon, J.H., Kwon, S., Song, J. and Lee, S. (2009) Representation of surface roughness in fused deposition modeling. *Journal of Materials Processing Technology* [online]. 209 (15–16), pp. 5593–5600. Available from: https://ac.els-cdn.com/S0924013609002039/1-s2.0-S0924013609002039-main.pdf?_tid=2b365ea9-68bf-48ae-9da6-6f88e5fbef83&acdnat=1552522806_f367b237969fb301de33bccef427a221 [Accessed 14 March 2019].

Ahonen, T., Hadid, A. and Pietikäinen, M. (2006) Face description with local binary patterns: Application to face recognition. *IEEE Transactions on Pattern Analysis and Machine Intelligence* [online]. 28 (12), pp. 2037–2041. [Accessed 11 April 2023].

Alicona (2023) InfiniteFocusSL, the 3D measurement system for shape & finish [Apparatus and software]. Available at: https://www.alicona.com/en/products/infinitefocussl [Access: 8/2023]

Autodesk (2023) Fusion 360 (version 2023) [Computer Program] Available at: https://www.autodesk.co.uk/products/fusion-360 [Access: 8/2023]

Belikovetsky, S., Yampolskiy, M., Toh, J. and Elovici, Y. (2016) dr0wned - Cyber-Physical Attack with Additive Manufacturing.

Belongie, S., Malik, J. and Puzicha, J. (2002) Shape matching and object recognition using shape contexts. *IEEE Transactions on Pattern Analysis and Machine Intelligence* [online]. 24 (4), pp. 509–522. [Accessed 22 April 2023].

Bochmann, L., Bayley, C., Helu, M., Transchel, R., Wegener, K. and Dornfeld, D. (2015) Understanding error generation in fused deposition modeling. *Surface Topography: Metrology and Properties* [online]. 3 (1), p. 014002. Available from: http://stacks.iop.org/2051-672X/3/i=1/a=014002?key=crossref.c7f819bde03b1b13d1c2140f04297746 [Accessed 7 March 2019].

Borrmann, D., Elseberg, J., Lingemann, K. and Nüchter, A. (2011) The 3D Hough Transform for plane detection in point clouds: A review and a new accumulator design. *3D Research* [online]. 2 (2), pp. 1–13. Available from: https://link.springer.com/article/10.1007/3DRes.02(2011)3 [Accessed 23 April 2023].

British Standards Institution (2015) *ISO/ASTM 52900:2015 - Additive manufacturing — General principles — Terminology British Standards Institution*. 2015 [online]. Available from: https://www.iso.org/standard/69669.html [Accessed 30 April 2023].

Bronstein, M.M. and Kokkinos, I. (2010) Scale-invariant heat kernel signatures for non-rigid shape recognition. *Proceedings of the IEEE Computer Society Conference on Computer Vision and Pattern Recognition* [online]. pp. 1704–1711. [Accessed 23 April 2023].

Brunelli, R. (2009) *Template Matching Techniques in Computer Vision: Theory and Practice Template Matching Techniques in Computer Vision: Theory and Practice* [online]. [Accessed 22 April 2023].

Cai, C., Tey, W.S., Chen, J., Zhu, W., Liu, X., Liu, T., Zhao, L. and Zhou, K. (2021) Comparative study on 3D printing of polyamide 12 by selective laser sintering and multi jet fusion. *Journal of Materials Processing Technology* [online]. 288, p. 116882. [Accessed 17 November 2021].

Cazón, A., Morer, P., Matey, L., Cazó, A., Morer, P. and Matey, L. (2014) PolyJet technology for product prototyping: Tensile strength and surface roughness properties. [online]. 228 (12), pp. 1664–1675.

Chen, C.C. and Chen, C.C. (1999) Filtering methods for texture discrimination. *Pattern Recognition Letters* [online]. 20 (8), pp. 783–790.

Chen, F., Luo, Y., Tsoutsos, N.G., Maniatakos, M., Shahin, K. and Gupta, N. (2019) Embedding Tracking Codes in Additive Manufactured Parts for Product Authentication. *Advanced Engineering Materials* [online]. 21 (4), pp. 1–8. Available from: https://onlinelibrary.wiley.com/doi/abs/10.1002/adem.201800495 [Accessed 15 November 2019].

Chen, F., Mac, G. and Gupta, N. (2017) Security features embedded in computer aided design (CAD) solid models for additive manufacturing. *Materials and Design* [online]. 128, pp. 182–194.

Chen, H. and Bhanu, B. (2007) 3D free-form object recognition in range images using local surface patches. *Pattern Recognition Letters* [online]. 28 (10), pp. 1252–1262.

Chiu, S.H., Chou, S., Liaw, J.J. and Wen, C.Y. (2002) Textural Defect Segmentation Using a Fourier-Domain Maximum Likelihood Estimation Method. *Textile Research Journal* [online]. 72 (3), pp. 253–258.

Choy, C., Gwak, J. and Savarese, S. (2019) 4D Spatio-Temporal ConvNets: Minkowski Convolutional Neural Networks. *Proceedings of the IEEE Computer Society Conference on Computer Vision and Pattern Recognition* [online]. 2019-June, pp. 3070–3079. Available from: https://arxiv.org/abs/1904.08755v4 [Accessed 23 April 2023].

Chua, C.K., Wong, C.H. and Yeong, W.Y. (2017) *Benchmarking for Additive Manufacturing Standards, Quality Control, and Measurement Sciences in 3D Printing and Additive Manufacturing* [online].

Clare Scott (2016) InfraTrac Successfully Applies Anti-Counterfeit Technology to 3D Printed Metal Parts. Available at: https://3dprint.com/157763/infratrac-3d-printed-metal-parts [Access: 8/2023]

Coggins, J.M. and Jain, A.K. (1985) A spatial filtering approach to texture analysis. *Pattern Recognition Letters* [online]. 3 (3), pp. 195–203.

Cole, E.S. (2008) Conventional Light Microscopy. *Current Protocols Essential Laboratory Techniques* [online]. 00 (1).

Dachowicz, A., Chaduvula, S.C., Atallah, M. and Panchal, J.H. (2017) Microstructure-Based Counterfeit Detection in Metal Part Manufacturing. *JOM* [online]. 69 (11), pp. 2390–2396.

Dalal, N. and Triggs, B. (2005) *Histograms of oriented gradients for human detection*. In: *Proceedings - 2005 IEEE Computer Society Conference on Computer Vision and Pattern Recognition, CVPR 2005* [online]. I, pp. 886–893. Available from: http://lear.inrialpes.fr [Accessed 23 April 2023].

Dey, A. and Yodo, N. (2019) A systematic survey of FDM process parameter optimization and their influence on part characteristics. *Journal of Manufacturing and Materials Processing* [online]. 3 (3).

Dhruv, B., Mittal, N. and Modi, M. (2018) Study of Haralick's and GLCM texture analysis on 3D medical images. *https://doi.org/10.1080/00207454.2018.1536052* [online]. 129 (4), pp. 350–362. Available from: https://www.tandfonline.com/doi/abs/10.1080/00207454.2018.1536052 [Accessed 11 April 2023].

Dilberoglu, U.M., Gharehpapagh, B., Yaman, U. and Dolen, M. (2017) The Role of Additive Manufacturing in the Era of Industry 4.0. *Procedia Manufacturing* [online]. 11, pp. 545–554. Available from: https://linkinghub.elsevier.com/retrieve/pii/S2351978917303529 [Accessed 3 April 2019].

Doubrovski, E.L., Verlinden, J.C. and Horvath, I. (2012) *First steps towards collaboratively edited design for additive manufacturing knowledge*. In: *23rd Annual International Solid Freeform Fabrication Symposium - An Additive Manufacturing Conference, SFF 2012*. pp. 891–901. [Accessed 30 April 2023].

Ferez, R., Silvestre, J. and Munoz, J. (2004) *Defect detection in repetitive fabric patterns*. In: *Proceedings of the Fourth IASTED International Conference on Visualization, Imaging, and Image Processing*. pp. 783–786.

Gao, Y., Wang, W., Jin, Y., Zhou, C., Xu, W. and Jin, Z. (2021) ThermoTag: A Hidden ID of 3D Printers for Fingerprinting and Watermarking. *IEEE Transactions on Information Forensics and Security* [online]. 16, pp. 2805–2820. [Accessed 22 April 2023].

Gordeev, E.G., Galushko, A.S. and Ananikov, V.P. (2018) Improvement of quality of 3D printed objects by elimination of microscopic structural defects in fused deposition modeling. *PLoS ONE* [online]. 13 (6).

Gueche, Y.A., Sanchez-Ballester, N.M., Cailleaux, S., Bataille, B. and Soulairol, I. (2021) Selective Laser Sintering (SLS), a New Chapter in the Production of Solid Oral Forms (SOFs) by 3D Printing. *Pharmaceutics 2021, Vol. 13, Page 1212* [online]. 13 (8), p. 1212. Available from: https://www.mdpi.com/1999-4923/13/8/1212/htm [Accessed 5 April 2023].

Gumhold, S. and Þ, R.M. (2001) Feature Extraction from Point Clouds CR Categories : *In Proceedings of the 10 th International Meshing Roundtable*. pp. 293–305.

Gunaydin, Kadir & S. Türkmen, H. (2018) Common FDM 3D Printing Defects. *International Congress on 3D Printing (Additive Manufacturing) Technologies and Digital Industry*. (April), pp. 1–8.

Hanbay, K., Talu, M.F. and Özgüven, Ö.F. (2016) Fabric defect detection systems and methods—A systematic literature review. *Optik* [online]. 127 (24), pp. 11960–11973.

Hornung, A., Wurm, K.M., Bennewitz, M., Stachniss, C. and Burgard, W. (2013) OctoMap: An Efficient Probabilistic 3D Mapping Framework Based on Octrees. *Autonomous Robots* [online]. Available from: http://octomap.github.com. [Accessed 23 April 2023].

Hou, J.U., Kim, D.G., Choi, S. and Lee, H.K. (2015) *3D print-scan resilient watermarking using a histogram-based circular shift coding structure*. In: *IH and MMSec 2015 - Proceedings of the 2015 ACM Workshop on Information Hiding and Multimedia Security* [online]. pp. 115–121.

Hou, J.U., Kim, D.G. and Lee, H.K. (2017) Blind 3D Mesh Watermarking for 3D Printed Model by Analyzing Layering Artifact. *IEEE Transactions on Information Forensics and Security* [online]. 12 (11), pp. 2712–2725.

HP and Jabil Revolutionize $12 trillion Manufacturing Industry | Jabil. (2021). 2021 [online]. Available from: https://www.jabil.com/case-studies/hp-and-jabil-revolutionize-manufacturing.html [Accessed 7 December 2021].

HP Labs (2017) *Progress in 3D authentication and identification brings 3D manufacturing closer*. 2017 [online]. Available from: https://garage.ext.hp.com/us/en/hp-labs/progress_in_3d_authenticationandidentificationbrings3dmanufactur.html [Accessed 20 April 2019].

HP (2023) HP 3D Structured Light Scanner Pro S3. [Apparatus and software]. HP Development Company, L.P. Available at: https://3dscanexpert.com/hp-3d-scanner-pro-s3-david-sls-3-review/ [Access: 8/2023]

Huang, Z. and Zhou, Y. (2010) *Three-Dimensional Model Analysis and Processing Advanced Topics in Science and Technology in China* [online]. 1 (4).

Heidi Milkert (2014) Quantum Materials Corporation Secures Technology to 3D Print Quantum Dots for Anti-Counterfeiting. Available at: https://3dprint.com/7701/quantum-dots-3d-print [Access: 8/2023]

Hügli, H. and Mure-Dubois, J.C.C. (2006) 3D vision methods and selected experiences in micro and macro applications. *Proceedings of the SPIE*. 6382–10.

Joshi, S.C. and Sheikh, A.A. (2015) 3D printing in aerospace and its long-term sustainability. *Virtual and Physical Prototyping* [online]. 10 (4), pp. 175–185.

Kazhdan, M., Funkhouser, T. and Rusinkiewicz, S. (2003) *Rotation Invariant Spherical Harmonic Representation of 3D Shape Descriptors Eurographics Symposium on Geometry Processing*. [Accessed 21 January 2020].

Kechagias, J.D. and Maropoulos, S. (2015) An Investigation of Sloped Surface Roughness of Direct Poly-Jet 3D Printing. pp. 1–4.

Keselman, L. and Hebert, M. (2019) Direct fitting of Gaussian mixture models. *Proceedings - 2019 16th Conference on Computer and Robot Vision, CRV 2019* [online]. pp. 25–32.

Khan, A. and Professor, A. (2020) A NOVEL TEXTURE DESCRIPTOR USING FUSED MULTI-RESOLUTION LBP AND TAMURA FEATURES FOR IMAGE RETRIEVAL SYSTEM. *Dogo Rangsang Research Journal UGC Care Group I Journal*. 10 (03). [Accessed 11 April 2023].

Kim, H., Zhao, Y. and Zhao, L. (2016) Process-level modeling and simulation for HP's Multi Jet Fusion 3D printing technology. *2016 1st International Workshop on Cyber-Physical Production Systems, CPPS 2016* [online]. [Accessed 22 February 2021].

Knopp, J., Prasad, M., Willems, G., Timofte, R. and Van Gool, L. (2010) *Hough Transform and 3D SURF for Robust Three Dimensional Classification*. In: Daniilidis, K., Maragos, P. and Paragios, N., eds. *Computer Vision -- ECCV 2010*. Berlin, Heidelberg, Springer Berlin Heidelberg, pp. 589–602.

Kristiawan, R.B., Imaduddin, F., Ariawan, D., Ubaidillah and Arifin, Z. (2021) A review on the fused deposition modeling (FDM) 3D printing: Filament processing, materials, and printing parameters. *Open Engineering* [online]. 11 (1), pp. 639–649. [Accessed 5 April 2023].

Krzewina, L. (2006) Structured light for three-dimensional microscopy. *Camera* [online]. Available from: http://scholarcommons.usf.edu/etd/2593/.

Kumar, A. and Pang, G.K.H. (2002) Defect detection in textured materials using optimized filters. *IEEE Transactions on Systems, Man, and Cybernetics, Part B: Cybernetics* [online]. 32 (5), pp. 553–570.

Lalegani Dezaki, M., Mohd Ariffin, M.K.A. and Hatami, S. (2021) *An overview of fused deposition modelling (FDM): research, development and process optimisation Rapid Prototyping Journal* [online]. 27 (3), pp. 562–582. Available from: https://www.emerald.com/insight/1355-2546.htm [Accessed 5 April 2023].

Leach, R.K., Senin, N., Feng, X., Stavroulakis, P., Su, R., Syam, W.P. and Widjanarko, T. (2017) Information-rich metrology : Changing the game.

Li, B., Furukawa, T., Lynn, C.A., Andrew, A., Kurdila, J., Taheri, S. and Ahmadian, M. (2016) *Photometric Stereo for Micro-scale Shape Reconstruction*.

Li, Y. and Gu, P. (2004) *Free-form surface inspection techniques state of the art review*. In: *CAD Computer Aided Design* [online]. 36 (13), pp. 1395–1417. Available from: www.elsevier.com/locate/cad [Accessed 9 April 2019].

Li, Z., Singh Rathore, A., Song, C., Wei, S., Wang, Y., Xu, W. and Rathore, A.S. (2018) PrinT-racker: Fingerprinting 3D Printers using Commodity Scanners. [online].

de Lima, G.V.L., Saito, P.T.M., Lopes, F.M. and Bugatti, P.H. (2019) Classification of texture based on Bag-of-Visual-Words through complex networks. *Expert Systems with Applications* [online]. 133, pp. 215–224. [Accessed 23 April 2023].

Lishchenko, N., Piteľ, J. and Larshin, V. (2022) Online Monitoring of Surface Quality for Diagnostic Features in 3D Printing. *Machines* [online]. 10 (7), p. 541.

Liu, L., Meng, L., Peng, Y. and Wang, X. (2021) A data hiding scheme based on U-Net and wavelet transform. *Knowledge-Based Systems* [online]. 223, p. 107022. [Accessed 22 April 2023].

Lowe, D.G. (2004) Accepted for publication in the. *International Journal of Computer Vision*. [Accessed 23 April 2023].

Macq, B., Alface, P.R. and Montanola, M. (2015) *Applicability of watermarking for intellectual property rights protection in a 3D printing scenario*. In: *Proceedings - Web3D 2015: 20th International Conference on 3D Web Technology* [online]. pp. 89–95.

Madrigal, C.A., Branch, J.W., Restrepo, A. and Mery, D. (2017) A method for automatic surface inspection using a model-based 3D descriptor. *Sensors (Switzerland)* [online]. 17 (10).

Materka, A. and Strzelecki, M. (1998) *Texture Analysis Methods-A Review*.

Maturana, D. and Scherer, S. (2015) *VoxNet: A 3D Convolutional Neural Network for real-time object recognition*. In: *IEEE International Conference on Intelligent Robots and Systems* [online]. 2015-Decem, IEEE, pp. 922–928.

Melchels, F.P.W., Feijen, J. and Grijpma, D.W. (2010) A review on stereolithography and its applications in biomedical engineering. *Biomaterials* [online]. 31 (24), pp. 6121–6130. [Accessed 30 April 2023].

Miyoshi, K. (2021) Surface Characterization Techniques: An Overview. *Mechanical Tribology* [online]. 2 (July), pp. 45–68. Available from: http://ntrs.nasa.gov/archive/nasa/casi.ntrs.nasa.gov/20020070606.pdf.

Michael Molitch-Hou (2023) InfraTrac brings anti-counterfeiting tech to 3d printing. Available at: https://3dprintingindustry.com [Access: 8/2023].

Mualla F, Aubreville M, Maier A. Microscopy. 2018 Aug 3. In: Maier A, Steidl S, Christlein V, et al., editors. Medical Imaging Systems: An Introductory Guide [Internet]. Cham (CH): Springer; 2018. Available from: https://www.ncbi.nlm.nih.gov/books/NBK546149/figure/ch5.fig4/ doi: 10.1007/978-3-319-96520-8_5

Myshkin, N.K., Grigoriev, A.Y., Chizhik, S.A., Choi, K.Y. and Petrokovets, M.I. (2003) Surface roughness and texture analysis in microscale. *Wear* [online]. 254 (10), pp. 1001–1009. [Accessed 22 January 2020].

N, R.T. and M B, V. (2020) *Analysis of Polynomial Co-Efficient Based Authentication for 3D Fingerprints*. In: *2020 IEEE International Conference for Innovation in Technology (INOCON)* [online]. IEEE, pp. 1–6.

Negi, S., Dhiman, S. and Sharma, R.K. (2014) Investigating the Surface Roughness of SLS Fabricated Glass-Filled Polyamide Parts Using Response Surface Methodology. *Arabian Journal for Science and Engineering* [online]. 39 (12), pp. 9161–9179.

Niepert, M., Ahmad, M. and Kutzkov, K. (2016a) *Learning convolutional neural networks for graphs*. In: *33rd International Conference on Machine Learning, ICML 2016*. 4, pp. 2958–2967. [Accessed 23 April 2023].

Niepert, M., Ahmad, M. and Kutzkov, K. (2016b) Learning Convolutional Neural Networks for Graphs. *33rd International Conference on Machine Learning, ICML 2016* [online]. 4, pp. 2958–2967. Available from: https://arxiv.org/abs/1605.05273v4 [Accessed 23 April 2023].

nTopology (2023) nTop (version 2023) [Computer Program] Available at: https://www.ntop.com [Access: 8/2023]

Ojala, T., Pietikainen, M., Maenpaa, T., Pietikäinen, M. and Mäenpää, T. (2002) Multiresolution gray-scale and rotation invariant texture classification with local binary patterns. *IEEE Transactions on Pattern Analysis and Machine Intelligence* [online]. 24 (7), pp. 971–987. Available from: http://ieeexplore.ieee.org/document/1017623/ [Accessed 24 August 2019].

OpenCV (2023) ArUco marker dictionary (version 2023) [Computer program]. Available at https://opencv.org [Access: 8/2023]

Ovsjanikovs, M. (2011) SPECTRAL METHODS FOR ISOMETRIC SHAPE MATCHING AND SYMMETRY DETECTION. [online]. (March). Available from: http://purl.stanford.edu/xb493fy4331 [Accessed 23 April 2023].

Patpatiya, P., Chaudhary, K., Shastri, A. and Sharma, S. (2022) A review on polyjet 3D printing of polymers and multi-material structures. [online]. 236 (14), pp. 7899–7926. Available from: https://journals.sagepub.com/doi/abs/10.1177/09544062221079506?journalCode=picb [Accessed 4 April 2023].

Peng, F., Yang, J. and Long, M. (2019) 3-D Printed Object Authentication Based on Printing Noise and Digital Signature. *IEEE Transactions on Reliability* [online]. 68 (1), pp. 342–353. Available from: https://ieeexplore.ieee.org/document/8482279/ [Accessed 28 May 2020].

Pérez, M., Medina-Sánchez, G., García-Collado, A., Gupta, M. and Carou, D. (2018) Surface quality enhancement of fused deposition modeling (FDM) printed samples based on the selection of critical printing parameters. *Materials* [online]. 11 (8).

Pernkopf, F. and O'Leary, P. (2003) Image acquisition techniques for automatic visual inspection of metallic surfaces. *NDT and E International* [online]. 36 (8), pp. 609–617.

Petzold, S., Klett, J., Schauer, A. and Osswald, T.A. (2019) Surface roughness of polyamide 12 parts manufactured using selective laser sintering. *Polymer Testing* [online]. 80. [Accessed 5 April 2023].

Pham, G.N., Lee, S.H., Kwon, O.H. and Kwon, K.R. (2018) A watermarking method for 3D printing based on menger curvature and K-mean clustering. *Symmetry* [online]. 10 (4), pp. 1–16.

Pollard, S., Adams, G., Azhar, F. and Dickin, F. (2018) Authentication of 3D Printed Parts using 3D Physical Signatures. *NIP & Digital Fabrication Conference* [online]. 2018 (1), pp. 196–201. Available from: http://www.ingentaconnect.com/content/10.2352/ISSN.2169-4451.2018.34.196.

Qi, C.R., Su, H., Mo, K. and Guibas, L.J. (2017a) *PointNet: Deep learning on point sets for 3D classification and segmentation*. In: *Proceedings - 30th IEEE Conference on Computer Vision and Pattern Recognition, CVPR 2017* [online]. 2017-Janua, pp. 77–85. [Accessed 1 December 2019].

Qi, C.R., Yi, L., Su, H. and Guibas, L.J. (2017b) PointNet++: Deep Hierarchical Feature Learning on Point Sets in a Metric Space. *Advances in Neural Information Processing Systems* [online]. 2017-Decem, pp. 5100–5109. Available from: https://arxiv.org/abs/1706.02413v1 [Accessed 20 January 2020].

Randen, T. and Husøy, J.H. (1999) Filtering for texture classification: A comparative study. *IEEE Transactions on Pattern Analysis and Machine Intelligence* [online]. 21 (4), pp. 291–310.

Ravishankar, S., Dutt, H.N.V. and Gurumoorthy, B. (2010) Automated inspection of aircraft parts using a modified ICP algorithm. *International Journal of Advanced Manufacturing Technology* [online]. 46 (1–4), pp. 227–236.

Rebaioli, L. and Fassi, I. (2017) A review on benchmark artifacts for evaluating the geometrical performance of additive manufacturing processes. *International Journal of Advanced Manufacturing Technology* [online]. 93 (5–8), pp. 2571–2598.

Reddy, B. (2018) Effect of Process Parameters on the Mechanical Behavior of FDM processed PLA Parts. 8 (718), pp. 718–723.

Reuter, M., Biasotti, S., Giorgi, D., Patanè, G. and Spagnuolo, M. (2009) Discrete Laplace–Beltrami operators for shape analysis and segmentation. *Computers & Graphics* [online]. 33 (3), pp. 381–390. Available from: https://linkinghub.elsevier.com/retrieve/pii/S0097849309000272 [Accessed 13 June 2019].

Rubinsztein-Dunlop, H. *et al.* (2017) Roadmap on structured light. *Journal of Optics (United Kingdom)* [online]. 19 (1), pp. 1–51. Available from: http://dx.doi.org/10.1088/2040-8978/19/1/013001.

Rusu, R.B. and Cousins, S. (2011) *3D is here: Point Cloud Library (PCL)*. In: *Proceedings - IEEE International Conference on Robotics and Automation* [online]. Available from: http://pointclouds.org [Accessed 23 April 2023].

Sai, P.C. and Yeole, S. (2010) Fused Deposition Modeling. [online]. (July).

Santos, F.N., Moreira, A.P. and Costa, P.C. (2013) *Towards extraction of topological maps from 2D and 3D occupancy grids*. In: *Lecture Notes in Computer Science (including subseries Lecture Notes in Artificial Intelligence and Lecture Notes in Bioinformatics)* [online]. 8154 LNAI, pp. 307–318. [Accessed 7 November 2022].

Scovanner, P., Ali, S. and Shah, M. (2007) A 3-dimensional sift descriptor and its application to action recognition. *Proceedings of the ACM International Multimedia Conference and Exhibition* [online]. pp. 357–360. Available from: https://dl.acm.org/doi/10.1145/1291233.1291311 [Accessed 23 April 2023].

Sharma, A. and Rai, A. (2022) Fused deposition modelling (FDM) based 3D & 4D Printing: A state of art review. *Materials Today: Proceedings* [online]. 62, pp. 367–372. [Accessed 4 April 2023].

Shi, L., Wang, X. and Shen, Y. (2020) Research on 3D face recognition method based on LBP and SVM. *Optik* [online]. 220, p. 165157. [Accessed 11 April 2023].

Silapasuphakornwong, P., Suzuki, M., Unno, H., Torii, H., Uehira, K. and Takashima, Y. (2016) Nondestructive Readout of Copyright Information Embedded in Objects Fabricated with 3-D Printers. In: *Lecture Notes in Computer Science (including subseries Lecture Notes in Artificial Intelligence and Lecture Notes in Bioinformatics)* [online]. 9569, Springer Verlag, pp. 232–238.

Simplify3D (2018) Part Quality Troubleshooting Guide. (September).

Sobel, I. and Feldman, G. (1990) An Isotropic 3×3 image gradient operator. [online]. [Accessed 23 April 2023].

Sola, A., Sai, Y., Trinchi, A., Chu, C., Shen, S. and Chen, S. (2022) How Can We Provide Additively Manufactured Parts with a Fingerprint? A Review of Tagging Strategies in Additive Manufacturing. *Materials* [online]. 15 (1).

Straub, J. (2017) *A combined system for 3D printing cybersecurity*. In: Harding, K.G. and Zhang, S., eds. *Dimensional Optical Metrology and Inspection for Practical Applications VI* [online]. 10220, International Society for Optics and Photonics, p. 102200N.

Straub, J. (2018) An approach to detecting deliberately introduced defects and micro-defects in 3D printed objects. Alam, M.S., ed. *Pattern Recognition and Tracking XXVIII* [online]. 27, pp. 25–28.

Straub, J. (2015) Initial Work on the Characterization of Additive Manufacturing (3D Printing) Using Software Image Analysis. *Machines* [online]. 3 (2), pp. 55–71.

Sünderhauf, N., Shirazi, S., Jacobson, A., Dayoub, F., Pepperell, E., Upcroft, B. and Milford, M. (2015) Place Recognition with ConvNet Landmarks: Viewpoint-Robust, Condition-Robust, Training-Free. [Accessed 23 April 2023].

Suzuki, M., Dechrueng, P., Techavichian, S., Silapasuphakornwong, P., Torii, H. and Uehira, K. (2017) Embedding information into objects fabricated with 3-D printers by forming fine cavities inside them. *IS and T International Symposium on Electronic Imaging Science and Technology* [online]. pp. 6–9.

Suzuki, M., Silapasuphakornwong, P., Uehira, K., Unno, H. and Takashima, Y. (2015) Copyright protection for 3D printing by embedding information inside real fabricated objects. *VISAPP 2015 - 10th International Conference on Computer Vision Theory and Applications; VISIGRAPP, Proceedings* [online]. 3, pp. 180–185.

Tan, X. and Triggs, B. (2010) Enhanced local texture feature sets for face recognition under difficult lighting conditions. *IEEE Transactions on Image Processing* [online]. 19 (6), pp. 1635–1650. Available from: https://dl.acm.org/doi/10.1109/TIP.2010.2042645 [Accessed 23 April 2023].

Tey, W.S., Cai, C. and Zhou, K. (2021) A Comprehensive Investigation on 3D Printing of Polyamide 11 and Thermoplastic Polyurethane via Multi Jet Fusion. *Polymers 2021, Vol. 13, Page 2139* [online]. 13 (13), p. 2139.

Thompson, M.K. and Mischkot, M. (2015) Design of Test Parts to Characterize Micro Additive Manufacturing Processes. *Procedia CIRP* [online]. 34, pp. 223–228. Available from: https://linkinghub.elsevier.com/retrieve/pii/S2212827115008240 [Accessed 8 March 2021].

Tong, L., Wong, W.K. and Kwong, C.K. (2016) Differential evolution-based optimal Gabor filter model for fabric inspection. *Neurocomputing* [online]. 173, pp. 1386–1401.

Tuceryan, M. and Jain, A.K. (1993) Handbook of Pattern Recognition & Computer Vision. In: Chen, C.H., Pau, L.F. and Wang, P.S.P., eds. River Edge, NJ, USA, World Scientific Publishing Co., Inc., pp. 235–276.

Tumbleston, J.R. *et al.* (2015) Additive manufacturing. Continuous liquid interface production of 3D objects. *Science (New York, N.Y.)* [online]. 347 (6228), pp. 1349–1352. Available from: https://pubmed.ncbi.nlm.nih.gov/25780246/ [Accessed 30 April 2023].

Valerga, A.P., Batista, M., Fernandez-Vidal, S.R. and Gamez, A.J. (2019) Impact of chemical post-processing in fused deposition modelling (FDM) on polylactic acid (PLA) surface quality and structure. *Polymers* [online]. 11 (3).

Valerga, A.P., Batista, M., Salguero, J. and Girot, F. (2018) Influence of PLA filament conditions on characteristics of FDM parts. *Materials* [online]. 11 (8).

Vora, H.D. and Sanyal, S. (2020) A comprehensive review: metrology in additive manufacturing and 3D printing technology. [online]. 5, pp. 319–353. Available from: https://doi.org/10.1007/s40964-020-00142-6 [Accessed 2 December 2021].

Vyavahare, S., Teraiya, S., Panghal, D. and Kumar, S. (2020) *Fused deposition modelling: a review Rapid Prototyping Journal* [online]. 26 (1), pp. 176–201. Available from: https://www.emerald.com/insight/1355-2546.htm [Accessed 1 April 2023].

Wang, J., Zha, H. and Cipolla, R. (2006) Efficient Topological Localization Using Orientation Adjacency Coherence Histograms. *18th International Conference on Pattern Recognition (ICPR'06)* [online].

Wang, X., Ding, X. and Liu, C. (2005) Gabor filters-based feature extraction for character recognition. *Pattern Recognition* [online]. 38 (3), pp. 369–379. [Accessed 22 April 2023].

Wei, X., Zeng, L. and Pei, Z. (2019) *Experimental investigation of polyjet 3D printing process: Effects of finish type and material color on color appearance*. In: *ASME International Mechanical Engineering Congress and Exposition, Proceedings (IMECE)* [online]. 2A-2019, pp. 1–9.

Wickramasinghe, S., Do, T. and Tran, P. (2020) FDM-Based 3D printing of polymer and associated composite: A review on mechanical properties, defects and treatments. *Polymers* [online]. 12 (7), pp. 1–42.

Wong, K. V. and Hernandez, A. (2012) A Review of Additive Manufacturing. *ISRN Mechanical Engineering* [online]. 2012, pp. 1–10.

Woodham, R.J. (1978) PHOTOMETRIC STEREO - A REFLECTANCE MAP TECHNIQUE FOR DETERMINING SURFACE ORIENTATION FROM IMAGE INTENSITY. Nevatia, R., ed. *Proceedings of the Society of Photo-Optical Instrumentation Engineers* [online]. 155, pp. 136–143. Available from: http://proceedings.spiedigitallibrary.org/proceeding.aspx?articleid=1227659 [Accessed 26 August 2019].

Wu, L., Guo, X., Zhao, L. and Jian, M. (2017) A Quality Evaluation Scheme to 3D Printing Objects Using Stereovision Measurement. *Lecture Notes in Computer Science* [online]. pp. 458–467.

Wu, Z., Song, S., Khosla, A., Yu, F., Zhang, L., Tang, X. and Xiao, J. (2014) 3D ShapeNets: A Deep Representation for Volumetric Shapes. *Proceedings of the IEEE Computer Society Conference on Computer Vision and Pattern Recognition* [online]. 07-12-June-2015, pp. 1912–1920. Available from: https://arxiv.org/abs/1406.5670v3 [Accessed 23 April 2023].

Xie, X. (2008) A Review of Recent Advances in Surface Defect Detection using Texture analysis Techniques. 7 (3), pp. 1–22.

Xu, C., Dai, Y., Lin, R. and Wang, S. (2020) Deep clustering by maximizing mutual information in variational auto-encoder. *Knowledge-Based Systems* [online]. 205, p. 106260. [Accessed 11 April 2023].

Yamazaki, S., Kagami, S. and Mochimaru, M. (2014) *Extracting Watermark from 3D Prints*. In: *Proceedings - International Conference on Pattern Recognition* [online]. Institute of Electrical and Electronics Engineers Inc., pp. 4576–4581.

Yampolskiy, M., King, W.E., Gatlin, J., Belikovetsky, S., Brown, A., Skjellum, A. and Elovici, Y. (2018) Security of additive manufacturing: Attack taxonomy and survey. *Additive Manufacturing* [online]. 21, pp. 431–457. Available from: https://linkinghub.elsevier.com/retrieve/pii/S221486041730502X [Accessed 8 April 2019].

Yang, L., Zhao, Y., Yang, M.-H., Zhang, Z., Song, Y., Hong, S., Xu, R., Zhang, W. and Cui, B. (2023) Diffusion Models: A Comprehensive Survey of Methods and Applications; Diffusion Models: A Comprehensive Survey of Methods and Applications. [online]. Available from: https://doi.org/XXXXXXX. [Accessed 23 April 2023].

Yin, Y., Liu, X., Peng, X., Gao, B.Z. and Wang, M. (2015) Fringe projection 3D microscopy with the general imaging model. *Optics Express* [online]. 23 (5), p. 6846.

Yu, Q. and Wang, K. (2013) 3D vision based quality inspection with computational intelligence. *Assembly Automation* [online]. 33 (3), pp. 240–246.

Zamofing, T. and Hugli, H. (2004) *Applied multifocus 3D microscopy* Batchelor, B.G. and Hugli, H., eds. [online]. p. 134.

Zeltmann, S.E., Gupta, N., Tsoutsos, N.G., Maniatakos, M., Rajendran, J. and Karri, R. (2016) Manufacturing and Security Challenges in 3D Printing. *JOM* [online]. 68 (7), pp. 1872–1881.

Zhang, S. (2018) High-speed 3D shape measurement with structured light methods: A review. *Optics and Lasers in Engineering* [online]. 106, pp. 119–131. Available from: https://doi.org/10.1016/j.optlaseng.2018.02.017 [Accessed 1 April 2023].

Zhang, S. and Feng, Y. (2021) Modeling Concentrated Cross-Attention for Neural Machine Translation with Gaussian Mixture Model. *Findings of the Association for Computational Linguistics, Findings of ACL: EMNLP 2021* [online]. pp. 1401–1411. Available from: https://arxiv.org/abs/2109.05244v2 [Accessed 23 April 2023].

Zhao, S., Gao, Y. and Zhang, B. (2008) *Sobel-LBP*. In: *Proceedings - International Conference on Image Processing, ICIP* [online]. pp. 2144–2147. [Accessed 24 August 2019].

11. APPENDIX

Table 15: Taxonomy of anomalies

Printing technology	Materials Used	Benefits	Anomalies	Characteristics	Anomaly sources
FDM	PLA	Low Cost	Under-Extrusion, Over-Extrusion, Gaps in Top Layers, Stringing or Oozing, Overheating, Layer Shifting, Layer Separation and Splitting, Stops Extruding Mid Print, Weak Infill, Blobs and Zits, Gaps Between Infill and Outline, Curling or Rough Corners, Scars on Top Surface, Gaps in Floor Corners, Lines on the Side of Print, Vibrations and Ringing, Gaps in Thin Walls, Inconsistent Extrusion, Warping, Poor Surface Above Supports, Dimensional Accuracy, Poor Bridging	**Dimensional Accuracy**: ±0.5% **Layer Thickness Range**: 50-400 µm **Surface Roughness /Texture**: Can vary widely depending on settings	Material: temperature, viscosity, density, type of material and mechanical properties.
	ABS	High print speed			Platform: temperature, pressure, vibrations, position of the platform, system coordinates and heat evacuation.
	PETG	Easy to use			Printer head: speed, angle of inclination, diameter of extrusion, position of the extruder, vibration and acceleration.
Polyjet/ DLP/SLA	Photopolymer	High print speed	Layer Shifting, Layer Separation and Splitting, Warping, Curling or Rough Corners, Scars on Top Surface, Gaps in Thin Walls, Poor Surface Above Supports, Dimensional Accuracy	**Dimensional Accuracy**: ±0.1% **Layer Thickness Range**: 16-100 µm **Surface Roughness /Texture**: Very smooth surfaces	Material: viscosity, density and mechanical properties.
		Fine resolution			Platform: position of the platform and system coordinates.
		Smooth surface finish			Light source: intensity, wavelength, and exposure time.
		Complex geometries			Curing: layer compression and layer separation
MJF	Nylon based Polymer	Fine resolution	Top layer compression, Overheating, Layer Shifting, Layer Separation and Splitting, Weak Infill, Blobs and Zits, Gaps Between Infill and Outline, Curling or Rough Corners, Scars on Top Surface, Gaps in Floor Corners, Lines on the Side of Print, Vibrations and Ringing, Gaps in Thin	**Dimensional Accuracy**: ±0.3% **Layer Thickness Range**: 80 µm	Material: temperature, viscosity, density, type of material, and mechanical properties.
		High quality print			Platform: temperature and vibrations.
		Strong tensile strength			Laser: speed, angle of inclination,

			Walls, Inconsistent powder deposition, Warping	**Surface Roughness /Texture**: Very smooth surfaces but depends heavily on the powder used and post-processing	intensity, and acceleration.
		High print speed			
SLS	Polymer	Fine resolution	Overheating, Layer Shifting, Layer Separation and Splitting, Stops Extruding Mid Print, Weak Infill, Blobs and Zits, Gaps Between Infill and Outline, Curling or Rough Corners, Scars on Top Surface, Gaps in Floor Corners, Lines on the Side of Print, Vibrations and Ringing, Gaps in Thin Walls, Inconsistent Extrusion, Warping, Poor Surface Above Supports, Dimensional Accuracy	**Dimensional Accuracy**: ±0.3% **Layer Thickness Range**: 100-120 µm **Surface Roughness /Texture**: Slightly rougher than MJF but can be improved with post-processing	Material: temperature, viscosity, density, type of material and mechanical properties.
	Ceramic	High quality print			Platform: temperature, pressure, vibrations, position of the platform, position of the laser, system coordinates and heat evacuation.
	Composites	Strong tensile strength			Laser: speed, accuracy, laser intensity, diameter of extrusion, vibration, and acceleration.
LOM	Metal foil	Low material cost	Poor surface quality, low resolution, weak part strength, slow process	**Dimensional Accuracy**: ±1% **Layer Thickness Range**: 20-200 µm **Surface Roughness /Texture**: Depends on the material	Material: adhesive type, material properties, and sheet thickness.
					Laser or cutting blade: accuracy, power, and cutting speed.
					Adhesion process: pressure, temperature, and bonding uniformity.
					Platform: positioning accuracy and stability.